Electronic Supplementary Material (ESI) for Catalysis Science & Technology.

Supporting Information

Ruthenium(II) Arene Complexes Bearing Simple Dioxime Ligands: Effective Catalysts for the One-Pot Transfer Hydrogenation/N-Methylation of Nitroarenes with Methanol

Roberta Colaiezzi,[a] Chiara Saviozzi[b,c], Nicola di Nicola,[a] Stefano Zacchini,[d] Guido Pampaloni,[b,c] Marcello Crucianelli,[a] Fabio Marchetti,[b,c] Andrea Di Giuseppe,[a] Lorenzo Biancalana,[b,c*]*

[a] Università dell'Aquila, Dipartimento di Scienze Fisiche e Chimiche, Via Vetoio, I-67100 L'Aquila, Italy.

[b] Università di Pisa, Dipartimento di Chimica e Chimica Industriale, Via G. Moruzzi 13, I-56124 Pisa, Italy.

[c] Consorzio Interuniversitario Reattività Chimica e Catalisi (CIRCC), Via Celso Ulpiani 27, I-70126 Bari, Italy.

[d] Università di Bologna, Dipartimento di Chimica Industriale "Toso Montanari", Viale del Risorgimento 4, I-40136 Bologna, Italy.

* Email: lorenzo.biancalana@unipi.it , andrea.digiuseppe@univaq.it

Preparation and characterization of starting materials and reference Ru compounds

$[RuCl_2(\eta^6\text{-}p\text{-cymene})]_2$, D1 (Chart S1).

Chart S1. Structure of $[RuCl_2(\eta^6\text{-}p\text{-cymene})]_2$.

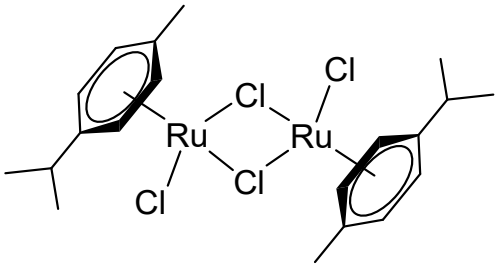

A scaled-up version of the previously-reported procedure[1] is herein described, employing comparatively less solvent, less phellandrene and a reduced reaction time. In a 500 mL round-bottom Schlenk flask equipped with a reflux condenser, α-phellandrene (35 mL, 216 mmol) was added to a dark brown solution of $RuCl_3 \cdot xH_2O$ (8.108 g, 31.00 mmol as trihydrate) in deaerated EtOH (300 mL). The reaction mixture was refluxed for 13 h (oil bath T = 100 °C) under a N_2 atmosphere. Next, volatiles were removed under vacuum while the suspension was still hot (oil bath T = 100 °C). The residue was vigorously stirred in petroleum ether (100 mL) for some hours. The resulting suspension was filtered on a G4 sintered glass filter and the solid was thoroughly washed with petroleum ether to remove high-boiling aromatic compounds. Following dissolution with CH_2Cl_2 and filtration over a celite pad, volatiles were carefully removed under vacuum (600 mbar, 40 °C). The brick red solid was stirred in a Et_2O/petroleum ether 1:1 *v*/*v* mixture (*ca*. 150 mL) until a fine power was obtained then the suspension was filtered. The solid was washed with petroleum ether and dried under vacuum (50 °C), while acquiring an orange coloration. Yield: 9.429 g, 30.79 mmol, 99 %. The purity was assessed by ^{1}H NMR (Figure S1).

$[RuCl_2(\eta^6\text{-}C_6Me_6)]_2$, D3 (Chart S2).

Chart S2. Structure of $[RuCl_2(\eta^6\text{-}C_6Me_6)]_2$.

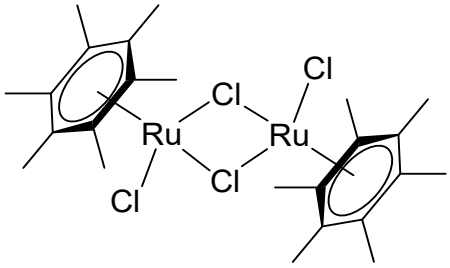

An optimized procedure is herein described, requiring a lower amount of C_6Me_6 and leading to a higher yield.[2] Solid $[RuCl_2(\eta^6\text{-}p\text{-cymene})]_2$ (2.00 g, 3.266 mmol) and hexamethylbenzene (7.6 g, 47 mmol) were intimately mixed and transferred in a 50 mL round bottom Schlenk flask with a narrow neck together with a large stir bar. The flask was equipped with a sintered glass filter on top, placed under a N_2 atmosphere and immersed into a pre-heated silicone oil bath at 210 °C. The dark red melt was stirred for 2 h while keeping the heating bath at 210-220 °C and gently tapping the upper side of the flask to drop the sublimed hexamethylbenzene. Next, the reaction mixture was cooled to room temperature. The resulting dark red solid was crushed, transferred into a 250 mL round bottom flask and suspended in CH_2Cl_2 (200 mL) under vigorous stirring for 1 h. The suspension was allowed to settle and the solution was filtered on a G4 sintered-glass filter. The filtrate was collected into a 1 L round bottom flask. The residual solid was suspended in fresh CH_2Cl_2 and the operations were repeated until complete dissolution of the red component (only a dark brown residue should remain on the filter). The red-orange filtrate solution was taken to dryness under vacuum and the residue was suspended in THF under vigorous stirring. The suspension was filtered on a G3 glass filter and the resulting brick red solid was thoroughly washed with THF to remove the aromatic species (checked by fluorescent silica / UV lamp), Et_2O, hexane and dried under vacuum (40 °C). Yield (**D3**): 1.98 g, 91 %. The pale yellow-orange THF filtrate was dried under vacuum and hexamethylbenzene was recovered by sublimation under vacuum at 100 °C. Yield (C_6Me_6): 6.3 g, 96 % of the molar excess. It is important to perform the reaction above 200 °C; one attempt at 180-185 °C resulted in the quantitative recovery of unreacted $[RuCl_2(\eta^6\text{-}p\text{-cymene})]_2$. Compound $[RuCl_2(\eta^6\text{-}C_6Me_6)]_2$ is soluble

in DMSO,[3] less soluble in CH_2Cl_2 > $CHCl_3$, poorly soluble in MeOH, MeCN, insoluble in THF, Et_2O, hexane. Anal. Calcd. for $C_{24}H_{36}Cl_4Ru_2$: C: 43.12, H: 5.43. Found: C: 43.31, H: 5.44. IR (solid state): $\tilde{\upsilon}/cm^{-1}$ = 3019w-sh, 2966w-sh, 2919m, 1499m-sh, 1442m, 1385s, 1373s, 1066s, 1015s, 760w, 750w. ^1H NMR (DMSO-d_6 or $CDCl_3$): δ/ppm = 2.02 ppm.

$[RuCl_2(\eta^6\text{-}1,3,5\text{-}C_6H_3Me_3)]_2$, D4 (Chart S3).

Chart S3. Structure of $[RuCl_2(\eta^6\text{-}1,3,5\text{-}C_6H_3Me_3)]_2$ (numbering refers to C atoms).

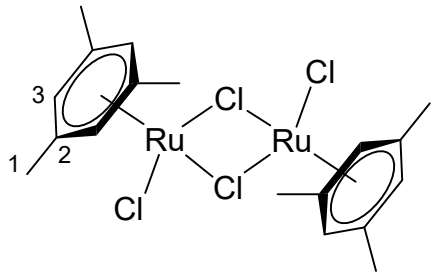

The original and most common preparation method involves the reaction of $RuCl_3$ hydrate with 10 eq. of 1,4-dihydromesitylene (1,3,5-trimethylcyclohexa-1,4-diene) in refluxing ethanol (66-77 % yield).[2c,4,5] A *brown* solid is obtained without a proper workup, *e.g.* sequential treatment with AgOAc and concentrated HCl as proposed by M. A. Bennett.[4] We applied the arene exchange methodology, which has been briefly mentioned once,[6] and a new purification method. In a 100 mL Schlenk tube, a brick red suspension of $[RuCl_2(\eta^6\text{-}p\text{-cymene})]_2$ (435 mg, 0.710 mmol) in anhydrous mesitylene (30 mL) was stirred at reflux [oil bath temperature: 200 °C] under a N_2 atmosphere. The conversion was checked by ^1H NMR. After 16 h, volatiles were removed from the hot reaction mixture under vacuum. The resulting *brown* solid was suspended in DMF under vigorous stirring at *ca*. 70 °C. The hot suspension was filtered over a celite pad. The operations were repeated until complete dissolution of the *red* component (only a dark brown residue should remain on the filter). The red filtrate was taken to dryness under vacuum (60 °C). In order to remove traces of unreacted $[RuCl_2(\eta^6\text{-}p\text{-cymene})]_2$, the residue was triturated with Et_2O/CH_2Cl_2 1:1 *v*/*v* and stirred until a fine powder was obtained. Next, the suspension was filtered on a G3 glass filter. The resulting orange solid was washed with Et_2O/CH_2Cl_2 1:1 *v*/*v*, Et_2O, hexane (removal of aromatics was checked by fluorescent silica / UV

lamp) and dried under vacuum (40 °C). Yield: 320 mg, 77 %. Keeping the heating bath well above the boiling point of mesitylene (165 °C) for a prolonged time ensures the success of the reaction. Temperature/time/conversion: 150 °C, 72 h, 10 %; 180 °C, 24 h, < 30 %; 200 °C, 7 h, 35 %. Compound $[RuCl_2(\eta^6\text{-}1,3,5\text{-}C_6H_3Me_3)]_2$ is soluble in DMSO,[3] 37 % HCl and hot DMF, poorly soluble in CH_2Cl_2, $CHCl_3$, insoluble in THF, Et_2O, hexane. IR (solid state): 3054w, 3013m, 2981m-sh, 2969m-sh, 1523s, 1452s-sh, 1443s, 1387ms-h, 1377s, 1298w, 1164w, 1153w, 1027s, 1009m-sh, 983s, 926w, 919w, 879s. ^{1}H NMR (500 MHz, DMSO-d_6): δ/ppm = 5.14 (s, 3H, C^3H), 2.14 (s, 9H, C^1H). $^{13}C\{^1H\}$ NMR (500 MHz, DMSO-d_6): δ/ppm = 105.0 (C^2), 82.0 (C^3), 18.2 (C^1).

$[Ru_2Cl_2(\mu\text{-}Cl)(\mu\text{-}H)(\eta^6\text{-}p\text{-cymene})_2]$, D5 (Chart S4).

Chart S4. Structure of $[Ru_2Cl_2(\mu\text{-}Cl)(\mu\text{-}H)(\eta^6\text{-}p\text{-cymene})_2]$ (numbering refers to C atoms).

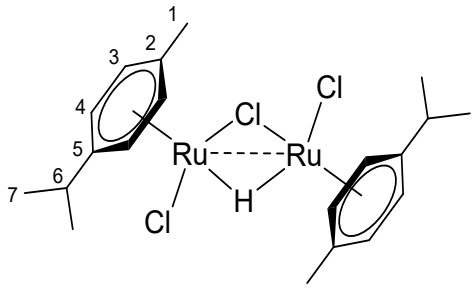

Previously obtained by the reaction of $[RuCl_2(\eta^6\text{-}p\text{-cymene})]_2$ with $H_{2(g)}/Et_3N$, $H_{2(g)}/Et_3SiH$ or $Na[HCO_2]$.[1,4,7] In a 25 mL Schlenk tube under N_2, an solution of $[RuCl_2(\eta^6\text{-}p\text{-cymene})]_2$ (93 mg, 0.152 mmol) in anhydrous THF (8 mL) was treated with $NaBH_4$ (15 mg, 0.40 mmol) and stirred at room temperature for 24 h. Conversion was checked by ^{1}H NMR ($CDCl_3$). The resulting red-violet solution was taken to dryness under vacuum. The residue was suspended in CH_2Cl_2 and filtered over celite. Volatiles were removed under vacuum from the filtrate solution, affording a red-violet solid, which was washed with pentane and dried under vacuum (40 °C). Yield: 88 mg, 99 %. Alternative procedure: a suspension of $[RuCl_2(\eta^6\text{-}p\text{-cymene})]_2$ (210 mg, 0.343 mmol) and $NaHCO_3$ (75 mg, 0.89 mmol) in deaerated ^{i}PrOH (10 mL) was stirred at room temperature for 4 days, affording a red-violet suspension. Conversion was checked by ^{1}H NMR ($CDCl_3$). Volatiles were removed under vacuum,

the residue was suspended in CH_2Cl_2 and moved on top of a silica column. A red-violet band was eluted with CH_2Cl_2/THF 5:1 *v*/*v*. The solution was taken to dryness under vacuum and the resulting red-violet solid was washed with pentane and dried under vacuum (40 °C). Yield: 148 mg, 75 %. ^{1}H NMR ($CDCl_3$): δ/ppm = 5.65 (d, $^3J_{HH}$ = 5.7 Hz, 2H, C^{4}H), 5.55 (d, $^3J_{HH}$ = 5.3 Hz, 2H, C$^{3'}$H), 5.31 (d, $^3J_{HH}$ = 5.8 Hz, 2H, C$^{4'}$H), 4.85 (d, $^3J_{HH}$ = 5.7 Hz, 2H, C^{3}H), 2.99 (hept, $^3J_{HH}$ = 6.9 Hz, 2H, C^{6}H), 2.29 (s, 6H, C^{1}H), 1.45 (d, $^3J_{HH}$ = 6.9 Hz, 6H, C^{7}H), 1.41 (d, $^3J_{HH}$ = 7.0 Hz, 6H, C$^{7'}$H), -10.18 (s, 1H, μ-H).

[RuCl{κ^2*N*-$H_2NCH_2CH_2NH_2$}(η^6-*p*-cymene)]Cl, N2 (Chart S5).

Chart S5. Structure of [RuCl(κ^2*N*-$H_2NCH_2CH_2NH_2$)(η^6-*p*-cymene)]Cl (numbering refers to C atoms).

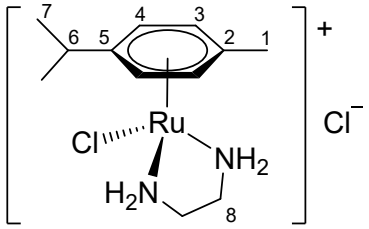

Differently from what reported in the literature,[8] by-products were observed by ^{1}H NMR in the final reaction mixture and purification by silica chromatography was necessary. In a 25 mL round bottom flask, a brick-red solution of [$RuCl_2$(η^6-p-cymene)]$_2$ (66 mg, 0.11 mmol), in CH_2Cl_2 (10 mL) was treated with ethylenediamine (16 μL, 0.24 mmol) and stirred at room temperature for 3 h. The final mixture (pale yellow solution + yellow solid) was moved on top of a silica gel column (d 2.3, h 2 cm; preliminarily washed with MeOH to remove NaCl). Impurities were eluted with CH_2Cl_2 and MeCN, then a yellow band was eluted with MeOH. Volatiles were removed under vacuum affording a yellow solid. Yield: 63 mg, 80 %. Soluble in MeOH, EtOH, poorly soluble in MeCN, ^{i}PrOH, insoluble in CH_2Cl_2. IR (solid state): ῡ/cm^{-1} = 3264m (NH), 3188m (NH), 3174m, 3081s, 3020m, 2961m, 2935m, 2877m, 1586w, 1567s,1532w, 1505m, 1469m, 1449m, 1438m, 1390m, 1362m, 1327w, 1280w, 1197s, 1168w, 1149s, 1109w, 1092w, 1062s, 1042m, 1034m, 1011s, 980w, 932w, 912w, 879s, 871s, 804m, 762w, 718m, 670m. ^{1}H NMR (CD_3OD): δ/ppm = 5.99 (s-br, 2H, NH); 5.61 (d, $^3J_{HH}$ = 6.0 Hz,

2H, C^{4}H), 5.44 (d, $^3J_{HH}$ = 5.9 Hz, 2H, C^{3}H), 4.07 (s-br, 2H, NH'), 2.87 (hept, $^3J_{HH}$ = 6.9 Hz, 1H, C^{6}H); 2.61–2.49 (m, 2H, C^{8}H), 2.47–2.35 (m, 2H, C^{8}H'), 2.23 (s, 3H, C^{1}H), 1.30 (d, $^3J_{HH}$ = 6.9 Hz, C^{7}H).

[RuCl{κ^2*N*-(*1S*,*2S*)-$H_2NC(Ph)C(Ph)NSO_2$(*p*-$C_6H_4CH_3$)}(η^6-*p*-cymene)], N3 (Chart S6).

Chart S6. Structure of [RuCl{κ^2*N*-(*1S*,*2S*)-$H_2NC(Ph)C(Ph)NSO_2$(*p*-$C_6H_4CH_3$)}(η^6-*p*-cymene)] (numbering refers to C atoms).

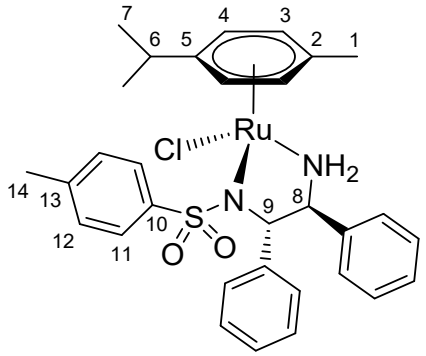

.

Prepared according to a slightly modified literature procedure.[9] In a 50 mL Schlenk tube under N_2, [$RuCl_2$(η^6-*p*-cymene)]$_2$ (82 mg, 0.13 mmol), (*1S*,*2S*)-(+)-*N*-*p*-tosyl-1,2-diphenylethylenediamine (102 mg, 0.278 mmol), deaerated ^{i}PrOH (10 mL) and Et_3N (50 μL, 0.36 mmol) were introduced. The orange suspension was stirred at 80 °C for 2 h. The resulting bright orange solution was concentrated up to *ca*. 1 mL under reduced pressure (no precipitation was observed at this stage, even at − 20 °C) then treated with H_2O (10 mL) under stirring. The suspension was filtered and the resulting yellow-orange solid was washed with H_2O and dried under vacuum (40 °C, over P_2O_5). Yield: 143 mg, 88 %. Soluble in ^{i}PrOH, $CHCl_3$, insoluble in water, Et_2O, hexane. IR (solid state): ῡ/cm^{-1} = 3271w, 3219w (NH); 3142w, 3083w, 3064w, 3031w, 2961w, 2921w, 2876w, 1599w, 1494m, 1469w-sh, 1454m, 1386w, 1374w, 1324w, 1266s, 1146w-sh, 1124s, 1112m-sh, 1083s, 1062w-sh, 1039m, 1002m, 994m, 945w, 915s, 901s, 861m, 841w, 819s, 809m-sh, 792m, 769m, 753m, 698s, 677m, 657m. ^{1}H NMR ($CDCl_3$): δ/ppm = 7.08–6.97 (m, 5H, Ph), 6.79–6.67 (m, 5H, Ph), 6.62 (app. t, 2H, $^3J_{HH}$ = 7.4 Hz, C^{11}H), 6.44 (d, 2H, $^3J_{HH}$ = 6.6 Hz, C^{12}H), 5.70 (d + m, 5H, C^{3}H + C^{4}H + NH), 3.77

(br, 1H, NH'), 3.62–3.52 (m, 2H, C^8H + C^9H), 3.12 (hept, $^3J_{HH}$ = 6.3 Hz, C^6H), 2.36 (s, 3H, C^1H), 2.21 (s, 3H, $C^{14}H$), 1.38 (app. t, $^3J_{HH}$ = 6.6 Hz, C^7H).

Figure S1. ^{1}H NMR spectrum (400 MHz, $CDCl_3$) of $[RuCl_2(\eta^6\text{-}p\text{-cymene})]_2$.

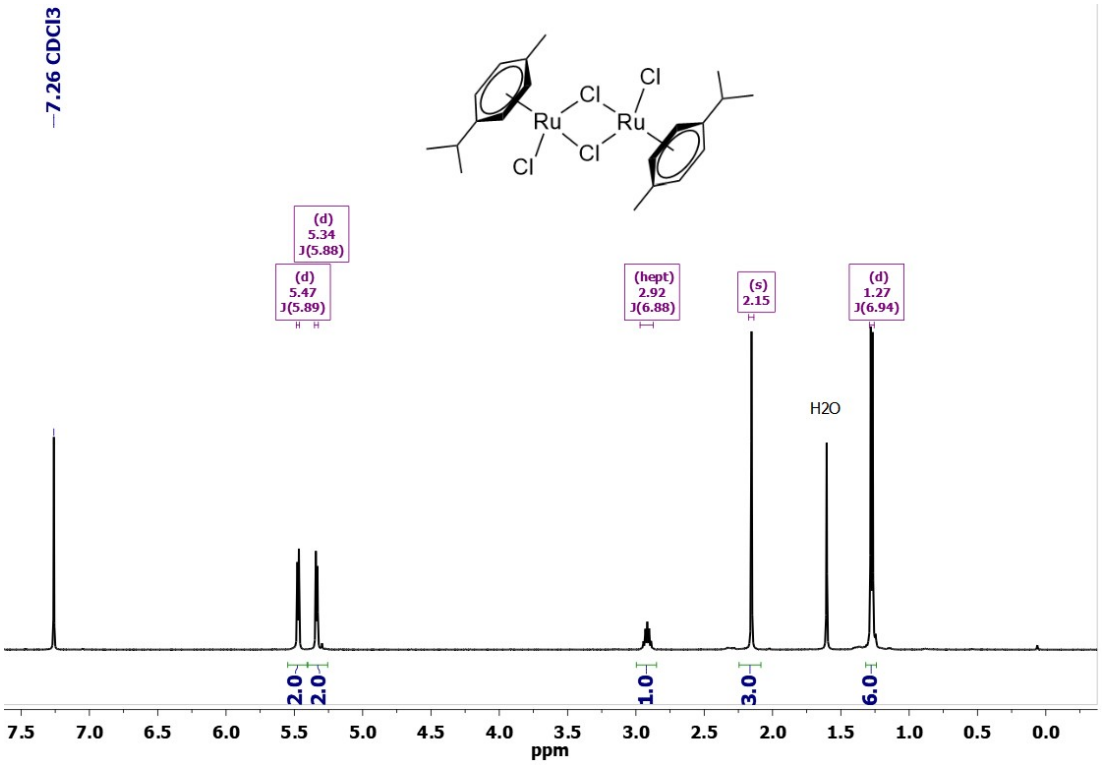

Figure S2. ^{1}H NMR spectrum (400 MHz, $CDCl_3$) of $[RuCl_2(\eta^6\text{-}C_6Me_6)]_2$.

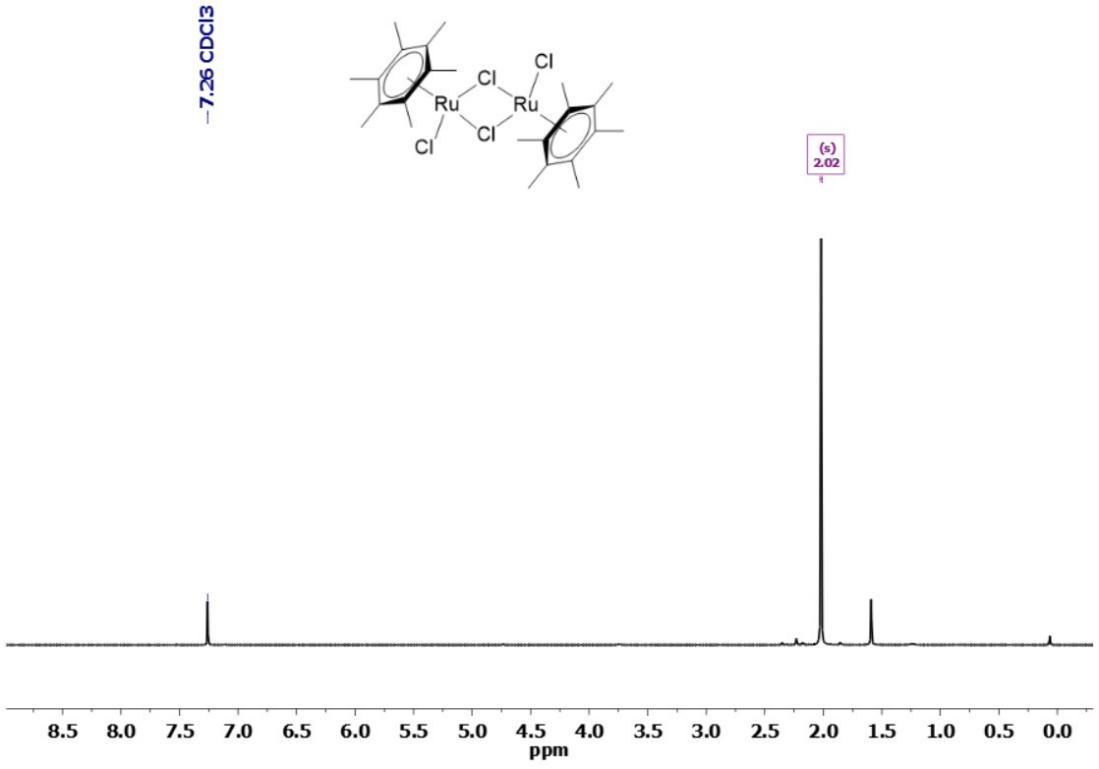

Figure S3. ^{1}H NMR spectrum (500 MHz, DMSO-d_6) of $[RuCl_2(\eta^6\text{-}1,3,5\text{-}C_6H_3Me_3)]_2$.

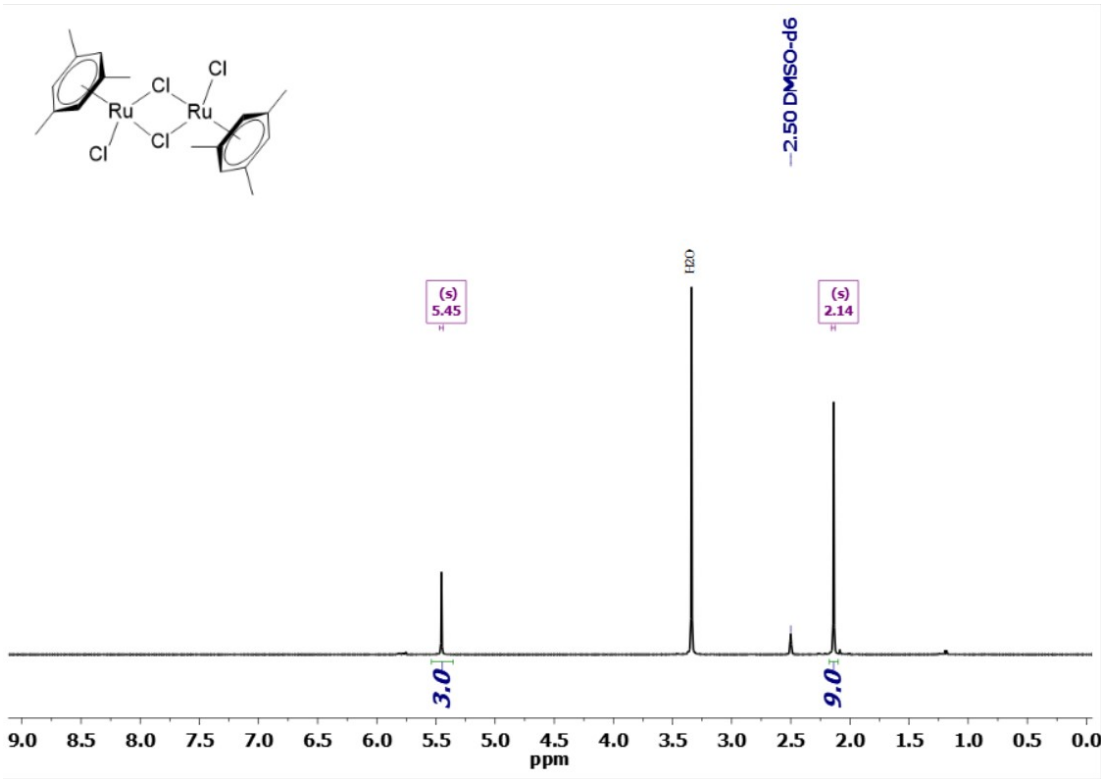

Figure S4. ^{1}H NMR spectrum (400 MHz, CD_3OD) of $[RuCl\{\kappa^2\text{-}N\text{-}H_2NCH_2CH_2NH_2\}(\eta^6\text{-}p\text{-cymene})]Cl$.

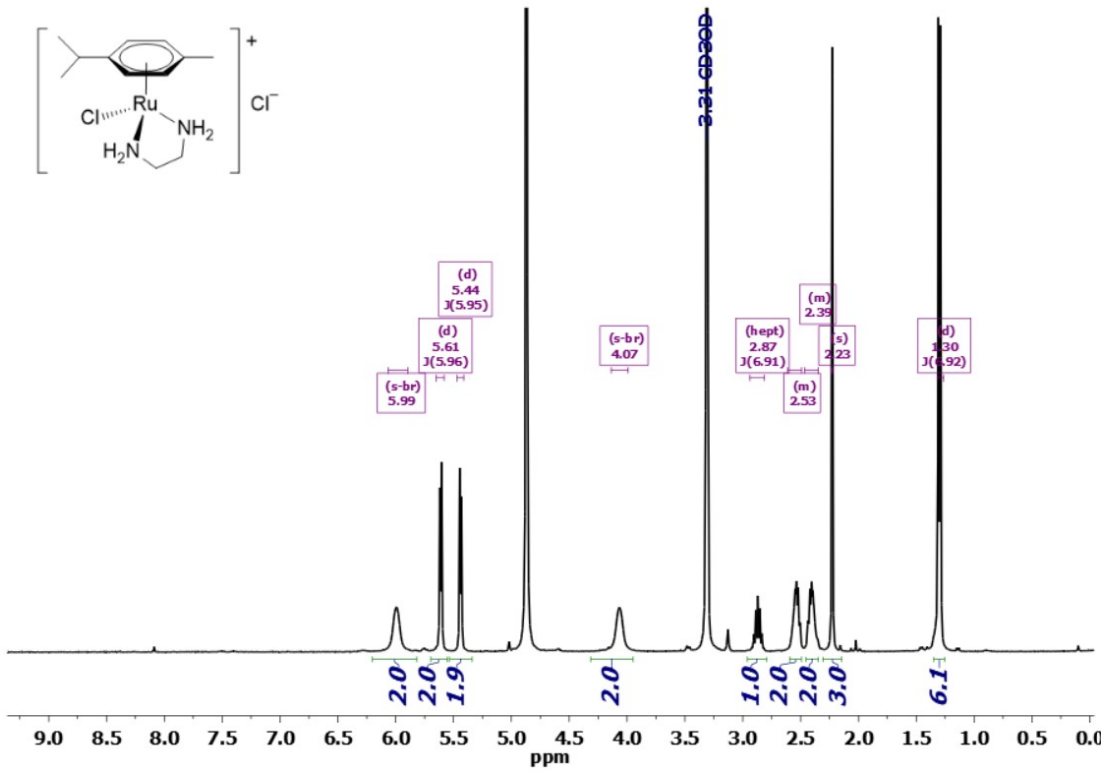

IR and NMR spectra of dioxime complexes

Figure S5. Solid-state IR spectrum (650-4000 cm^{-1}) of [RuCl(κ²*N*-{CH_3C=NOH}$_2$)(η⁶-*p*-cymene)]NO_3, [**1**]NO_3.

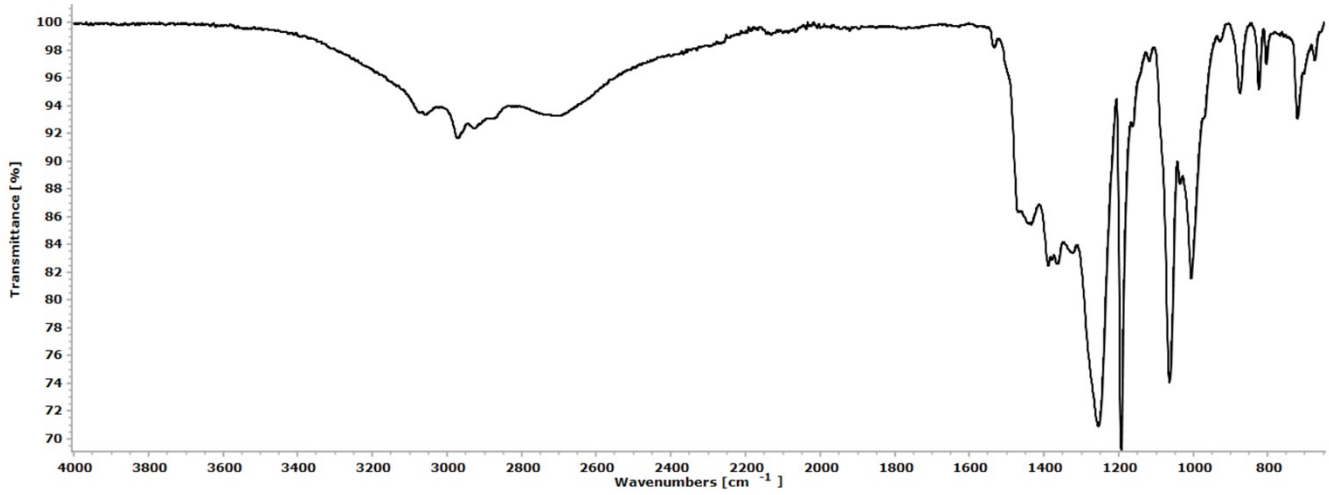

Figure S6. Solid-state IR spectra (650-4000 cm^{-1}) of [RuCl(κ²*N*-{CH_2CH_2C=NOH}$_2$)(η⁶-*p*-cymene)]$^+$, [**2**]$^+$ as NO_3^- (red line) or PF_6^- (blue line) salt.

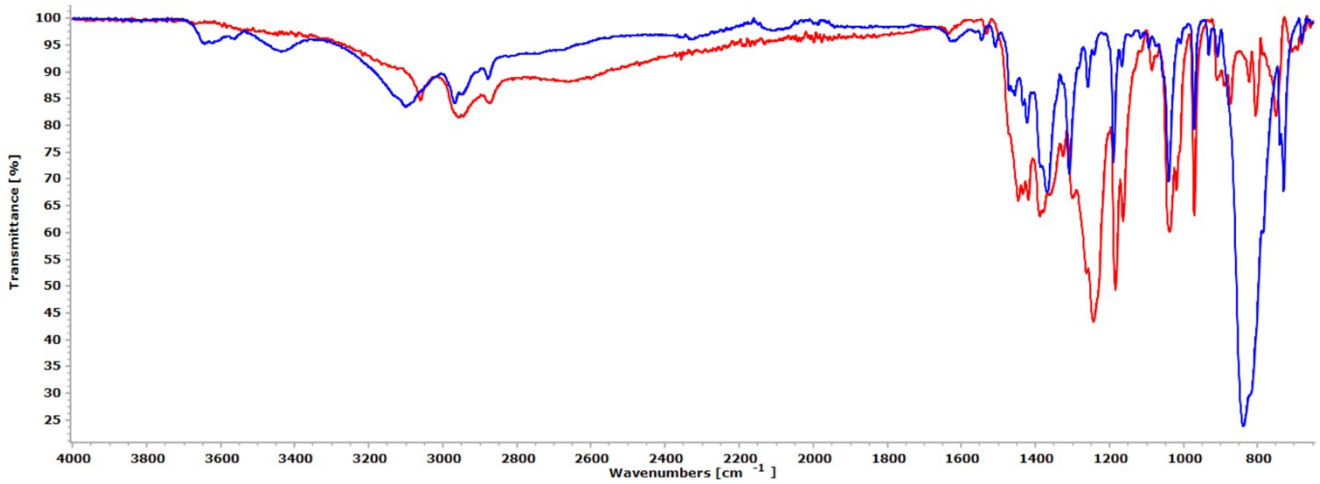

Figure S7. Solid-state IR spectrum (650-4000 cm^{-1}) of [RuI(κ^2*N*-{CH_2CH_2C=NOH}$_2$)(η^6-*p*-cymene)]NO_3, [**3**]NO_3.

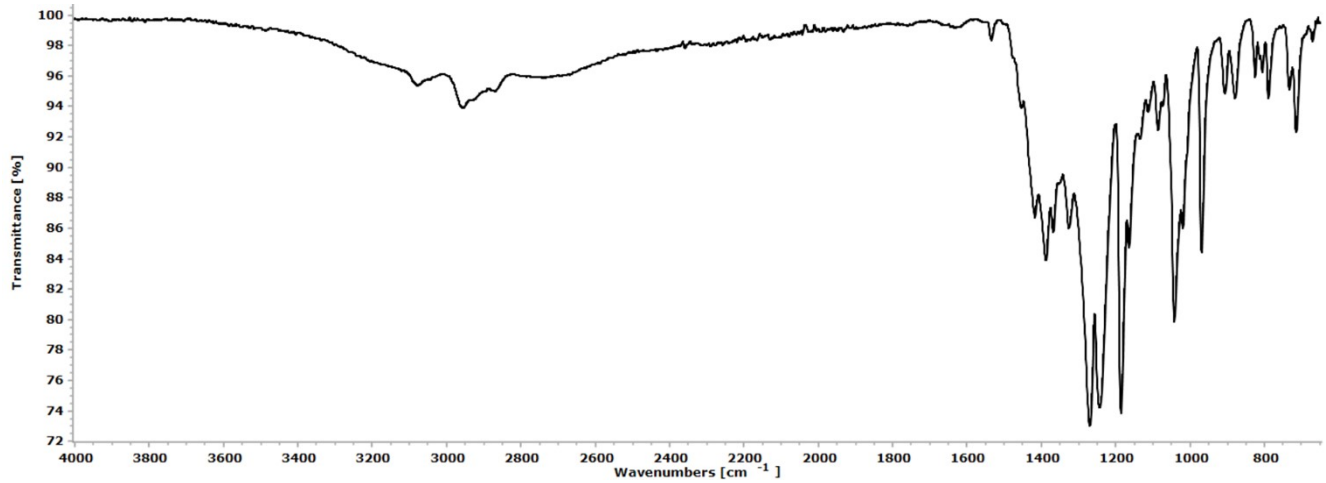

Figure S8. Solid-state IR spectrum (650-4000 cm^{-1}) of [RuCl(κ^2*N*-{CH_3C=NOH}$_2$)(η^6-C_6Me_6)]NO_3, [**4**]NO_3.

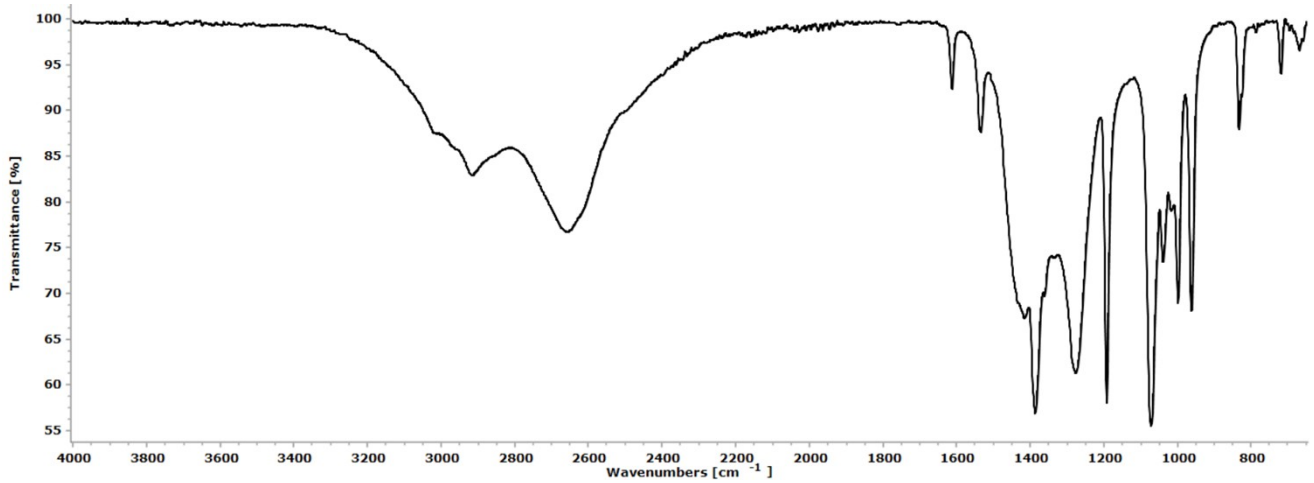

Figure S9. Solid-state IR spectrum (650-4000 cm^{-1}) of [RuCl(κ^2*N*-{CH_2CH_2C=NOH}$_2$)(η^6-C_6Me_6)]NO_3, [**5**]NO_3.

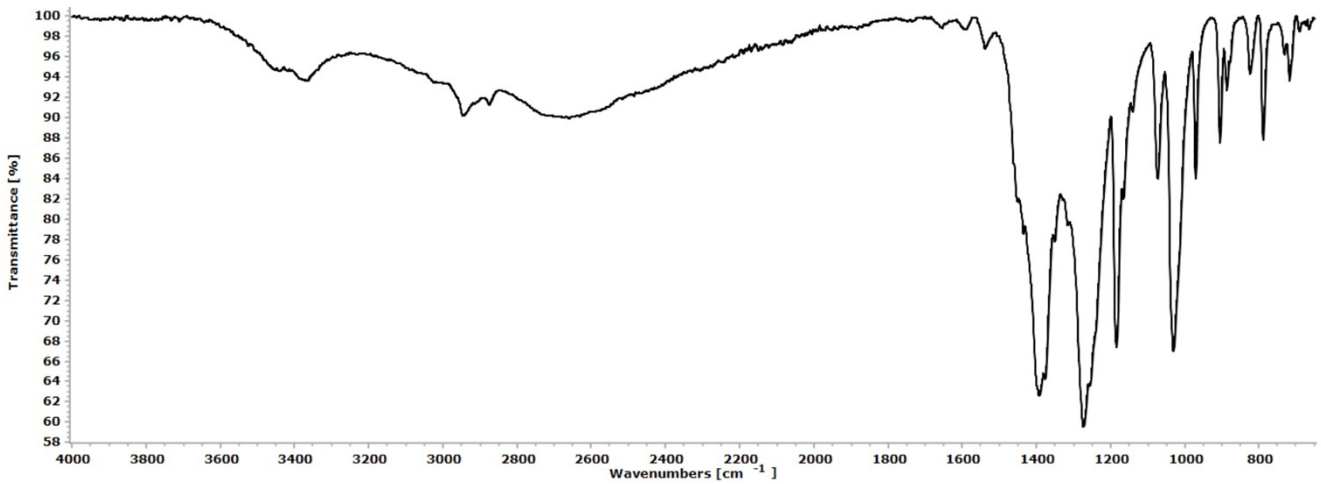

Figure S10. Solid-state IR spectrum (650-4000 cm^{-1}) of $[RuCl(\kappa^2N\text{-}\{PhC{=}NOH\}_2)(\eta^6\text{-}C_6Me_6)]NO_3$, [**6**]$NO_3$.

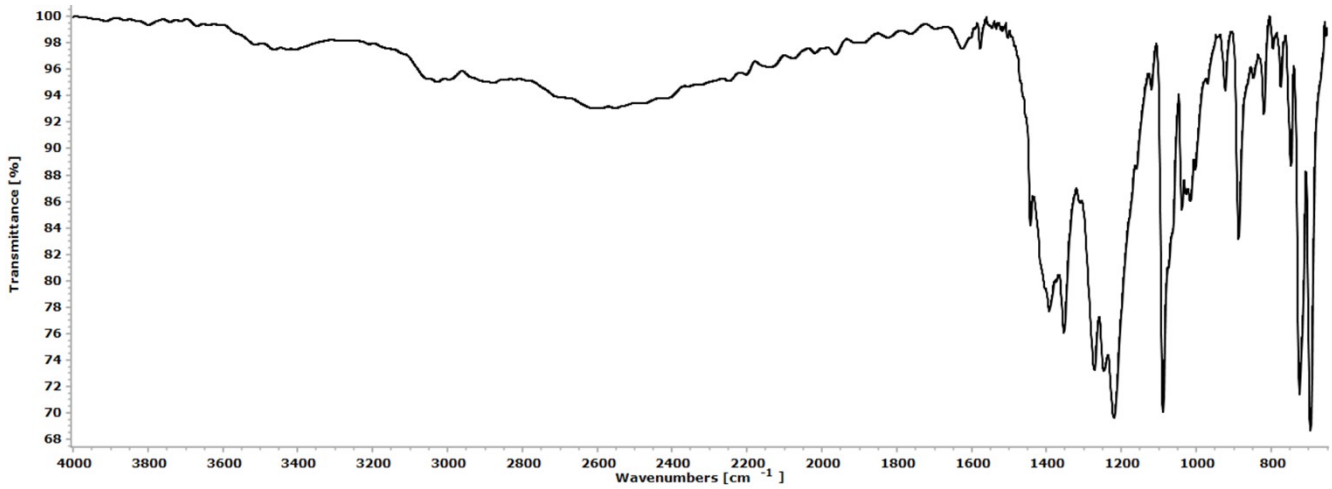

Figure S11. Solid-state IR spectrum (650-4000 cm^{-1}) of $[RuCl(\kappa^2N\text{-}\{CH_2CH_2C{=}NOH\}_2)(\eta^6\text{-}1,3,5\text{-}C_6H_3Me_3)]NO_3$, [**7**]$NO_3$.

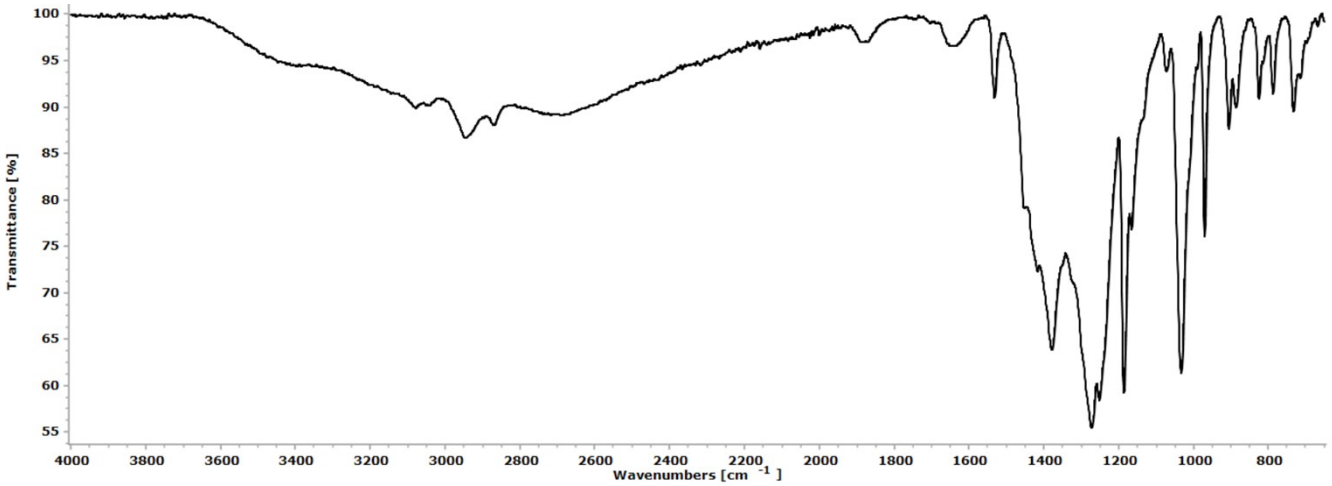

Figure S12. ^{1}H NMR spectrum (400 MHz, CD_3OD) of [RuCl(κ²*N*-{CH_3C=NOH}$_2$)(η⁶-*p*-cymene)]NO_3, [**1**]NO_3.

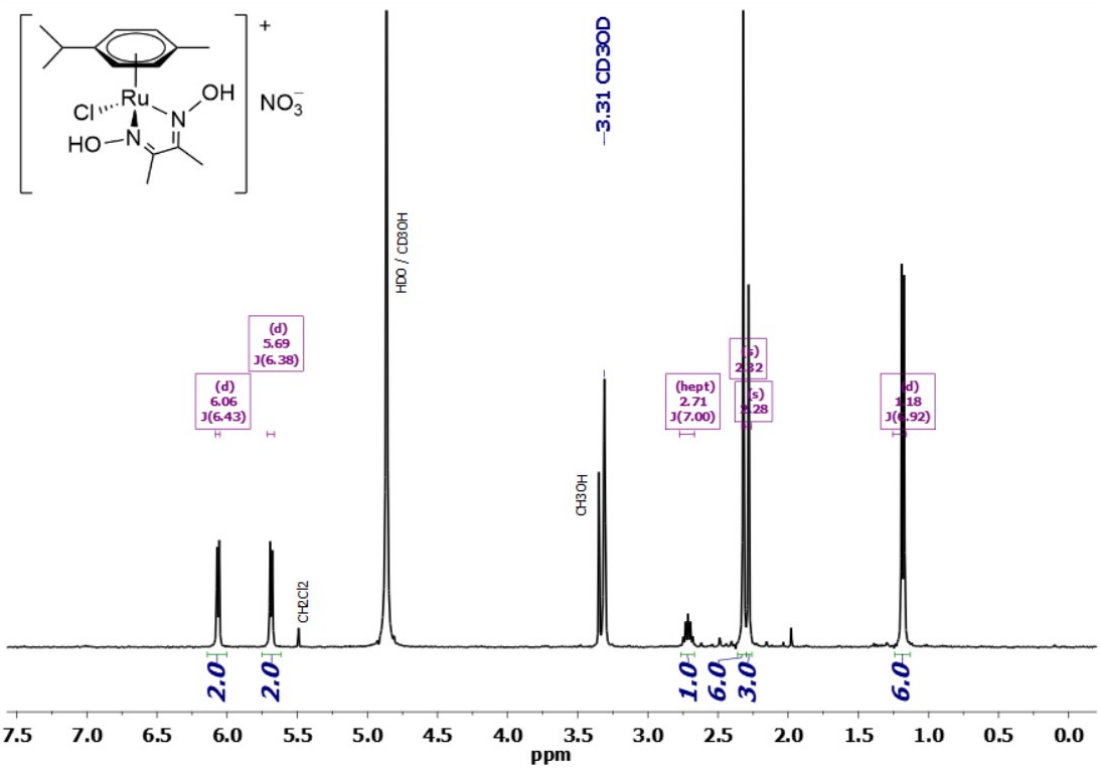

Figure S13. $^{13}C\{^{1}H\}$ NMR spectrum (100 MHz, CD_3OD) of [RuCl(κ²*N*-{CH_3C=NOH}$_2$)(η⁶-*p*-cymene)]NO_3, [**1**]NO_3.

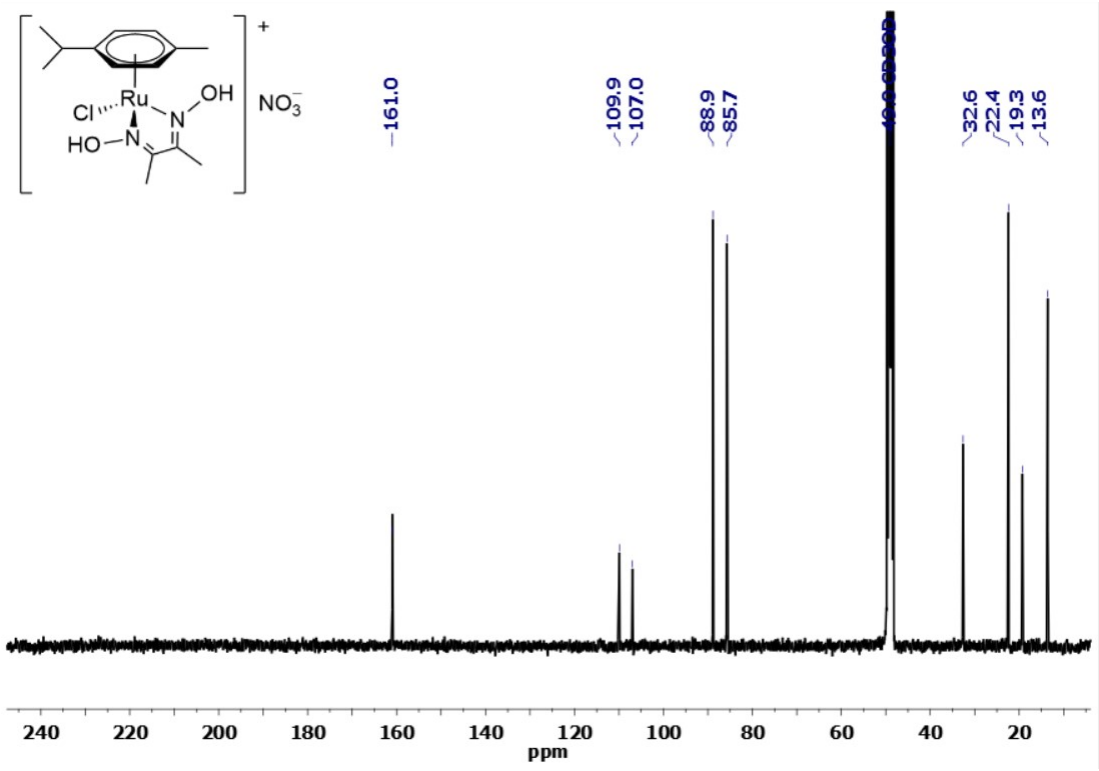

Figure S14. ^{1}H NMR spectrum (400 MHz, CD_3OD) of [RuCl(κ^2*N*-{CH_2CH_2C=NOH}$_2$)(η^6-*p*-cymene)]PF_6, [**2**]PF_6.

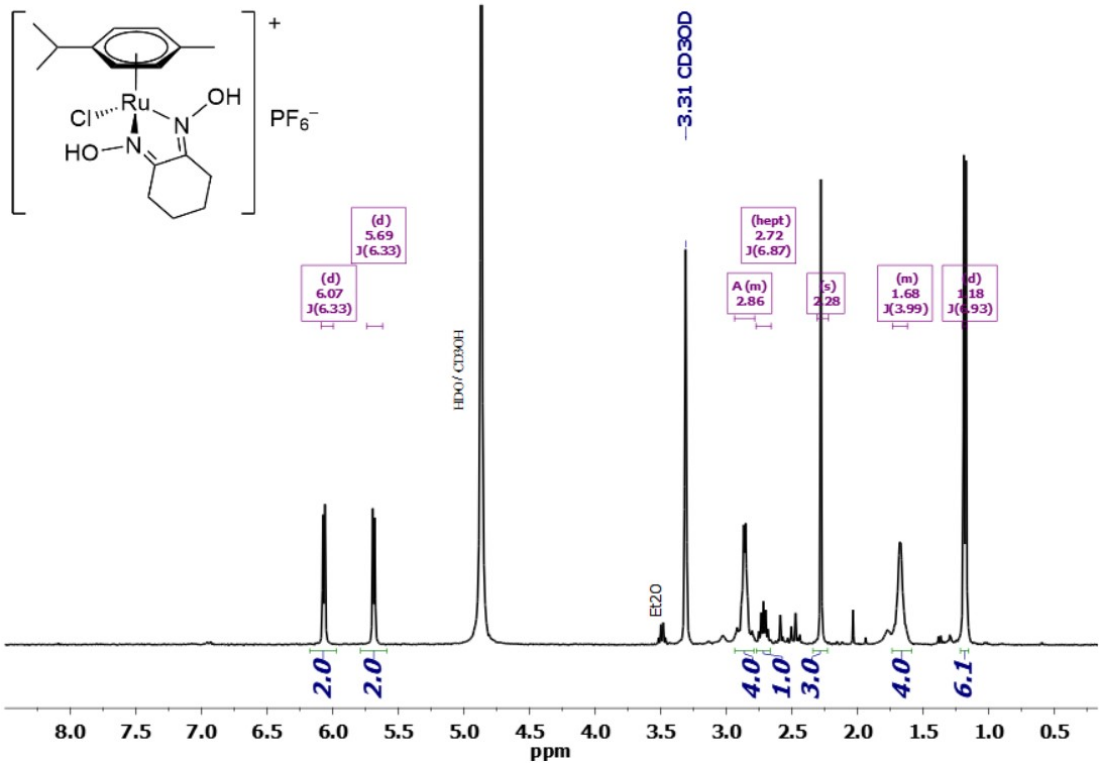

Figure S15. ^{1}H NMR spectra (400 MHz, CD_3OD) of [**2**]NO_3 (red line) and [**2**]PF_6 (blue line).

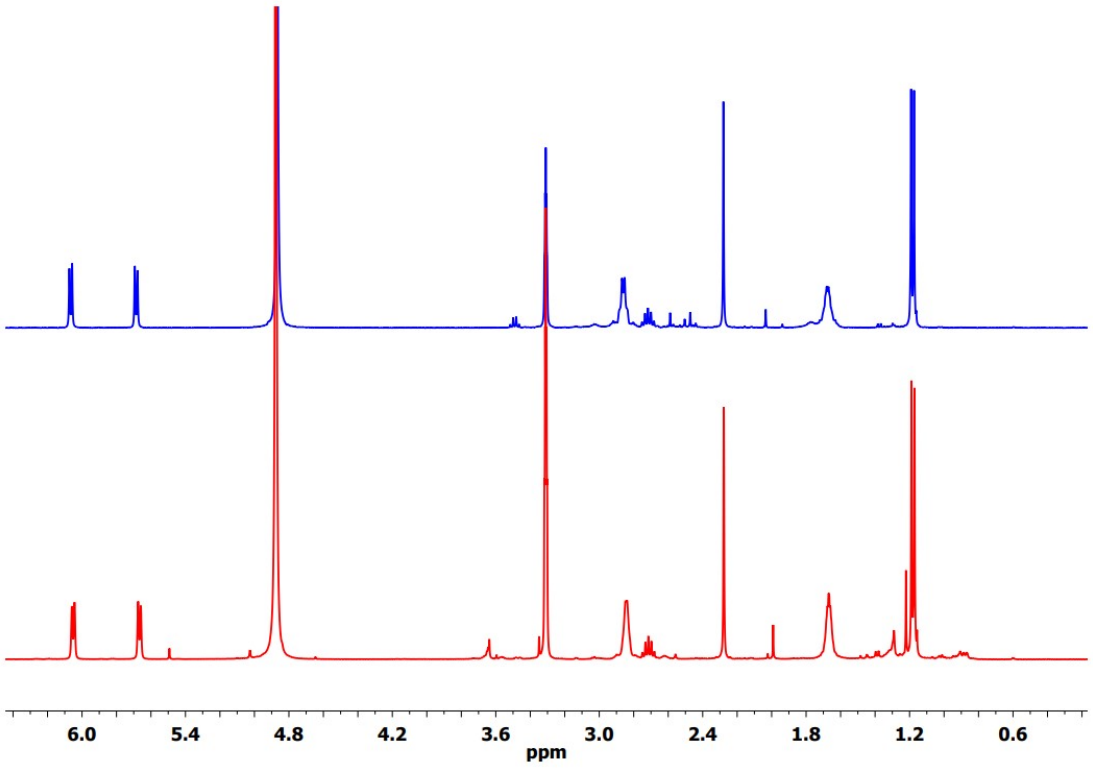

Figure S16. $^{13}C\{^{1}H\}$ NMR spectrum (100 MHz, CD_3OD) of $[RuCl(\kappa^2N\text{-}\{CH_2CH_2C{=}NOH\}_2)(\eta^6\text{-}p\text{-cymene})]PF_6$, [**2**]$PF_6$.

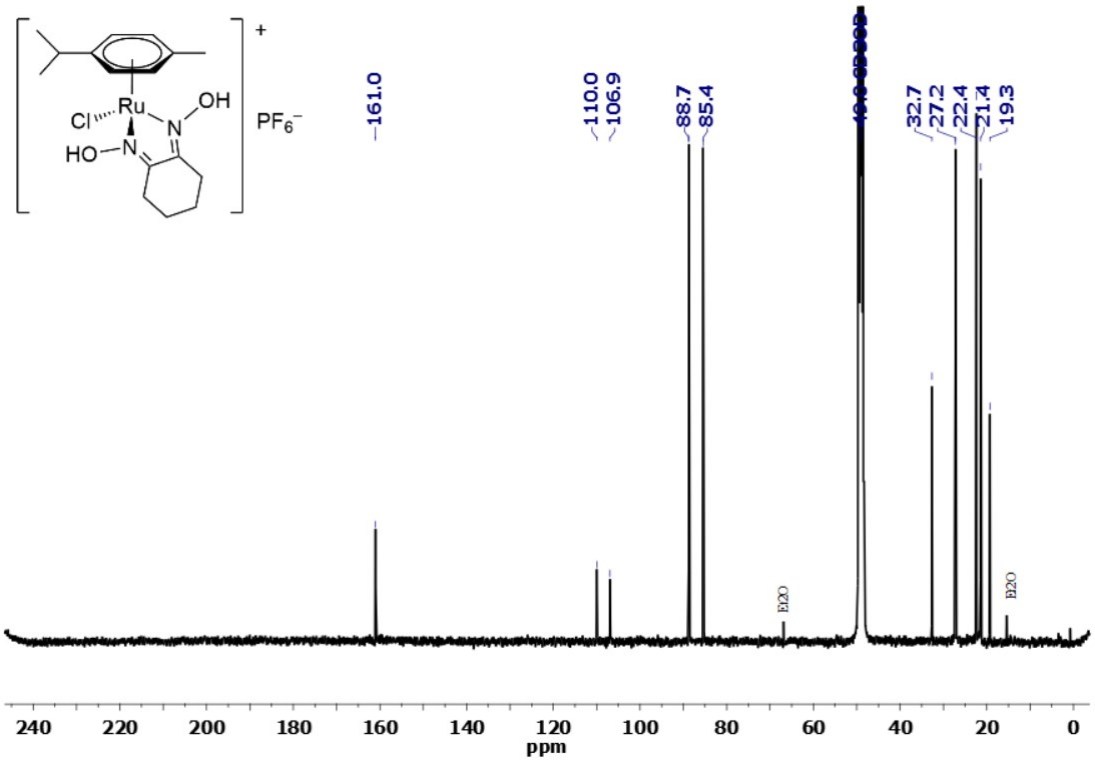

Figure S17. ^{1}H NMR spectrum (500 MHz, CD_3OD) of $[RuI(\kappa^2N\text{-}\{CH_2CH_2C{=}NOH\}_2)(\eta^6\text{-}p\text{-cymene})]NO_3$, [**3**]$NO_3$.

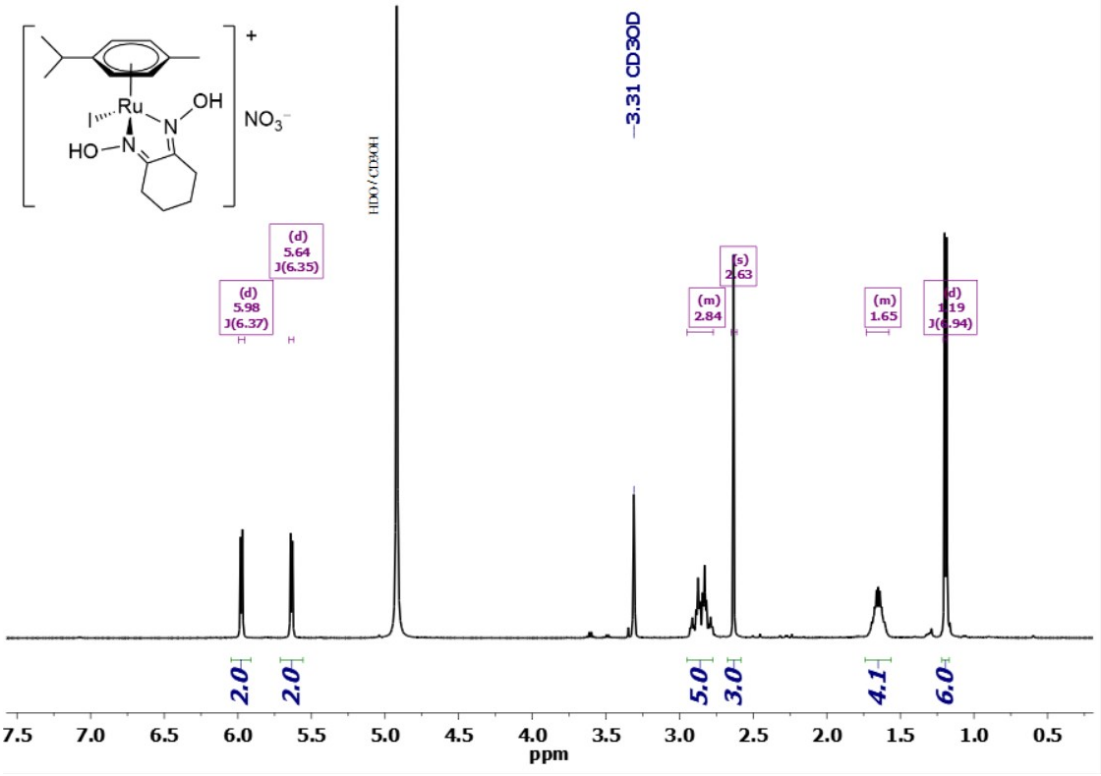

Figure S18. $^{13}C\{^{1}H\}$ NMR spectrum (126 MHz, CD_3OD) of [RuI(κ²*N*-{CH_2CH_2C=NOH}$_2$)(η⁶-*p*-cymene)]NO_3, [**3**]NO_3.

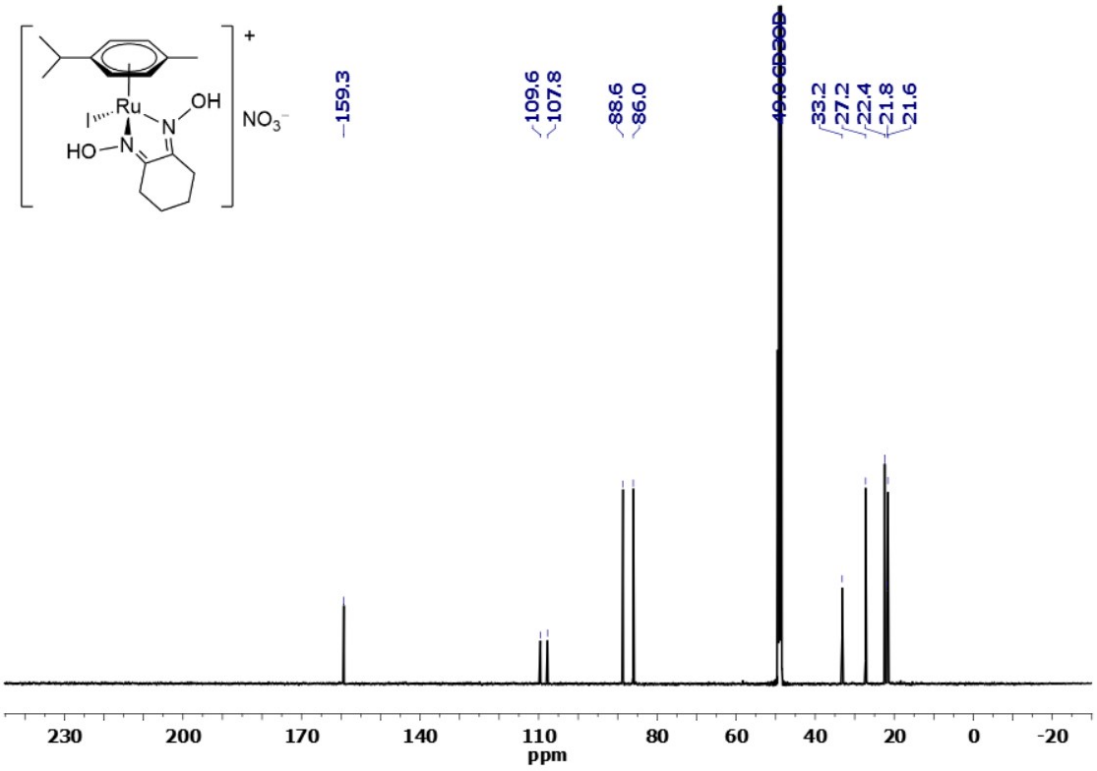

Figure S19. ^{1}H NMR spectrum (400 MHz, CD_3OD) of [RuCl(κ²*N*-{CH_3C=NOH}$_2$)(η⁶-C_6Me_6)]NO_3, [**4**]NO_3.

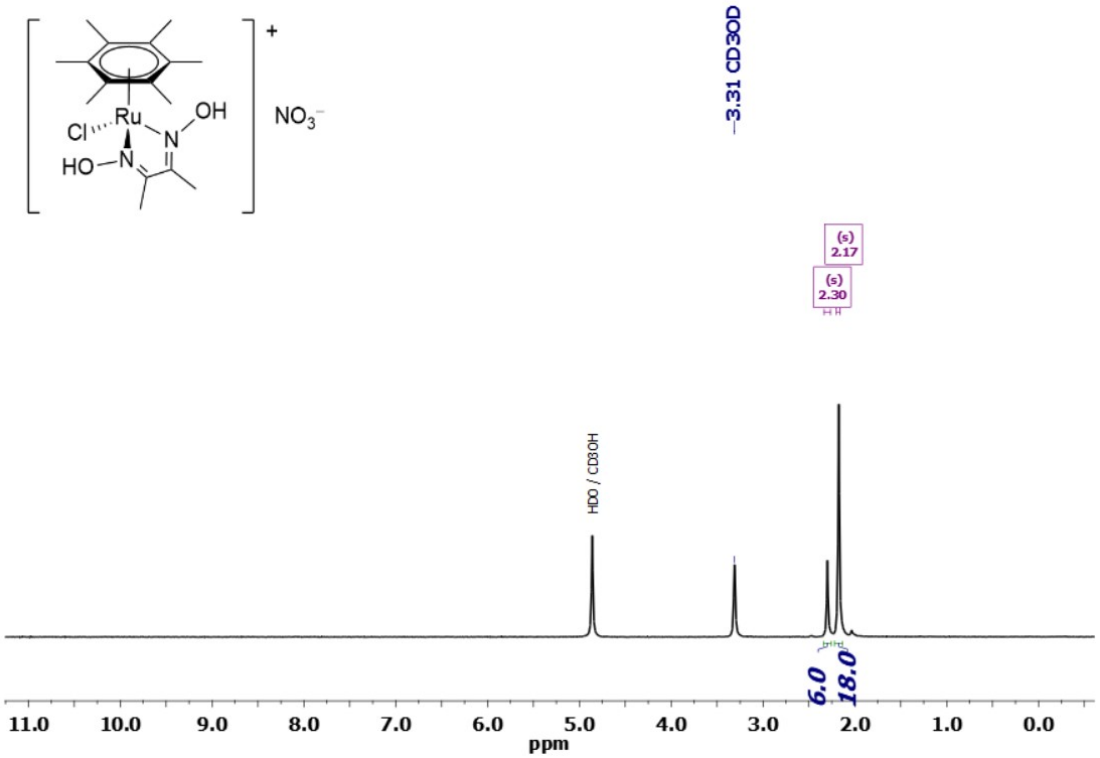

Figure S20. $^{13}C\{^{1}H\}$ NMR spectrum (100 MHz, CD_3OD) of $[RuCl(\kappa^2N\text{-}\{CH_3C{=}NOH\}_2)(\eta^6\text{-}C_6Me_6)]NO_3$, [**4**]$NO_3$.

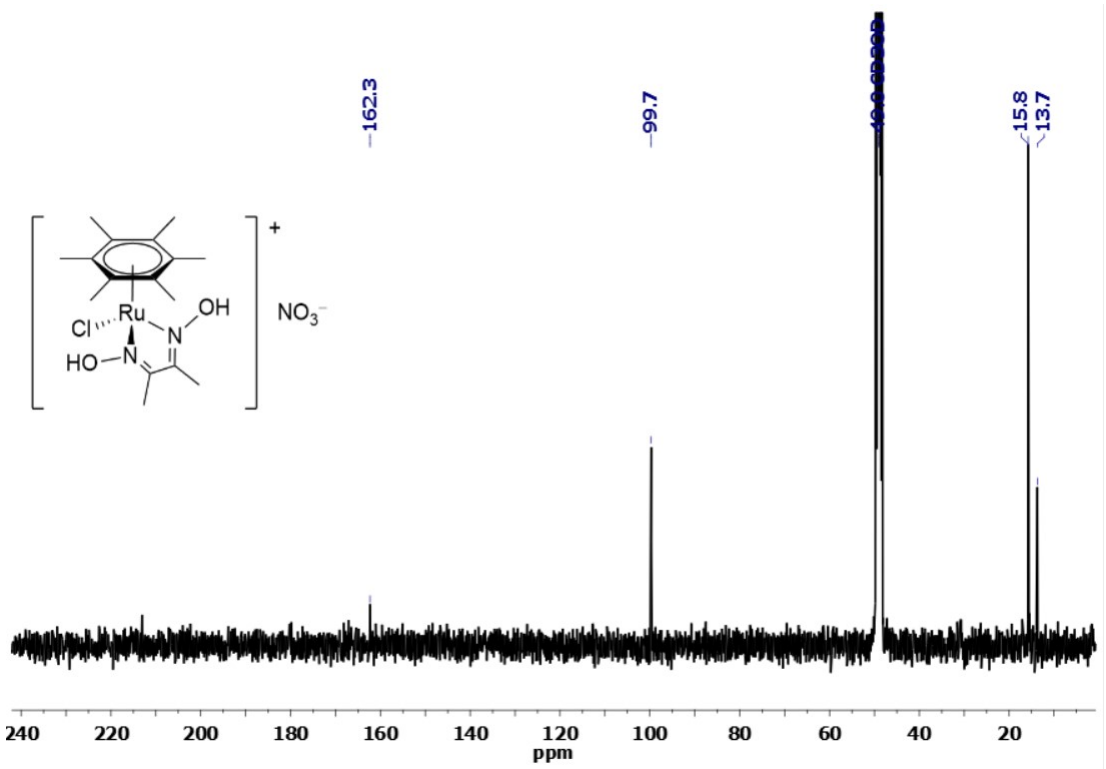

Figure S21. ^{1}H NMR spectrum (400 MHz, CD_3OD) of $[RuCl(\kappa^2N\text{-}\{CH_2CH_2C{=}NOH\}_2)(\eta^6\text{-}C_6Me_6)]NO_3$, [**5**]$NO_3$.

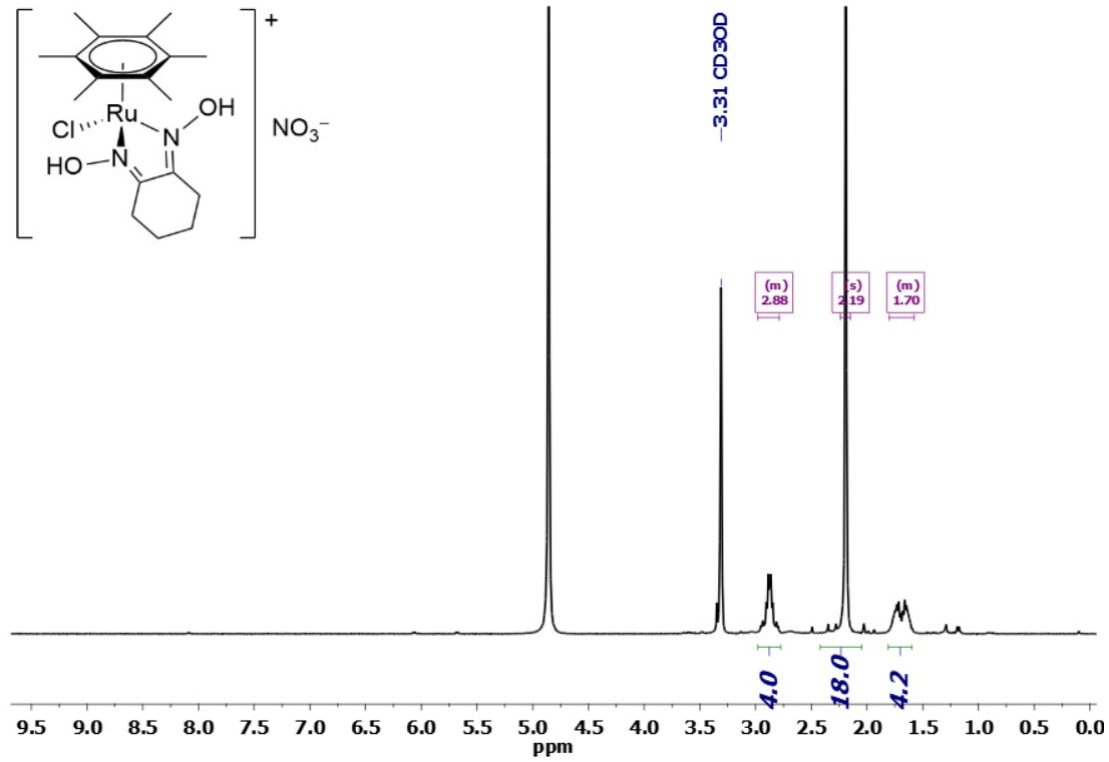

Figure S22. $^{13}C\{^{1}H\}$ NMR spectrum (100 MHz, CH_3OH/C_6D_6) of $[RuCl(\kappa^2N\text{-}\{CH_2CH_2C{=}NOH\}_2)(\eta^6\text{-}C_6Me_6)]NO_3$, [**5**]$NO_3$.

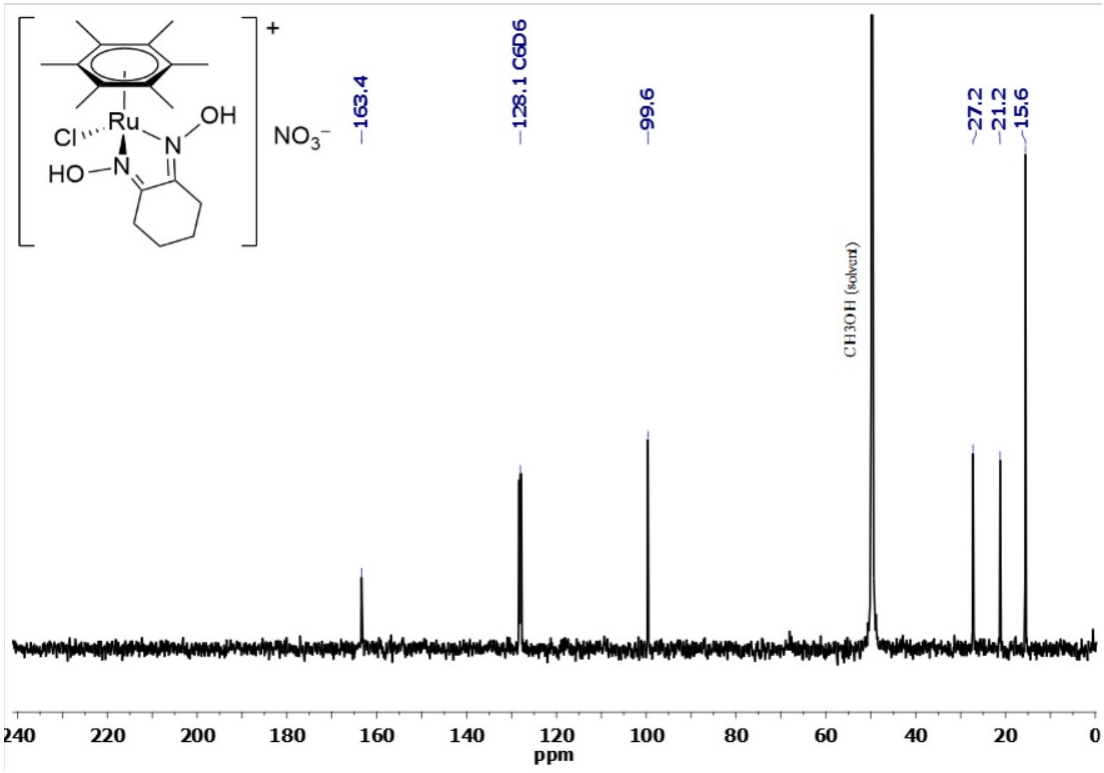

Figure S23. ^{1}H NMR spectrum (400 MHz, CD_3OD) of $[RuCl(\kappa^2N\text{-}\{PhC{=}NOH\}_2)(\eta^6\text{-}C_6Me_6)]NO_3$, [**6**]$NO_3$.

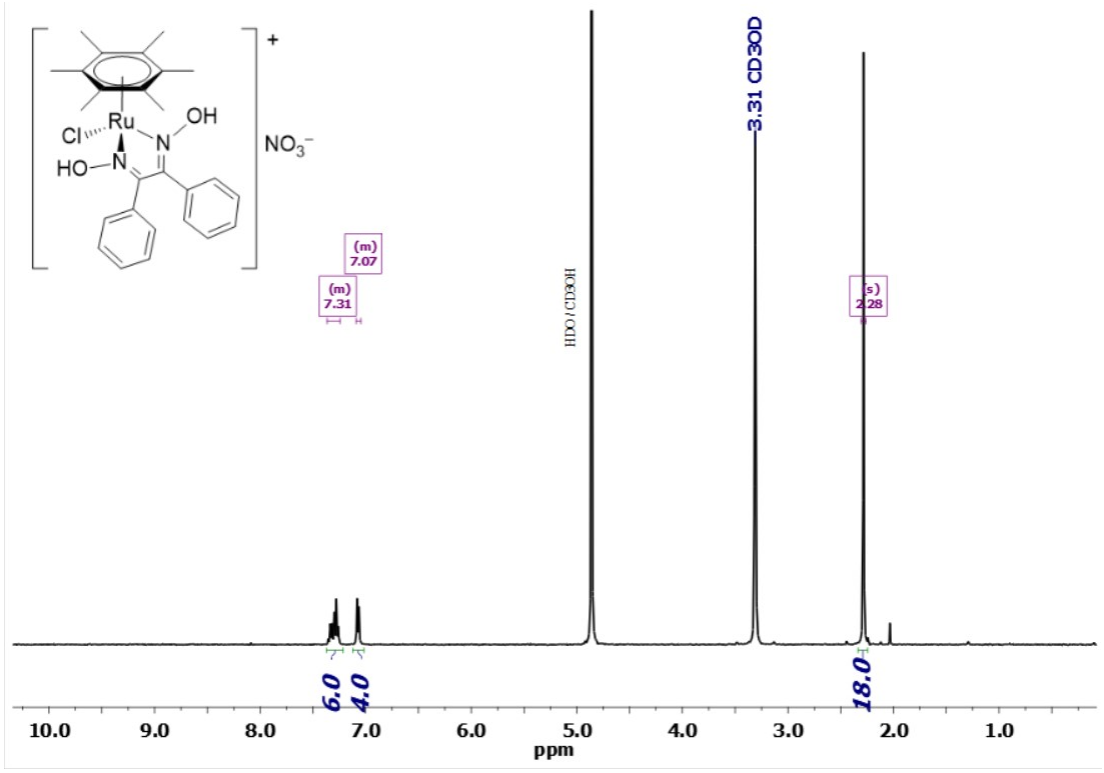

Figure S24. ^{1}H NMR spectra (400 MHz, CD_3OD) of [**6**]NO_3 (red line) and [**6**]PF_6 (blue line).

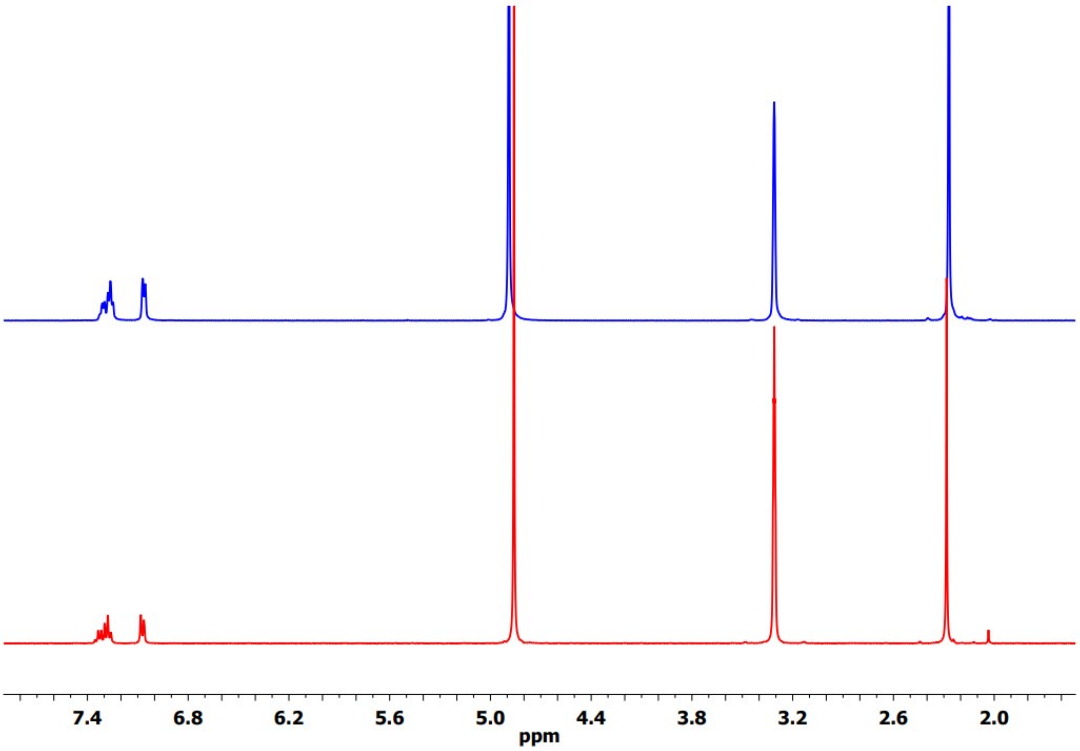

Figure S25. $^{13}C\{^{1}H\}$ NMR spectrum (100 MHz, CD_3OD) of [RuCl(κ^2*N*-{PhC=NOH}$_2$)(η^6-C_6Me_6)]NO_3, [**6**]NO_3.

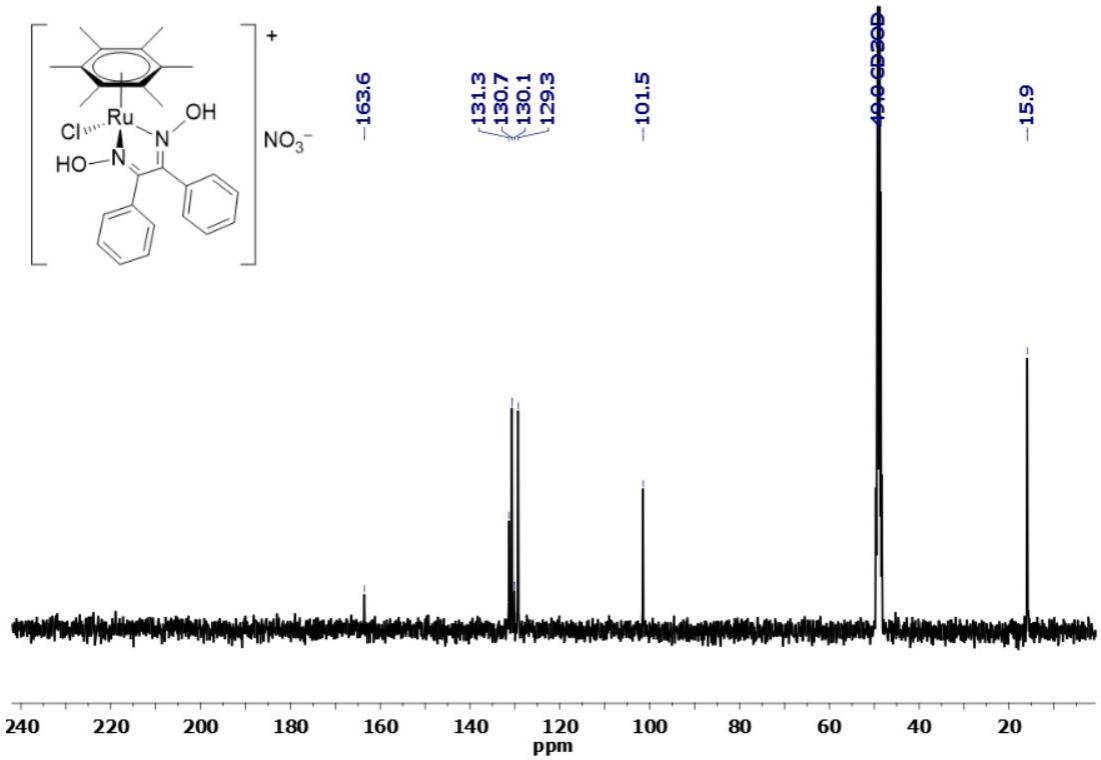

Figure S26. ^{14}N NMR spectrum (29 MHz, CD_3OD) of [RuCl(κ^2*N*-{PhC=NOH}$_2$)(η^6-C_6Me_6)]NO_3, [**6**]NO_3, (as a representative example) showing the resonance of the nitrate anion.

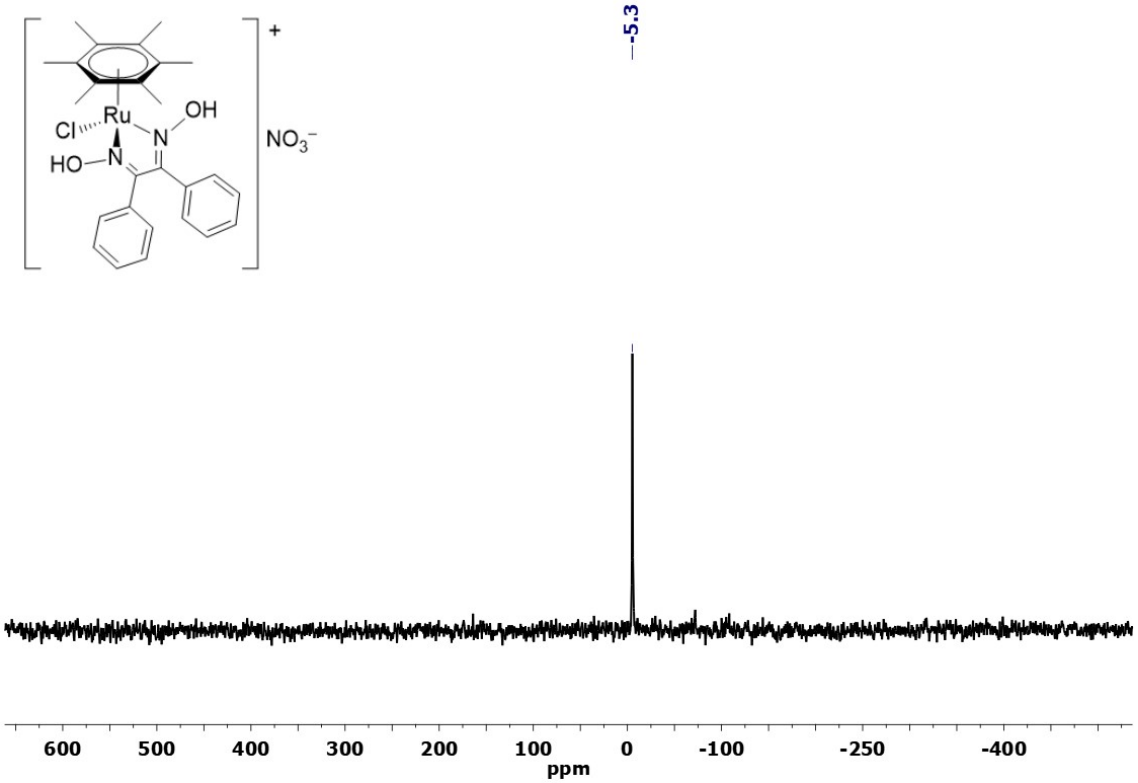

Figure S27. ^{1}H NMR spectrum (400 MHz, CD_3OD) of [RuCl(κ^2*N*-{CH_2CH_2C=NOH}$_2$)(η^6-1,3,5-$C_6H_3Me_3$)]NO_3, [**7**]NO_3.

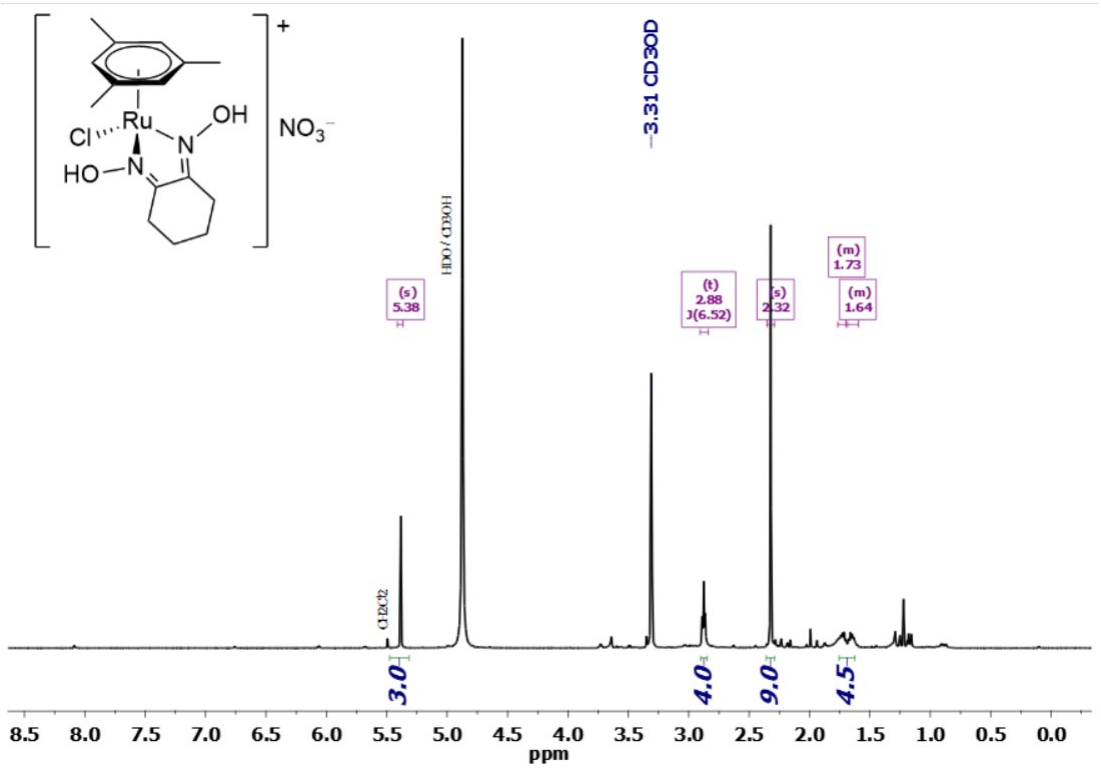

Figure S28. $^{13}C\{^{1}H\}$ NMR spectrum (100 MHz, CD_3OD) of $[RuCl(\kappa^2N\text{-}\{CH_2CH_2C{=}NOH\}_2)(\eta^6\text{-}1,3,5\text{-}C_6H_3Me_3)]NO_3$, [**7**]$NO_3$.

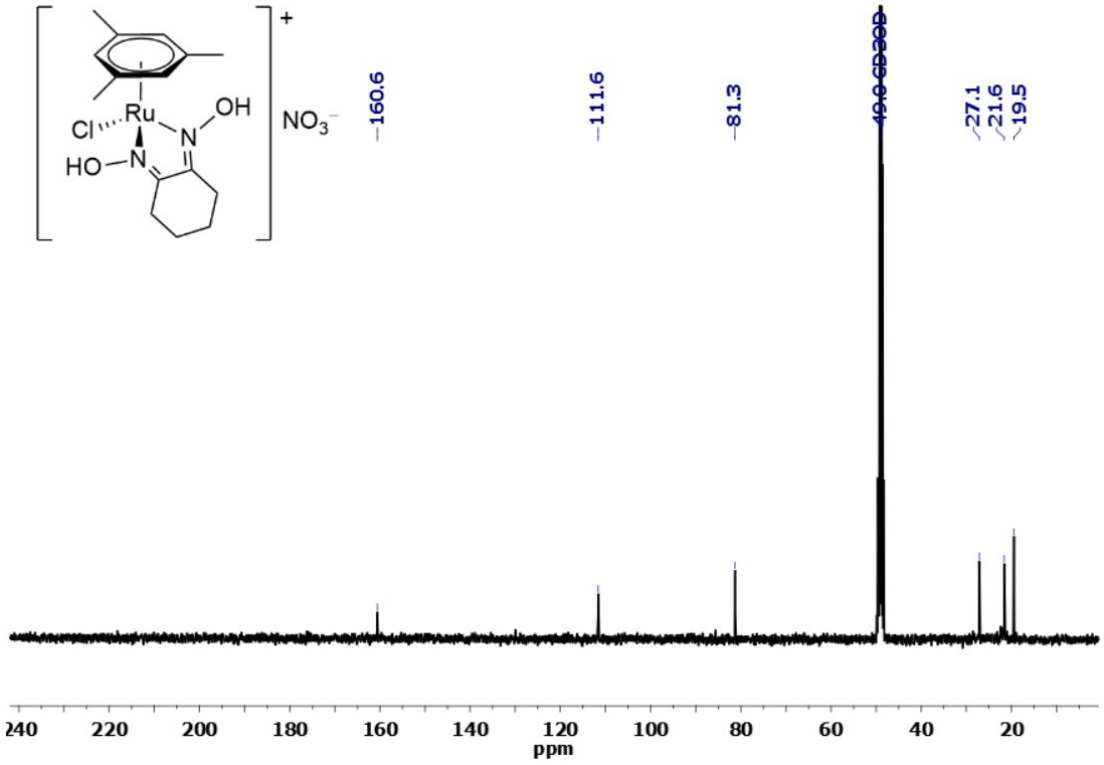

IR/NMR data of dioximes and comparison with their Ru complexes

Dimethylglyoxime. IR (solid state): ῦ/cm^{-1} = 3196m-br (OH), 3105m-sh, 3064m-sh, 2929m, 1436m, 1363s, 1143m, 978s (NO), 904s, 740m-sh, 707s. ^{1}H NMR (CD_3OD): δ/ppm = 1.98 (s, 6H, CH_3). $^{13}C\{^{1}H\}$ NMR (CD_3OD): δ/ppm = 155.3 (CN), 9.3 (CH_3).

Nioxime (1,2-cyclohexanone dioxime). IR (solid state): ῦ/cm^{-1} = 3382m (OH), 2947w, 2864w, 2823w, 1640w, 1573w, 1452w, 1414w, 1376m, 1336w, 1290m, 1256w, 1155w, 1122w, 1071w, 1003m-sh, 982m-sh, 960s (NO), 897w, 869s, 841s-sh, 812m-sh, 746m, 699m. ^{1}H NMR (CD_3OD): δ/ppm = 2.67−2.57 (m, 4H, NCH_2), 1.72−1.62 (m, 4H, CCH_2). $^{13}C\{^{1}H\}$ NMR (CD_3OD): δ/ppm = 154.5 (CN), 25.9 (NCH_2), 23.2 (CCH_2).

1,2-diphenyldioxime. IR (solid state): ῦ/cm^{-1} = 3270m (OH), 3064w, 1496w, 1444w, 1393m, 1227w, 1165w, 1072w, 1032w, 985s (NO), 922m, 869s, 752m, 706s, 691s. ^{1}H NMR (CD_3OD): δ (ppm) = 7.49-7.36 (10H, m, H Ph). $^{13}C\{^{1}H\}$ NMR (CD_3OD): δ/ppm = 156.7 (CN), 134.1 (Ph,C_{ipso}), 130.3 (Ph,C_{ortho}), 129.3 (Ph,C_{para}), 129.0 (Ph,C_{meta}).

Table S1. Comparison of selected IR and NMR data for nioxime and their Ru(η^6-arene) complexes.

Compound	Arene	monodentate ligand	^{13}C NMR (CD_3OD)		^{1}H NMR (CD_3OD)		IR (solid state):
			δ (CN) / ppm	Δ_c / ppm [a]	δ (NCH_x) / ppm	Δ_c / ppm [a]	ῦ (NO) / cm^{-1}
dimethylglyoxime	-	-	155.3		1.98		978s
[**1**]NO_3	*p*-cymene	Cl	161.0	+ 5.7	2.32	+ 0.34	1064s
[**4**]NO_3	C_6Me_6	Cl	162.3	+ 7.0	2.30	+ 0.32	1072s
4^{-H}	C_6Me_6	Cl	164.7	+ 9.4	2.10	+ 0.12	1109s (N=O) 1041s (N−O)
nioxime	-	-	154.5		2.62		960s
[**2**]PF_6	*p*-cymene	Cl	161.0	+ 6.5	2.86	+ 0.24	1039s
2^{-H}	*p*-cymene	Cl	165.8	+ 11.3	2.63	+ 0.01	1101s (N=O) 1029s (N−O)
[**3**]NO_3	*p*-cymene	I	159.8	+ 5.0	2.86	+ 0.24	1043s
3^{-H}	*p*-cymene	I	[b]		2.63	+ 0.01	1109s (N=O) 1035s (N−O)
[**5**]NO_3	C_6Me_6	Cl	163.4	+ 8.9	2.88	+ 0.26	1031s
[**7**]NO_3	$C_6H_3Me_3$	Cl	160.6	+ 6.1	2.82	+ 0.20	1033s
diphenyldioxime	-	-	156.7		-	-	985s
[**6**]NO_3	C_6Me_6	Cl	163.6	+ 6.9	-	-	1088s

[a] Coordination-induced shift: δ(complex) – δ(nioxime). [b] Not detected due to the low solubility of the compound.

Hydrogen bonding network in the crystal structures

Figure S29. Representation of the H-bond network within the solid-state structure of [**3**]NO_3. H-bonds are represented as dashed cyan lines.

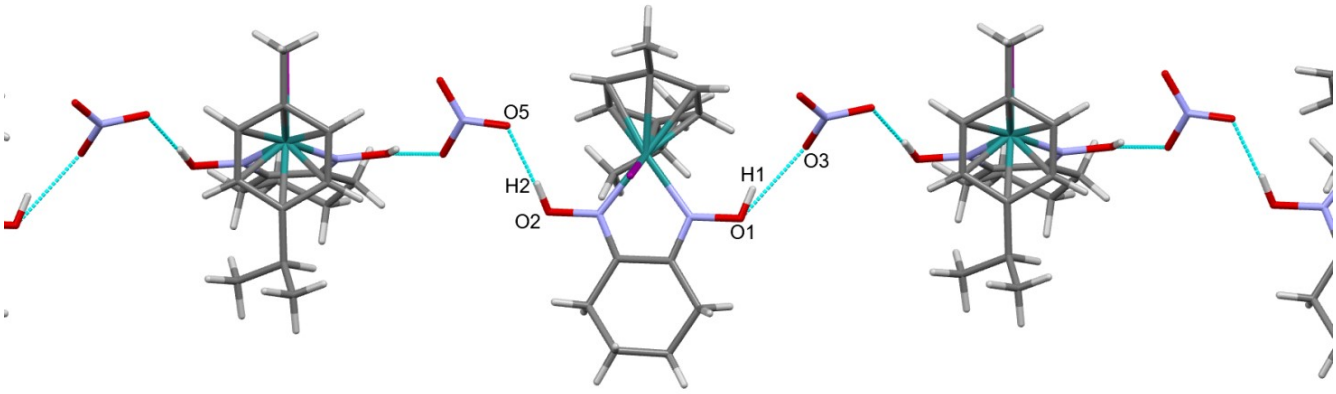

Table S2. Hydrogen bonds for [**3**]NO_3 [Å and °].

D-H···A	d(D-H)	d(H···A)	d(D···A)	<(DHA)
O(1)-H(1)···O(3)	0.84	1.86	2.623(3)	150.6
O(2)-H(2)···N(3)#1	0.84	2.62	3.375(4)	149.5
O(2)-H(2)···O(5)#1	0.84	1.84	2.675(4)	174.9

Symmetry transformations used to generate equivalent atoms: #1 x, -y+1/2, z-1/2.

Figure S30. Representation of the H-bond network within the solid-state structure of [**4**]NO_3. H-bonds are represented as dashed cyan lines.

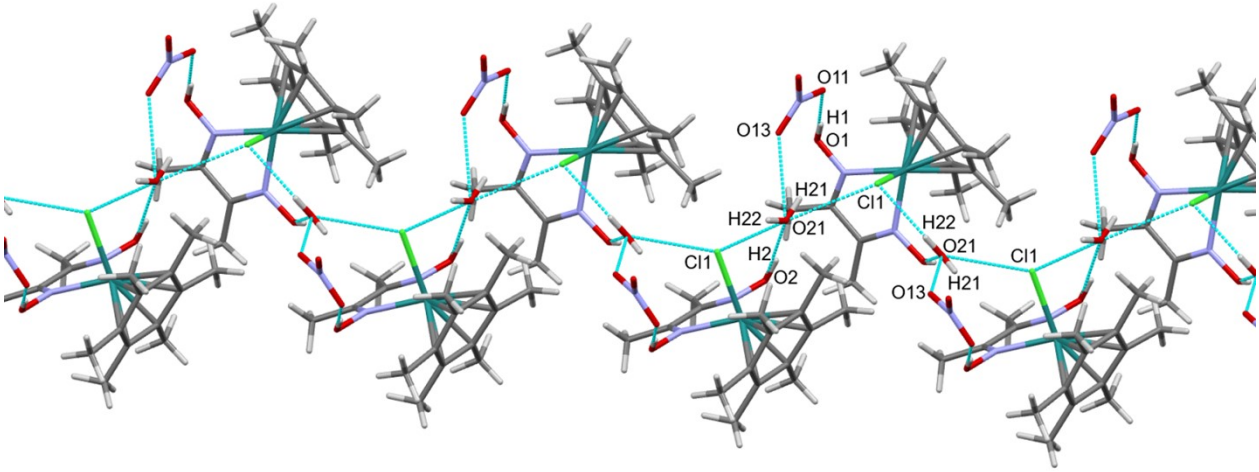

Table S3. Hydrogen bonds for [**4**]NO_3 [Å and °].

D-H···A	d(D-H)	d(H···A)	d(D···A)	<(DHA)
O(1)-H(1)···N(3)	0.84	2.54	3.304(4)	151.0
O(1)-H(1)···O(11)	0.84	1.74	2.574(3)	173.6
O(1)-H(1)···O(13)	0.84	2.65	3.201(4)	124.0
O(2)-H(2)···O(21)#1	0.84	1.72	2.545(4)	164.8
O(21)-H(21)···Cl(1)	0.84(3)	2.61(5)	3.213(3)	130(5)
O(21)-H(21)···O(13)	0.84(3)	2.28(5)	2.866(5)	127(5)
O(21)-H(22)···Cl(1)#2	0.86(3)	2.33(4)	3.111(4)	151(5)

Symmetry transformations used to generate equivalent atoms: #1 x+1/2, -y+1, z; #2 x-1/2, -y+1, z.

Figure S31. Representation of the H-bond network within the solid-state structure of **4**$^{-H}$. H-bonds are represented as dashed cyan lines.

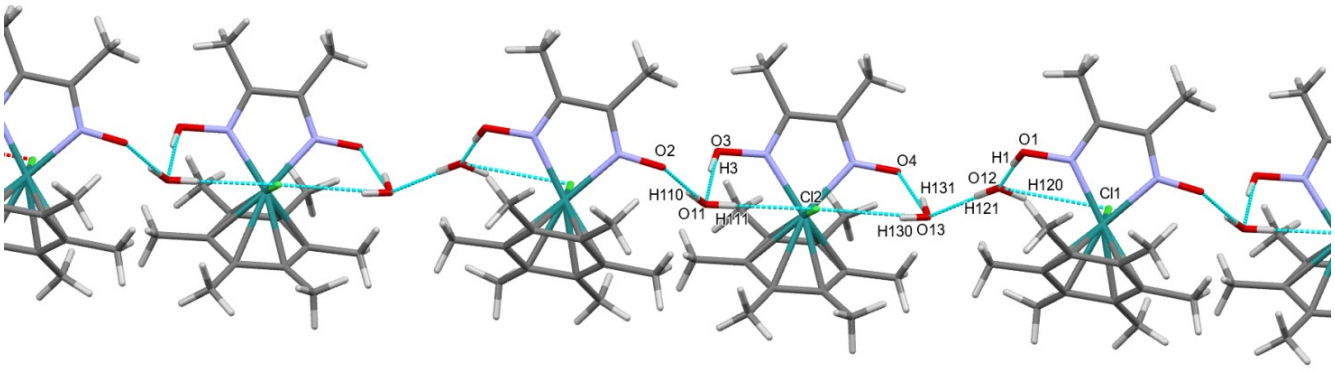

Table S4. Hydrogen bonds for **4**$^{-H}$ [Å and °].

D-H···A	d(D-H)	d(H···A)	d(D···A)	<(DHA)
O(1)-H(1)···O(12)	0.819(16)	1.795(17)	2.610(2)	173(3)
O(3)-H(3)···O(11)	0.812(16)	1.799(17)	2.601(2)	170(3)
O(11)-H(110)···N(2)	0.842(17)	2.669(18)	3.484(2)	163(2)
O(11)-H(110)···O(2)	0.842(17)	1.814(18)	2.649(2)	171(3)
O(11)-H(111)···Cl(2)	0.833(17)	2.374(19)	3.1703(17)	160(3)
O(12)-H(120)···Cl(1)	0.816(17)	2.46(2)	3.2018(18)	152(3)
O(12)-H(121)···O(13)	0.823(18)	1.864(18)	2.686(2)	177(3)
O(13)-H(130)···Cl(2)#1	0.826(17)	2.48(2)	3.2416(18)	153(3)
O(13)-H(131)···N(4)#1	0.825(17)	2.67(2)	3.364(2)	142(3)
O(13)-H(131)···O(4)#1	0.825(17)	1.922(19)	2.731(2)	166(3)

Symmetry transformations used to generate equivalent atoms: #1 x-1, y, z.

IR and NMR spectra of oxime-oximato complexes

Figure S32. Solid-state IR spectra (650-4000 cm^{-1}) of [RuCl(κ²*N*-{ONC(CH_2)$_4$CNOH})(η⁶-*p*-cymene)], **2**$^{-H}$ (black line) and [**2**]NO_3 (red line).

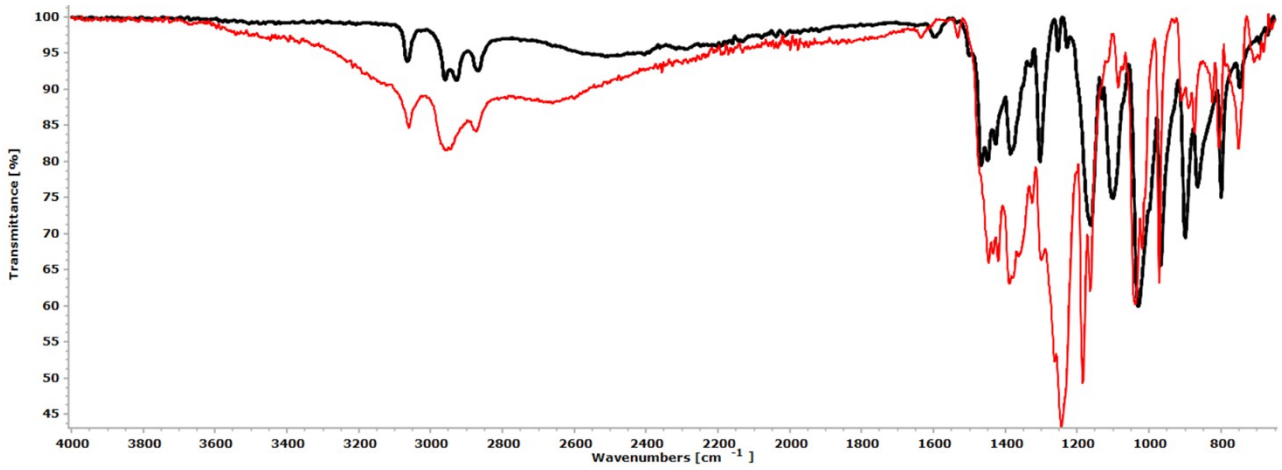

Figure S33. Solid-state IR spectra (650-4000 cm^{-1}) of [RuI(κ²*N*-{ONC(CH_2)$_4$CNOH})(η⁶-*p*-cymene)], **3**$^{-H}$ (black line) and [**3**]NO_3 (red line).

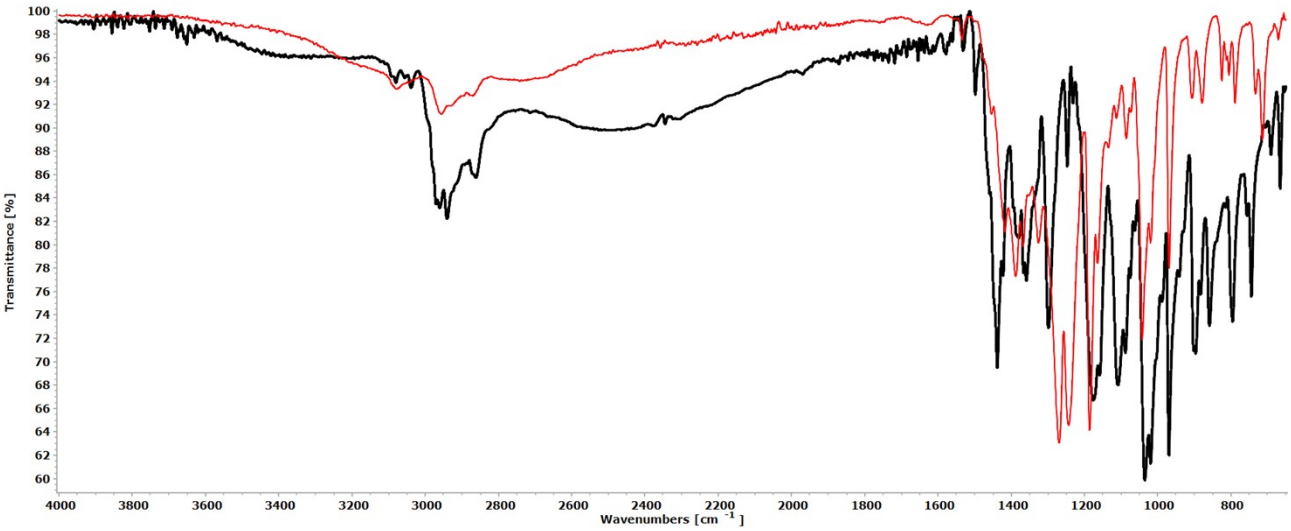

Figure S34. Solid-state IR spectra (650-4000 cm^{-1}) of [RuCl(κ²*N*-{ONC(CH_3)C(CH_3)NOH})(η⁶-C_6Me_6)], **4**$^{-H}$ (black line) and [**4**]NO_3 (red line).

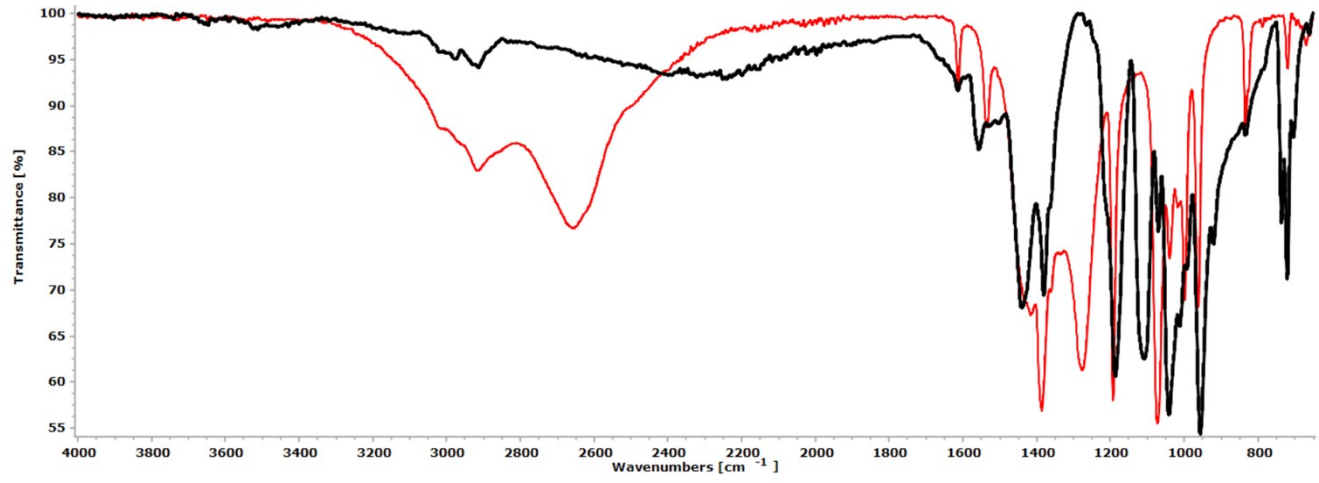

Figure S35. ^{1}H NMR spectrum (400 MHz, CD_3OD) of [RuCl(κ^2*N*-{ONC$(CH_2)_4$CNOH})(η^6-*p*-cymene)], **2^{-H}**.

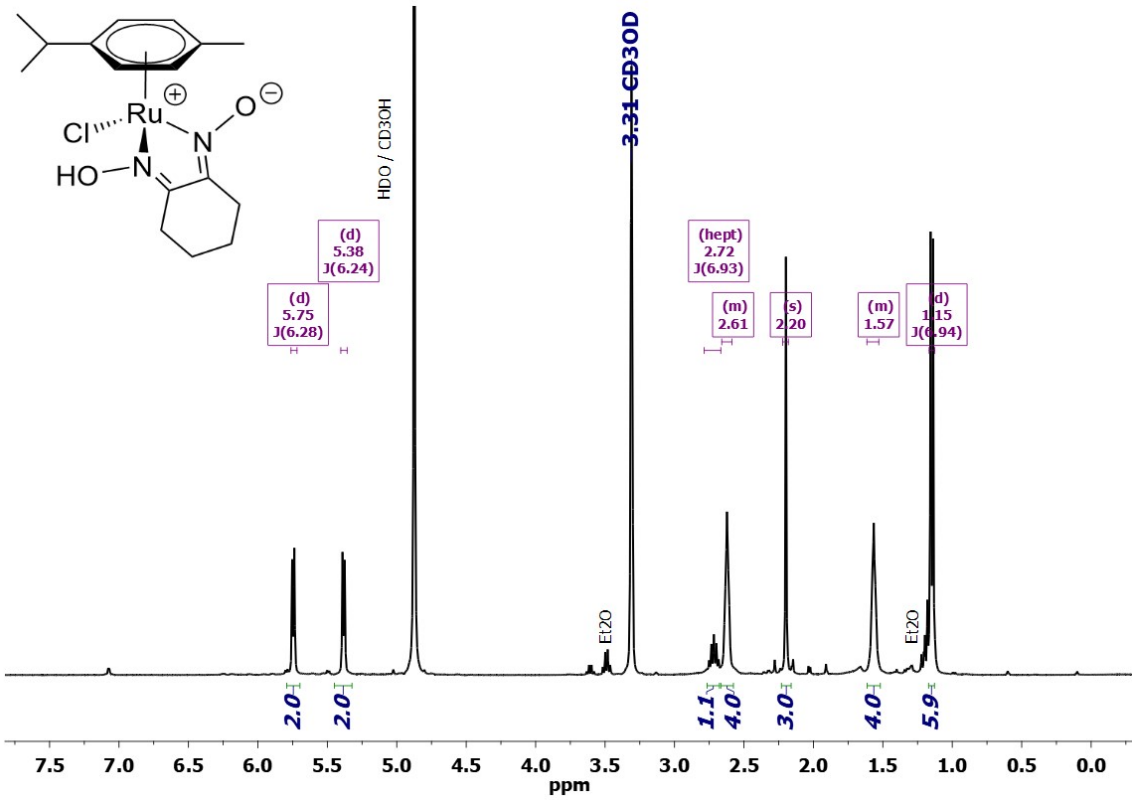

Figure S36. $^{13}C\{^{1}H\}$ NMR spectrum (125 MHz, CD_3OD) of [RuCl(κ^2*N*-{ONC$(CH_2)_4$CNOH})(η^6-*p*-cymene)], **2^{-H}**.

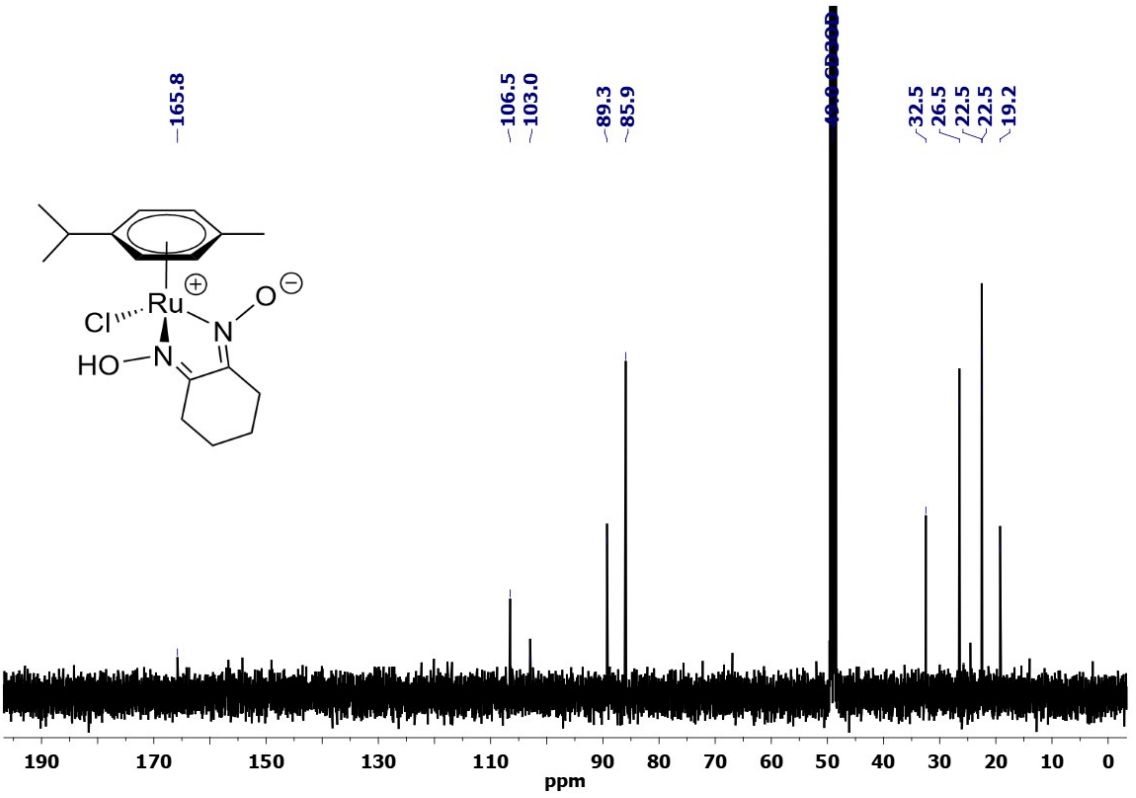

Figure S37. ^{1}H NMR spectrum (400 MHz, CD_3OD) of [RuI(κ^2*N*-{ONC$(CH_2)_4$CNOH})(η^6-*p*-cymene)], **3^{-H}**.

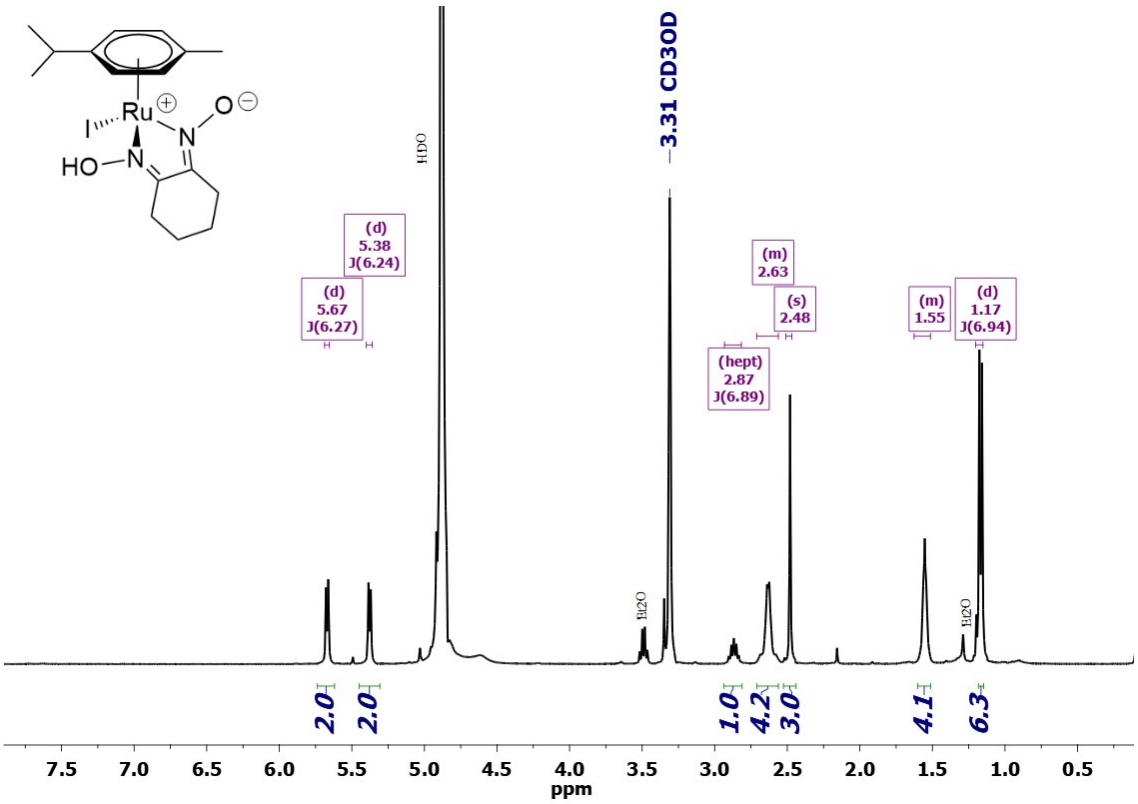

Figure S38. $^{13}C\{^{1}H\}$ NMR spectrum (100 MHz, CD_3OD) of [RuI(κ^2*N*-{ONC$(CH_2)_4$CNOH})(η^6-*p*-cymene)], **3^{-H}**.

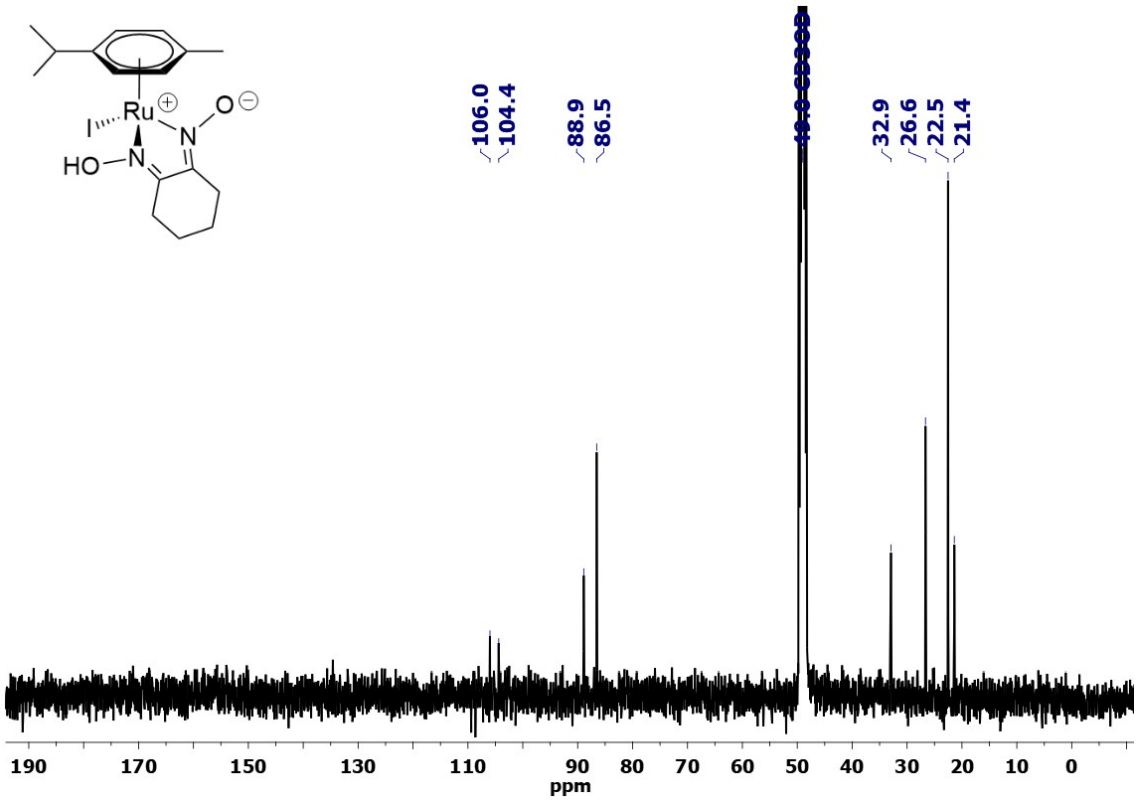

Figure S39. ^{1}H NMR spectrum (500 MHz, CD_3OD) of [RuCl(κ²*N*-{ONC(CH_3)C(CH_3)NOH})(η⁶-C_6Me_6)], **4-H**.

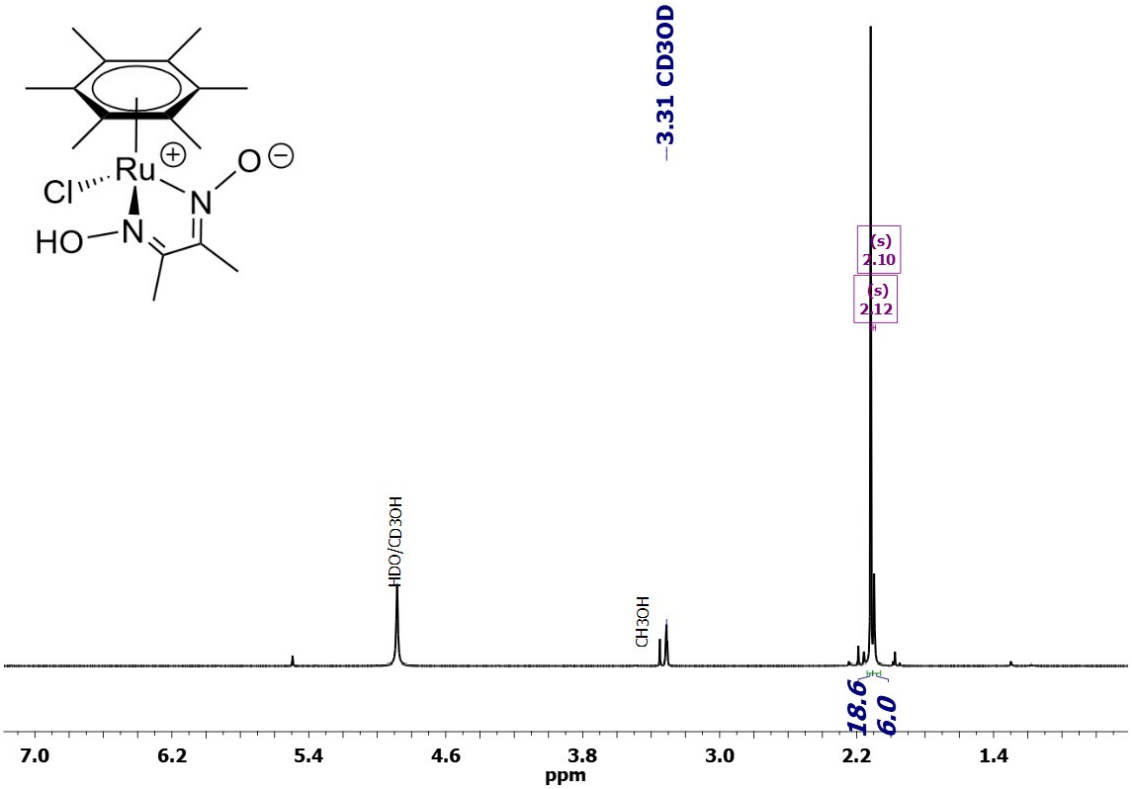

Figure S40. $^{13}C\{^{1}H\}$ NMR spectrum (125 MHz, CD_3OD) of [RuCl(κ²*N*-{ONC(CH_3)C(CH_3)NOH})(η⁶-C_6Me_6)], **4-H**.

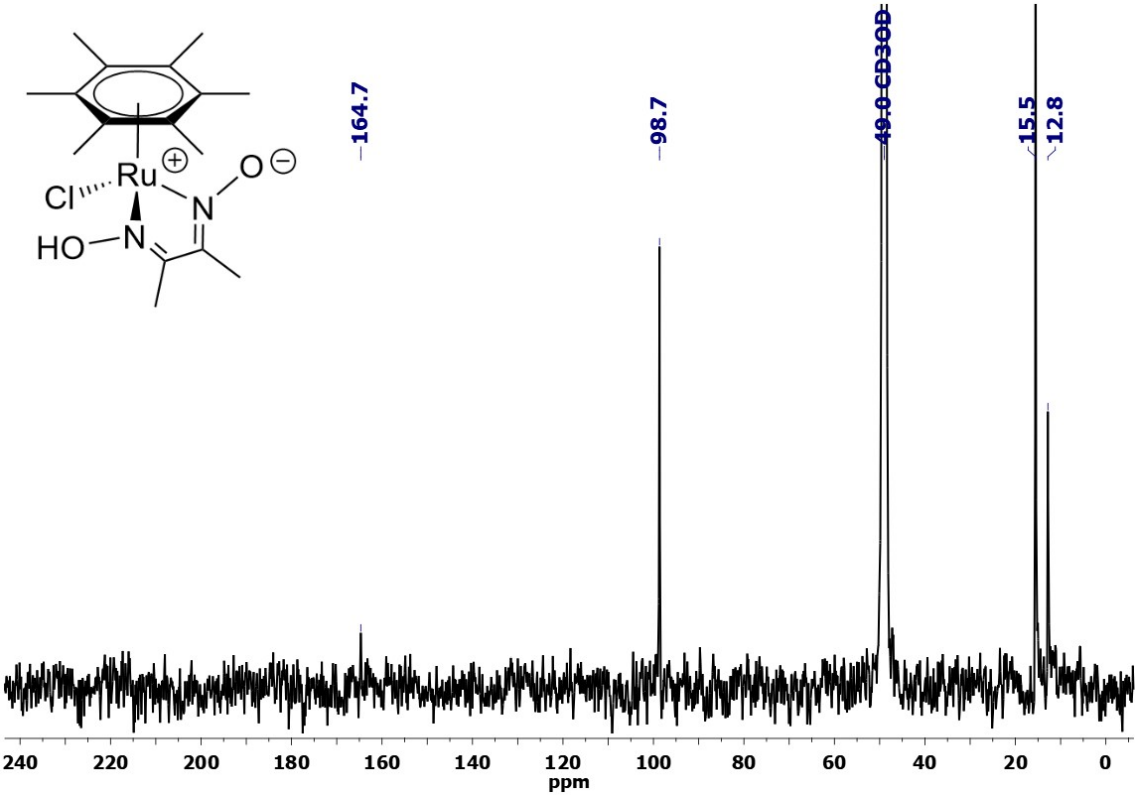

Figure S41. *Protonation shift*: comparison of ^{1}H NMR spectra (CD_3OD) for [**2**]PF_6 (top, violet line) **2**$^{-H}$ (cyan line), [**4**]NO_3 (olive green line) and **4**$^{-H}$ (bottom, red line).

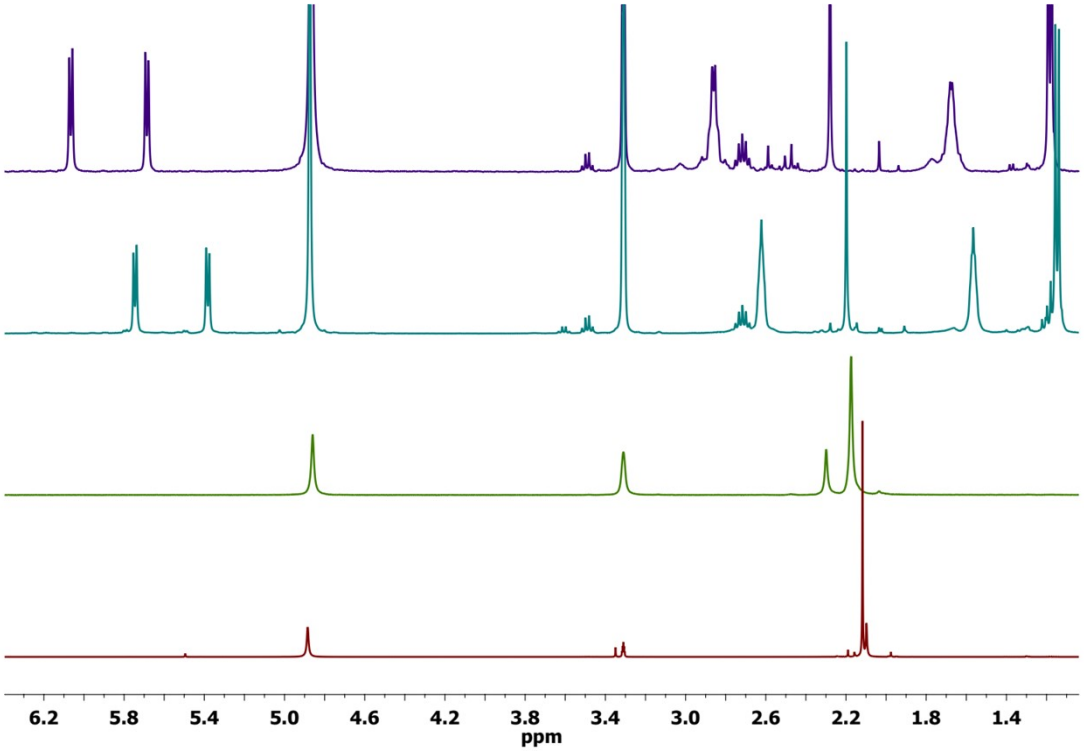

Reactivity of dioxime complexes in MeOH

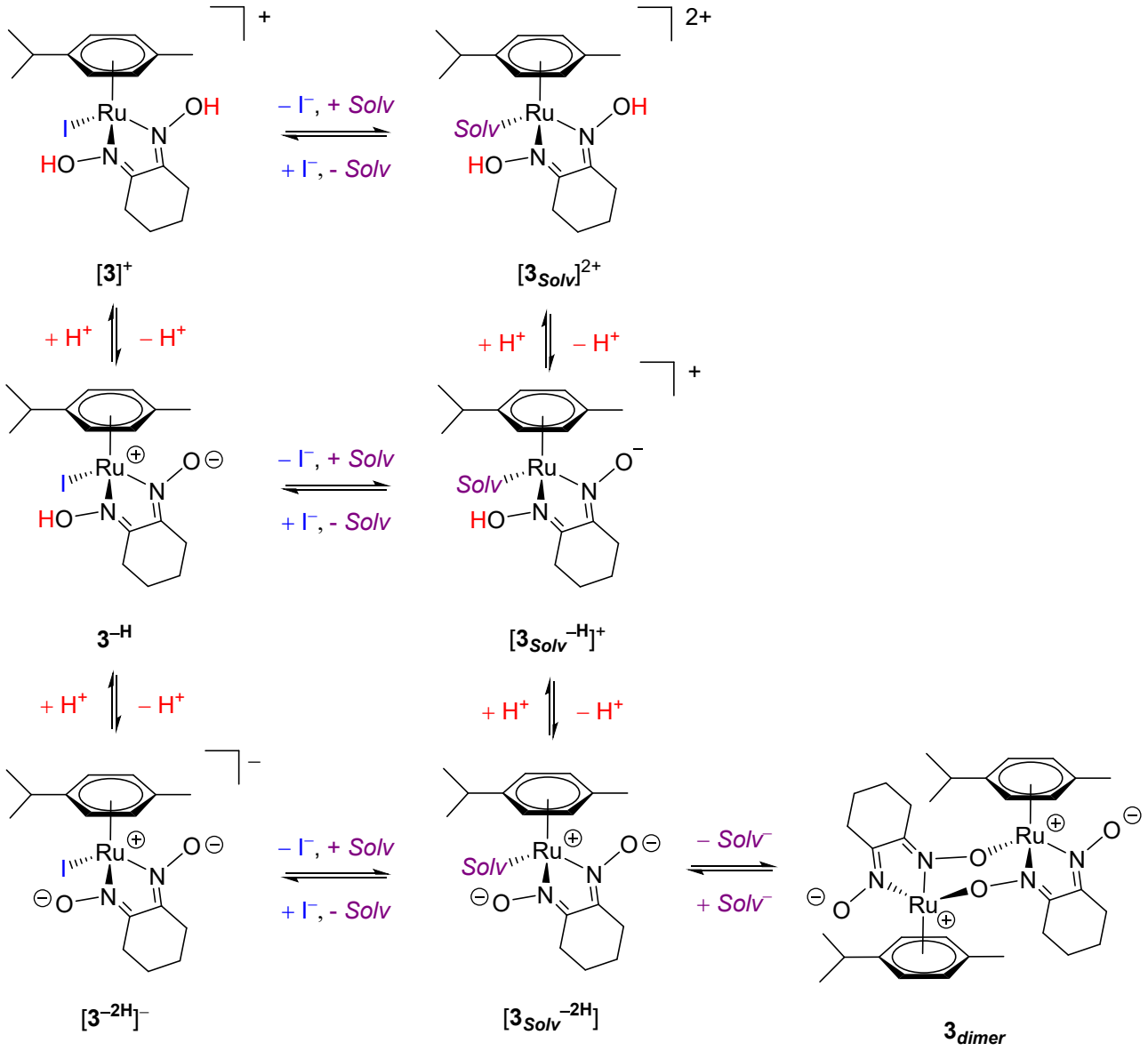

Scheme S1. Protonation, halide/solvent exchange and dimerization equilibria possibly involving ruthenium arene dioxime complexes of general formula [RuX(κ²*N*-{RC=NOH}$_2$)(η⁶-arene)]⁺ (X = halide). The reactions are represented starting from [RuI(κ²*N*-{CH_2CH_2C=NOH}$_2$)(η⁶-*p*-cymene)]⁺, [**3**]⁺, for clarity. *Solv* = MeOH or other coordinating solvent. Possible H⁺ intramolecular exchange between the dioxime and the solvent ligand in [$\mathbf{3}_{Solv}$-H]⁺ and [$\mathbf{3}_{Solv}$-2H] is not included.

Synthesis of [Ru(MeOH)(κ²*N*-{CH_2CH_2C=NOH}$_2$)(η⁶-*p*-cymene)][NO_3]$_2$, [$\mathbf{3}_{MeOH}$][NO_3]$_2$ (Chart S7)

Chart S7. Presumable structure of [$\mathbf{3}_{MeOH}$]$^{2+}$ in MeOH solution.

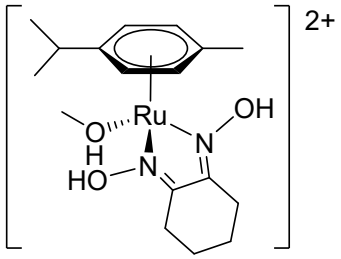

A suspension of [$RuCl_2$(η⁶-*p*-cymene)]$_2$ (50 mg, 0.082 mmol) and $AgNO_3$ (56 mg, 0.32 mmol) in MeOH was stirred at room temperature under protection from the light. After 1 h, the suspension was filtered over celite. The yellow filtrate, containing [Ru(NO_3)$_2$(η⁶-*p*-cymene)] or related solvato-species,[10] was treated with nioxime (24 mg, 0.17 mmol) and stirred at room temperature for 1 h. The resulting yellow-brown solution was taken to dryness under vacuum. The residue was dissolved in CH_2Cl_2 and filtered over celite. Volatiles were removed under vacuum, affording a brown solid. Yield: 66 mg, *ca*. 76 % (according to the proposed formula).[11] ^{1}H NMR (400 MHz, CD_3OD): δ/ppm = 6.33 (d, *J* = 6.4 Hz, 2H), 5.97 (d, *J* = 6.4 Hz, 2H), 2.97–2.78 (m, 4H), 2.65 (hept, *J* = 6.9 Hz, 1H), 2.20 (s, 3H), 1.78–1.59 (m, 4H), 1.19 (d, *J* = 6.9 Hz, 6H). Other ruthenium *p*-cymene byproducts (*ca*. 10 %) are present in the isolated material. The compound is unstable in the solid state (stored in air). After one week, it turned into a dark brown solid with complete release of *p*-cymene (^{1}H NMR).

Synthesis of [Ru(κ²*N*,κ*O*-{CH_2CH_2C=NO}$_2$)(η⁶-*p*-cymene)]$_2$, 3_{dimer} (Chart S8).

Chart S8. Structure of 3_{dimer}.

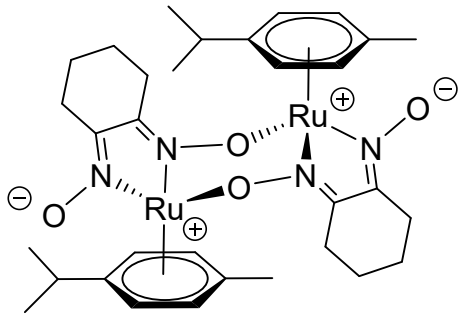

A suspension of [$RuCl_2$(η⁶-*p*-cymene)]$_2$ (50 mg, 0.087 mmol) and $AgNO_3$ (59 mg, 0.35 mmol) in MeOH was stirred at room temperature under protection from the light. After 1 h, the suspension was filtered over celite. The yellow filtrate was taken to dryness under vacuum and re-dissolved in anhydrous MeOH (6 mL) under N_2. The solution was treated with nioxime (26 mg, 0.18 mmol), stirred at room temperature for 30' (orange-brown solution) then treated with ^{t}BuOK (1 M in THF; 0.35 mL, 0.35 mmol). The resulting brown solution was stirred at room temperature for 30' then taken to dryness under vacuum. The residue was dissolved in acetone and filtered over celite. Volatiles were removed under vacuum and the residue was triturated in Et_2O/hexane 1:1 *v*/*v*. The suspension was filtered and the resulting orange-brown solid was washed with hexane and dried under vacuum (40 °C). Yield: 31 mg, 47 % (according to the proposed formula). ^{1}H NMR (400 MHz, CD_3OD): δ/ppm = 5.96 (d, *J* = 6.1 Hz, 2H), 5.62 (d, *J* = 5.9 Hz, 2H), 5.54 (d, *J* = 5.9 Hz, 2H), 5.30 (d, *J* = 6.1 Hz, 2H), 2.69–2.61 (m, 2H), 2.55 (hept, *J* = 6.9 Hz, 2H), 2.45 (dt, *J* = 18.9, 5.5 Hz, 2H), 2.32 (s, 6H), 2.29–2.22 (m, 2H), 2.00 (dt, *J* = 11.0, 5.3 Hz, 2H), 1.61–1.55 (m, 2H), 1.50–1.36 (m, 6H), 1.17 (d, *J* = 6.9 Hz, 6H), 1.04 (d, *J* = 6.9 Hz, 6H). Other ruthenium *p*-cymene byproducts (*ca*. 10 %) are present in the isolated material. The CD_3OD solution was maintained at room temperature, showing progressive release of *p*-cymene (4 h: 10 %; 18 h: 35 %).

Reactivity experiments with Bronsted bases / silver salts.

[**2**]PF_6 + Et_3N or $NaHCO_3$ (1 eq) at room temperature: quantitative and selective formation of $\mathbf{2^{-H}}$.

[**2**]PF_6 + Et_3N (3 eq) at reflux: formation of $\mathbf{2^{-H}}$, minor Ru byproducts and *p*-cymene (5 % mol).

[**2**]PF_6 + $NaHCO_3$ (4.5 eq) at reflux: formation of K[$\mathbf{2^{-2H}}$], minor Ru byproducts and *p*-cymene (36 % mol).

[**2**]PF_6 + K_2CO_3 (1.3 eq): quantitative and selective formation of K[$\mathbf{2^{-2H}}$]. After 24 h: release of *p*-cymene (18 % mol).

[**2**]PF_6 + $AgNO_3$ (1.0 eq): quantitative conversion, formation of > 3 unidentified Ru(*p*-cymene) complexes and *p*-cymene (23 % mol).

[**3**]NO_3 + $PhNH_2$ (1 eq): probable equilibrium mixture of [**3**]NO_3, [$PhNH_3$]NO_3 and $\mathbf{3^{-H}}$ (one set of signals, intermediate between [**3**]$^+$ and $\mathbf{3^{-H}}$).

[**3**]NO_3 + ^{t}BuOK or $NaHCO_3$ (1 eq): quantitative and selective formation of $\mathbf{3^{-H}}$. After 14 h: identical, aside from a light brown patina and free *p*-cymene (3 % mol).

[**3**]NO_3 + ^{t}BuOK (2 eq) or K_2CO_3 (1.4 eq). Quantitative and selective formation of [$\mathbf{3^{-2H}}$]$^-$. After 14 h: identical, aside from a light brown patina and free *p*-cymene (2 % mol).

[**3**]NO_3 + $AgNO_3$. Quantitative conversion, formation of [$\mathbf{3}_{MeOH}$]$^{2+}$, another unidentified Ru(*p*-cymene) complex (*ca*. 1:1 ratio) and *p*-cymene (9 % mol). After 14 h: brown solid, quantitative release of *p*-cymene.

[$\mathbf{3^{-H}}$] + $AgNO_3$. Quantitative conversion, formation of unidentified Ru(*p*-cymene) complexes (> 5) and *p*-cymene (30 % mol).

K[$\mathbf{3^{-2H}}$] + $AgNO_3$. Quantitative conversion, formation of unidentified Ru(*p*-cymene) complexes, a minor amount of $\mathbf{3}_{dimer}$ and *p*-cymene (6 % mol). After 14 h: brown solid and free *p*-cymene (27 % mol).

[$\mathbf{3_{MeOH}}$][NO_3]$_2$ + ^{t}BuOK (1 eq). Quantitative conversion, probable formation of [$\mathbf{3_{MeOH}^{-H}}$]$^+$ as major product along with other unidentified Ru(*p*-cymene) complexes (30 %) and *p*-cymene (6 % mol).

[$\mathbf{3_{MeOH}}$][NO_3]$_2$ + ^{t}BuOK (2 eq). Described above (formation of $\mathbf{3}_{dimer}$).

[**4**]NO_3 + $NaHCO_3$ (1.2 eq): formation of $\mathbf{4^{-H}}$.

[**4**]NO_3 + K_2CO_3 (1.3 eq): formation of a mixture of $[\mathbf{4^{-2H}}]^-$ and $[\mathbf{4_{MeOH}^{-2H}}]$ (1:2.6 ratio; assignment based on the characterization in aqueous solution).

NMR data (CD_3OD).

K[$\mathbf{2^{-2H}}$]. ^{1}H NMR: δ/ppm = 5.65 (d, *J* = 6.2 Hz, 2H), 5.26 (d, *J* = 6.2 Hz, 2H), 2.74 (hept, *J* = 6.9 Hz, 1H), 2.62–2.52 (m, 4H), 2.17 (s, 3H), 1.57–1.47 (m, 4H), 1.12 (d, *J* = 6.9 Hz, 6H).

$\mathbf{3^{-H}}$. ^{1}H NMR: δ/ppm = 5.67 (d, *J* = 6.2 Hz, 2H), 5.37 (d, *J* = 6.2 Hz, 2H), 2.87 (hept, *J* = 6.9 Hz, 1H), 2.72–2.55 (m, 4H), 2.48 (s, 3H), 1.58–1.52 (m, 4H), 1.16 (d, *J* = 6.9 Hz, 6H).

K[$\mathbf{3^{-2H}}$]. ^{1}H NMR: δ/ppm = 5.57 (d, *J* = 6.2 Hz, 2H), 5.24 (d, *J* = 6.2 Hz, 2H), 2.88 (hept, *J* = 6.9 Hz, 1H), 2.65–2.52 (m, 4H), 2.44 (s, 3H), 1.54–1.47 (m, 4H), 1.14 (d, *J* = 6.9 Hz, 6H).

[$\mathbf{3_{MeOH}^{-H}}$]NO_3. ^{1}H NMR: δ/ppm = 5.81 (d, *J* = 6.2 Hz, 2H), 5.45 (d, *J* = 6.1 Hz, 2H), 2.77–2.60 (m, 5H), 2.21 (s, 3H), 1.63–1.54 (m, 4H), 1.16 (d, *J* = 6.9 Hz, 6H).

K[$\mathbf{4^{-2H}}$]. ^{1}H NMR: δ/ppm = 2.12 (s, 18H), 2.01 (s, 6H).

[$\mathbf{4_{MeOH}^{-2H}}$]. ^{1}H NMR: δ/ppm = 2.11 (s, 18H), 2.04 (s, 6H).

K[$\mathbf{5^{-2H}}$]. ^{1}H NMR: δ/ppm = 2.57–2.53 (m, 4H), 2.08 (s, 18H), 1.53–1.48 (m, 4H).

***p*-cymene**. ^{1}H NMR: δ/ppm = 7.13–7.02 (m, 4H), 2.88–2.81 (m, 1H), 2.28 (s, 3H), 1.21 (d, *J* = 6.9 Hz, 6H).

Figure S42. ESI-MS spectrum of [**3**]NO_3 in methanol.

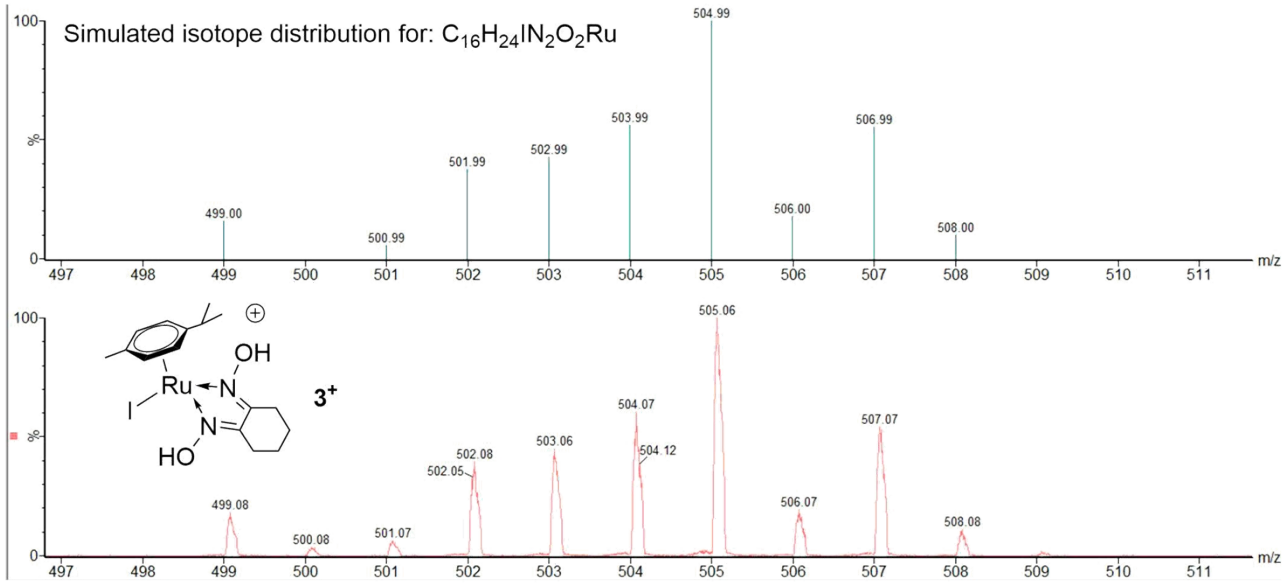

Figure S43. ^{1}H NMR spectra (500 MHz, CD_3OD) of [**2**]PF_6 (**a**) and after reaction with 1.0 eq. Et_3N (**b**, **2**$^{-H}$) or 1.3 eq. K_2CO_3 (**c**, **d**, [**2**$^{-2H}$]$^-$). Spectrum **c** refers to the freshly prepared solution (in CH_3OD) while spectrum **d** was acquired after 14 h at room temperature.

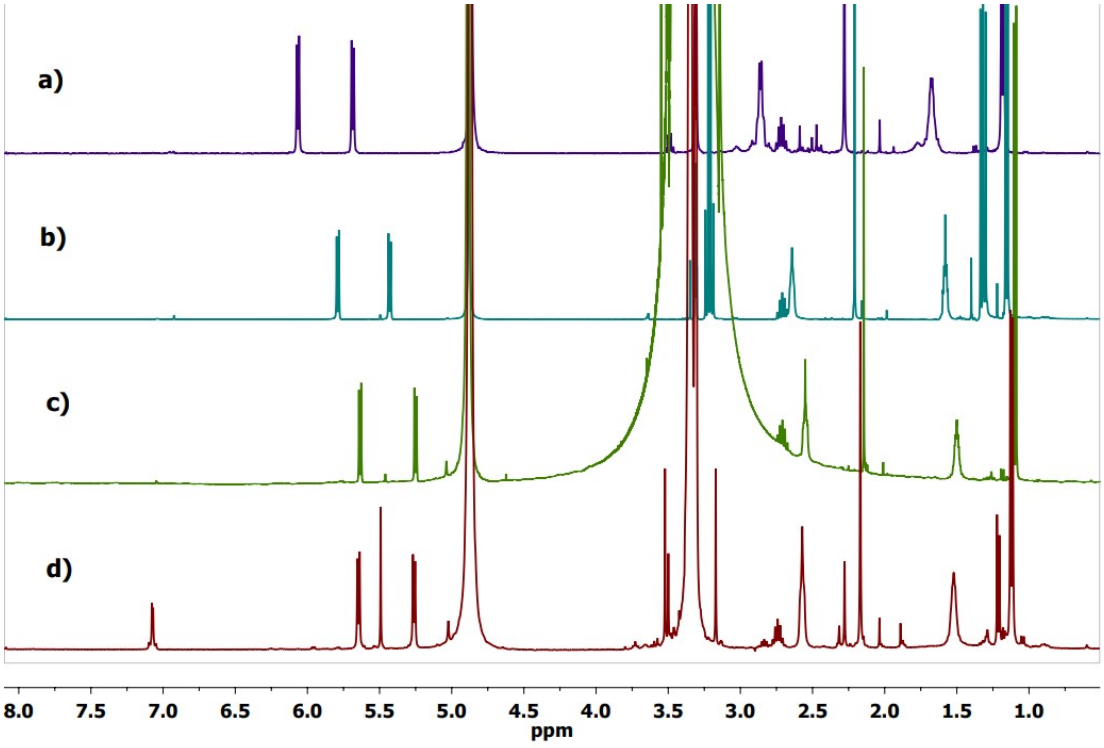

Figure S44. ^{1}H NMR spectra (500 MHz, CD_3OD) of [**3**]NO_3 (**a**) and after reaction with 1.0 eq. $PhNH_2$ (**b**, [$\mathbf{3^+}$]/$\mathbf{3^{-H}}$ equilibrium), 1.0 eq. ^{t}BuOK (**c**, $\mathbf{3^{-H}}$) or 2.0 eq. ^{t}BuOK (**d**, $[\mathbf{3^{-2H}}]^-$).

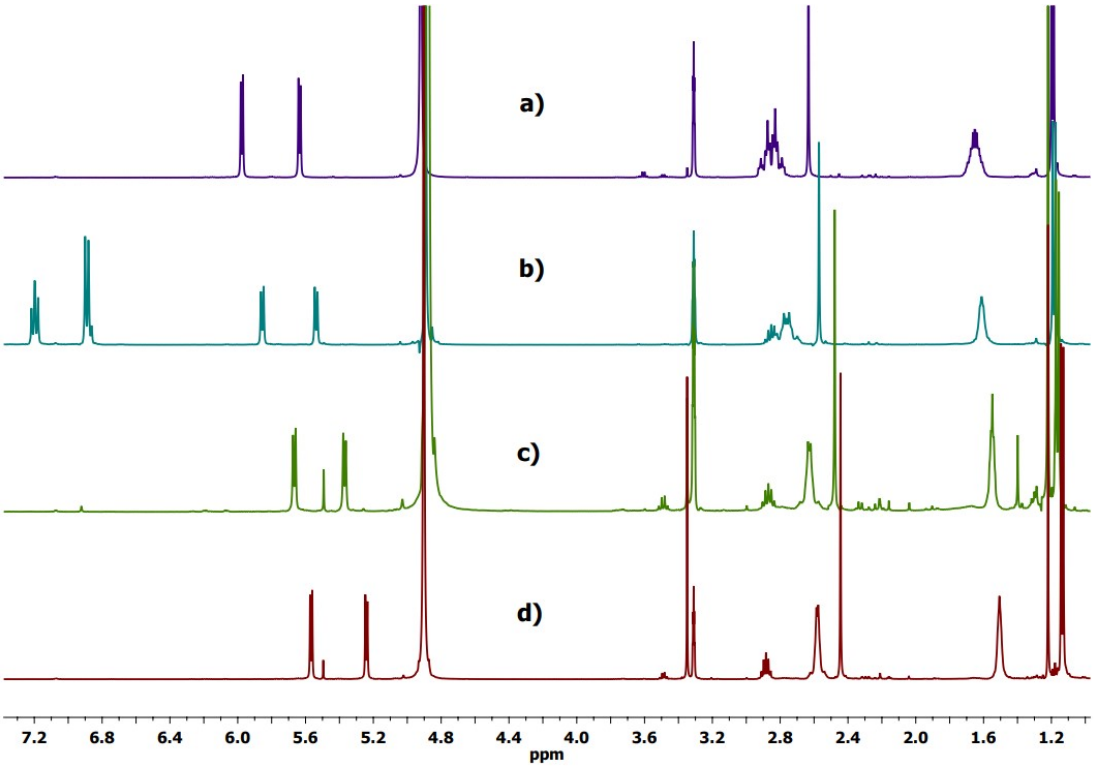

Figure S45. ^{1}H NMR spectra (500 MHz, CD_3OD) of [**4**]NO_3 (**a**) and after reaction with 1.2 eq. $NaHCO_3$ (**b**, $\mathbf{4^{-H}}$) or 1.3 eq. K_2CO_3 at room temperature (**c**, $[\mathbf{4^{-2H}}]^-$ + $[\mathbf{4_{MeOH}^{-2H}}]$).

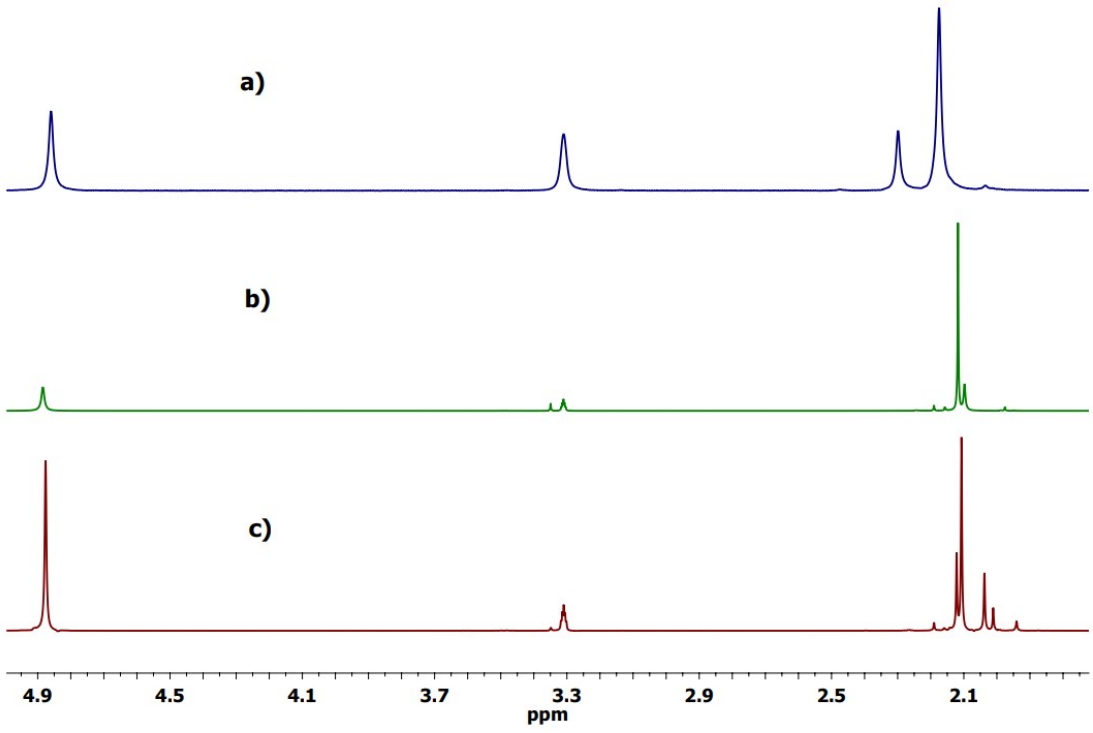

Figure S46. ESI-MS spectra of [**3**$^{-2H}$]$^{-}$ in methanol, *in situ* formed from [**3**]NO_3 + 3 eq. of ^{t}BuOK.

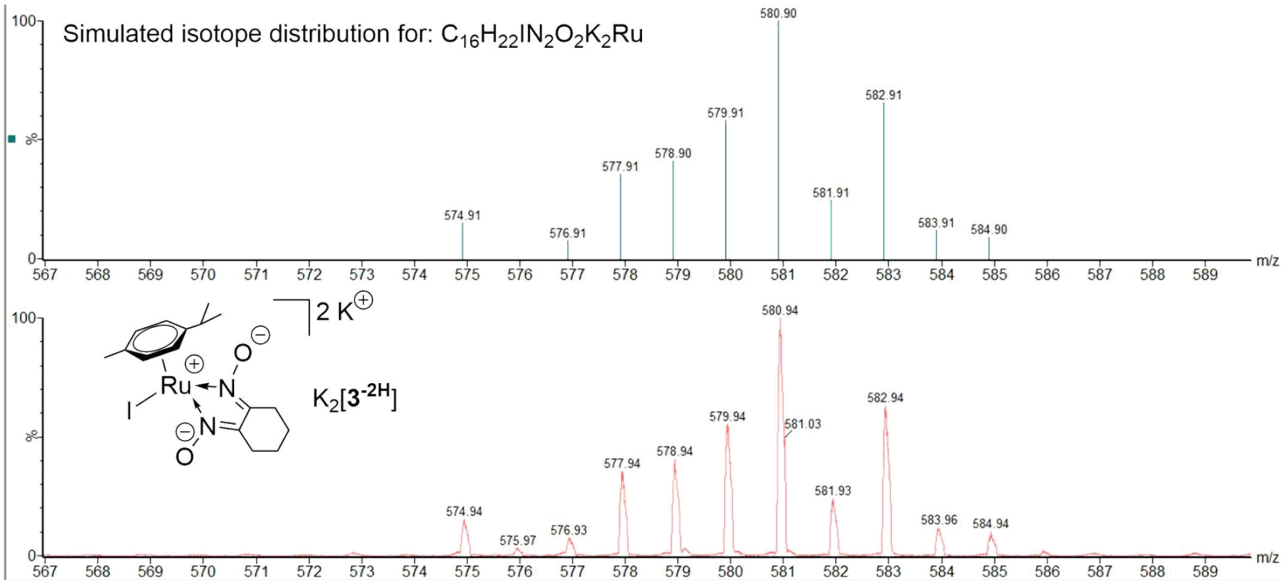

Figure S47. ^{1}H NMR spectra (500 MHz, CD_3OD) of the reactions of [$Ru(NO_3)_2(\eta^6$-*p*-cymene)] with nioxime (**a,** [**3**$_{MeOH}$]$^{2+}$), nioxime and ^{t}BuOK (1.0 eq) (**b**, [**3**$_{MeOH}^{-H}$]$^{+}$ as major product), nioxime and ^{t}BuOK (2.0 eq) (**c**, **3**$_{dimer}$ as major product).

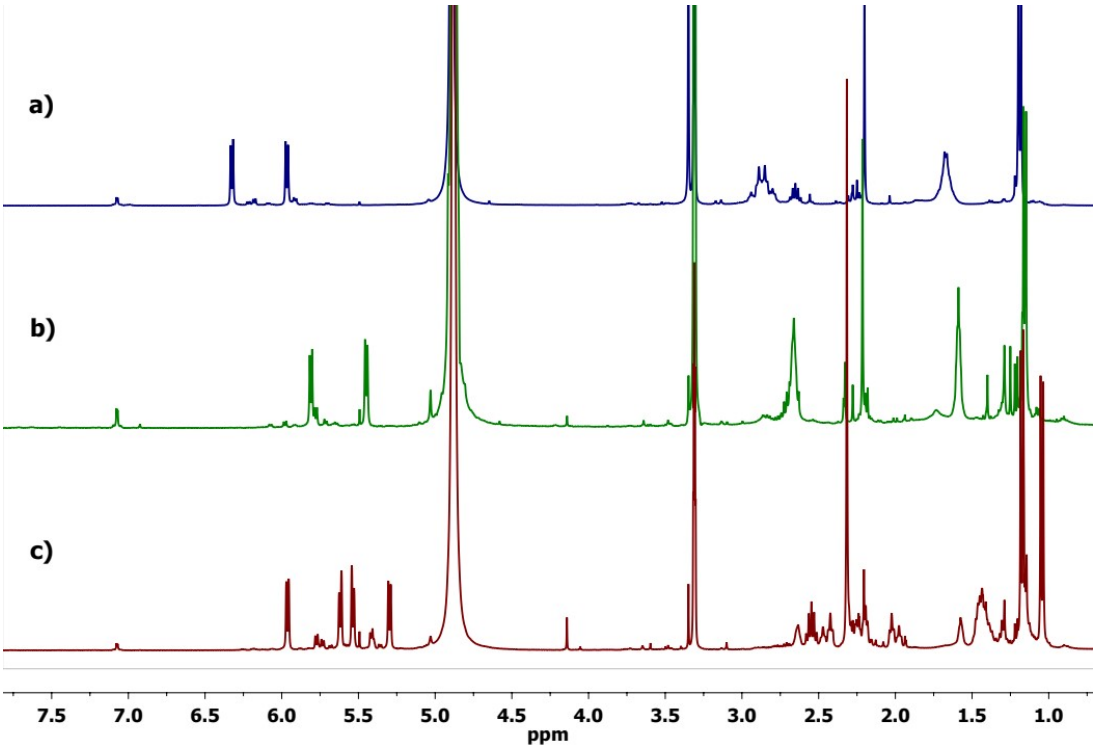

Figure S48. ^{1}H NMR spectra (500 MHz, CD_3OD) of $[\mathbf{3}^{-2H}]^-$ (from $[\mathbf{3}]NO_3$ + 2.0 eq. ^{t}BuOK) in the freshly-prepared solution (**a**) and after 18 h at room temperature (**b**); of $\mathbf{3}_{dimer}$ (from $[Ru(NO_3)_2(\eta^6\text{-}p\text{-cymene})]$ + nioxime + 2.0 eq. ^{t}BuOK) in the in the freshly-prepared solution (**c**) and after 18 h at room temperature (**d**).

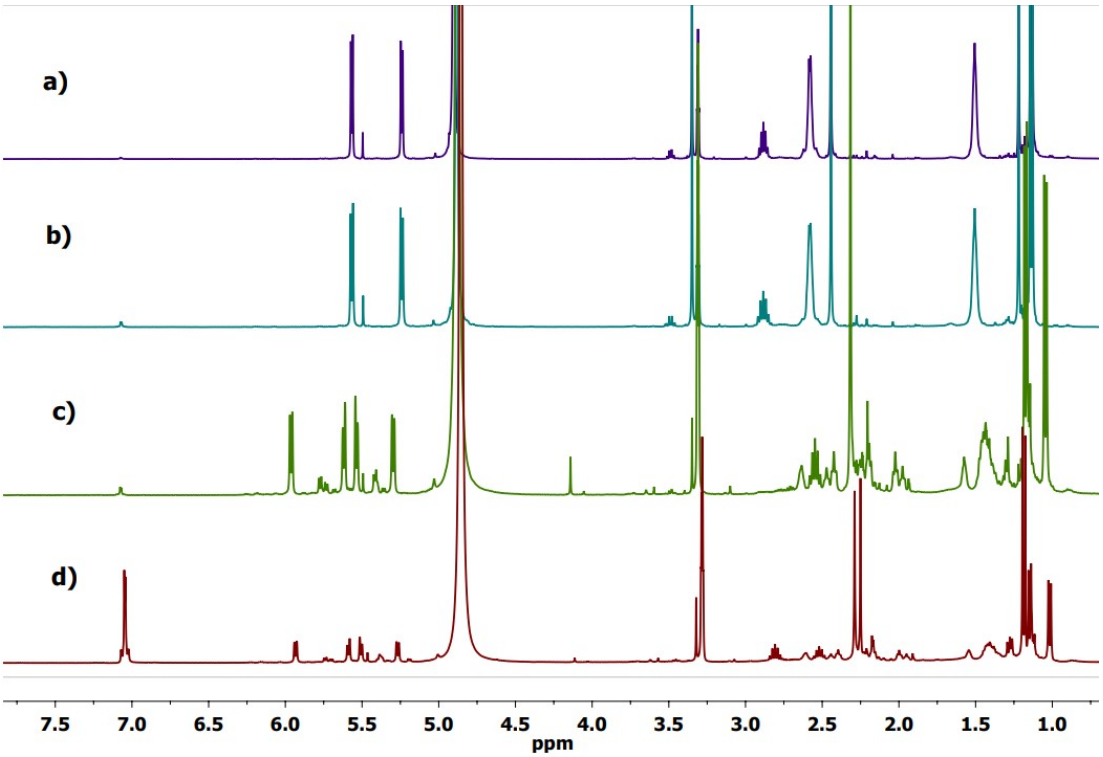

Figure S49. ^{1}H NMR spectra (500 MHz, CD_3OD) of the reactions of $AgNO_3$ (1.0 eq) with $[\mathbf{2}]PF_6$ (**a**, in CH_3OD), $[\mathbf{3}]NO_3$ (**b**), $\mathbf{3}^{-H}$ (**c**) and $[\mathbf{3}^{-2H}]^-$ (**d**).

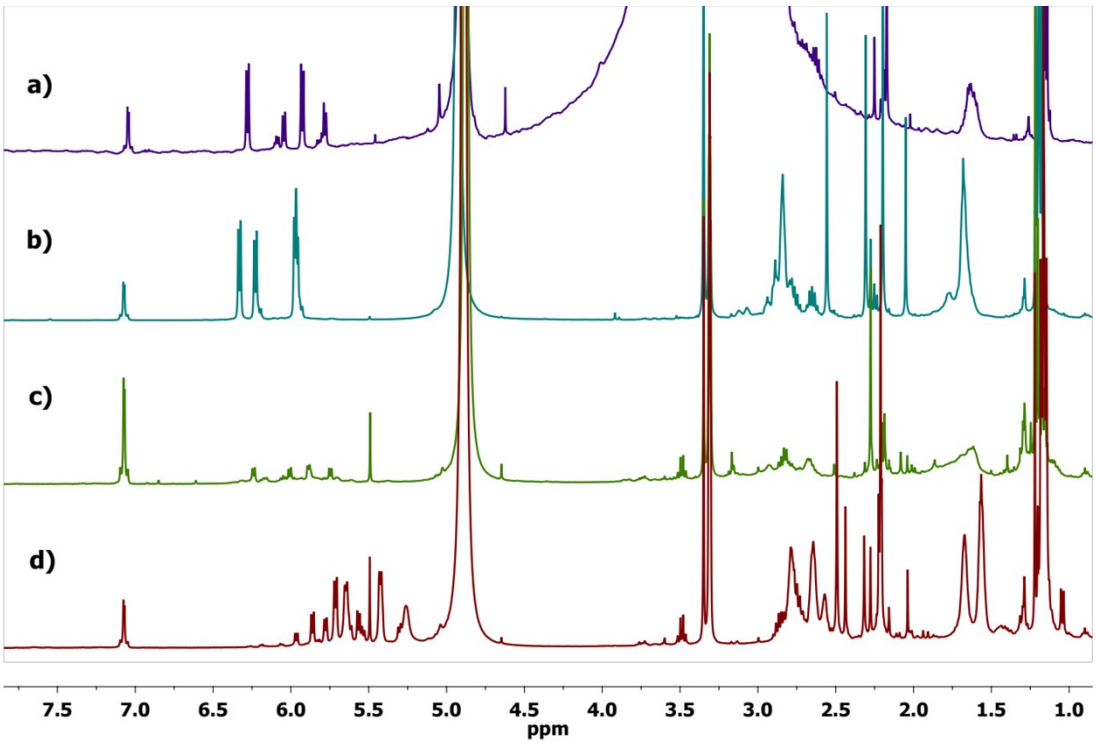

Isolation and characterization of *N*-methylated amines as hydrochloride salts

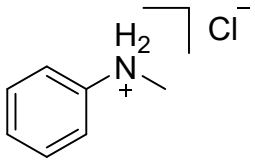

***N*-methylaniline·HCl**. Purification by column chromatography (hexane/ethyl acetate 9:1) obtaining 63.9 mg (isolated yield 89 %) as a white solid. ^{1}H NMR (400 MHz, D_2O): δ/ppm = 7.63–7.59 (m, 3H), 7.55–7.53 (m, 2H), 3.14 (s, 3H). ^{13}C{^{1}H} NMR (101 MHz, D_2O): δ/ppm = 136.3, 130.4, 129.8, 121.8, 36.8.

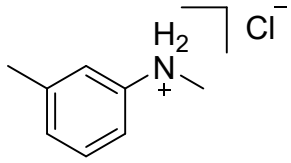

***N*,3-dimethylaniline·HCl**. Purification by column chromatography (hexane/ethyl acetate 9:1) obtaining 47.3 mg (isolated yield 78 %) as a white solid. ^{1}H NMR (400 MHz, D_2O): δ/ppm = 7.10 (t, 1H), 6.57 (m, 1H), 6.46-6.44 (m, 2H), 2.84 (s, 3H), 2.31 (s, 3H). ^{13}C{^{1}H} NMR (101 MHz, D_2O): δ/ppm = 149.5, 139.0, 129.2, 118.3, 113.3, 109.7, 30.8, 21.7.

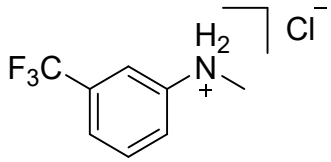

***N*-methyl-3-(trifluoromethyl)aniline·HCl**. Purification by column chromatography (hexane/ethyl acetate 9:1) obtaining 71.8 mg (isolated yield 82 %) as a white solid. ^{1}H NMR (400 MHz, D_2O): δ/ppm = 7.78-7.48 (m, 4H), 3.08 (s, 3H). ^{13}C{^{1}H} NMR (101 MHz, D_2O): δ/ppm = 131.3, 130.4, 129.9, 121.8, 36.8. ^{19}F NMR (376 MHz, D_2O): δ/ppm = 62.69

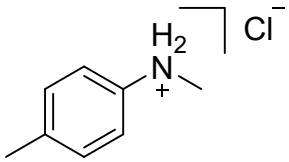

***N*,4-dimethylaniline·HCl**. Purification by column chromatography (hexane/ethyl acetate 9:1) obtaining 55.1 mg (isolated yield 91 %) as a white solid. ^{1}H NMR (400 MHz, D_2O): δ/ppm = 7.64-7.63 (d, 2H), 7.56-7.54 (d, 2H), 3.15 (s, 3H), 2.26 (s, 3H). ^{13}C{^{1}H} NMR (101 MHz, D_2O): δ/ppm = 136.2, 130.4, 129.9, 121.8, 36.8, 30.3.

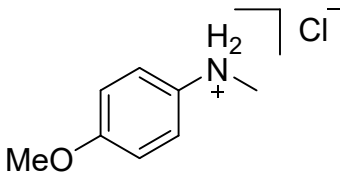

4-Methoxy-*N*-methylaniline·HCl. Purification by column chromatography (hexane/ethyl acetate 9:1) obtaining 44.5 mg (isolated yield 65 %) as a white solid. ^{1}H NMR (400 MHz, D_2O): δ/ppm = 7.50-7.48 (d, 2H), 7.21-7.18 (d, 2H), 3.94 (s, 3H), 3.12 (s, 3H). ^{13}C{^{1}H} NMR (101 MHz, D_2O): δ/ppm = 159.4, 129.7, 123.0, 115.5, 55.7, 36.8.

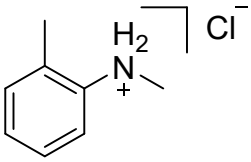

***N*,2-dimethylaniline·HCl**. Purification by column chromatography (hexane/ethyl acetate 9:1) obtaining 38.7 mg (isolated yield 64 %) as a white solid. ^{1}H NMR (400 MHz, D_2O): δ/ppm = 7.50 (m, 2H), 7.49 (m, 2H), 3.15 (s, 3H), 2.50 (s, 3H). ^{13}C{^{1}H} NMR (101 MHz, D_2O): δ/ppm = 134.9, 132.3, 131.0, 129.7, 127.9, 121.7, 35.7, 16.0.

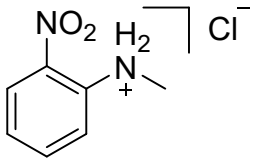

***N*-methyl-2-nitroaniline·HCl**. Purification by column chromatography (hexane/ethyl acetate 8:2) obtaining 63.9 mg (isolated yield 84 %) as a white solid. ^{1}H NMR (400 MHz, D_2O): δ/ppm = 7.45 (m, 2H), 7.41 (m, 2H), 2.42 (s, 3H). ^{13}C{^{1}H} NMR (101 MHz, D_2O): δ/ppm = 131.9, 131.7, 129.4, 128.5, 127.4, 123.2, 16.1.

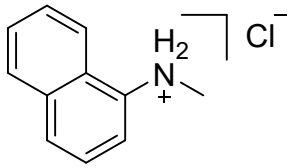

***N*-methylnaphthalen-1-amine·HCl**. Purification by column chromatography (hexane/ethyl acetate 95:5) obtaining 40.8 mg (isolated yield 52 %) as a white solid. ^{1}H NMR (400 MHz, D_2O): δ/ppm = 8.10 (m, 1H), 8.08 (m, 1H), 8.04 (m, 1H), 7.81 (m, 1H), 7.73 (m, 1H), 7.71 (m, 1H), 7.64 (m, 1H), 3.31 (s, 3H). ^{13}C{^{1}H} NMR (101 MHz, D_2O): δ/ppm = 134.1, 131.5, 130.4, 129.2, 128.3, 127.4, 125.4, 125.1, 120.1, 119.6, 36.0.

Figure S50. ^{1}H NMR spectrum (400 MHz, D_2O) of *N*-methylaniline·HCl.

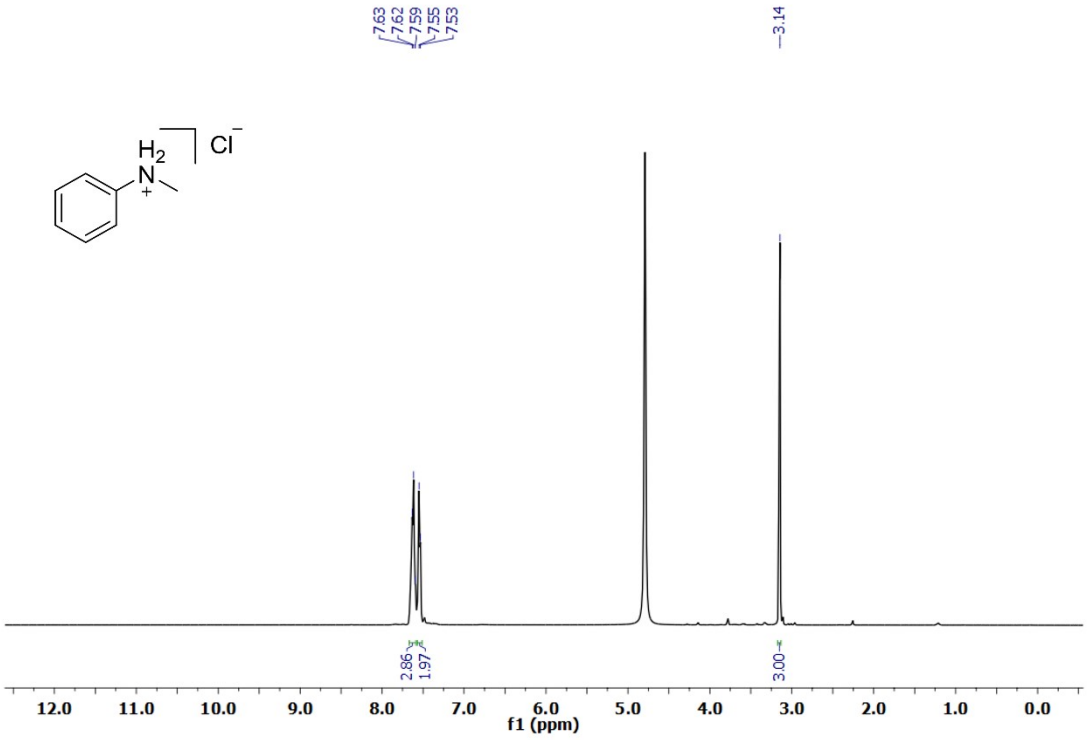

Figure S51. $^{13}C\{^{1}H\}$ NMR spectrum (101 MHz, D_2O) of *N*-methylaniline·HCl..

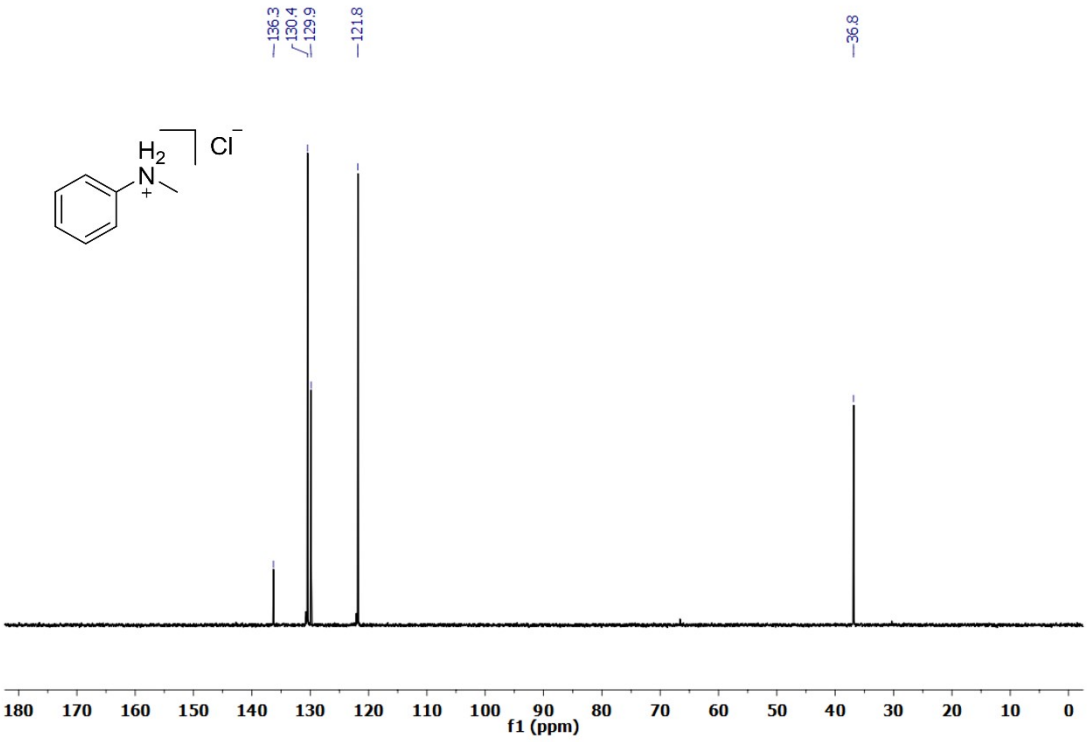

Figure S52. ^{1}H NMR spectrum (400 MHz, $CDCl_3$) of *N*,3-dimethylaniline·HCl.

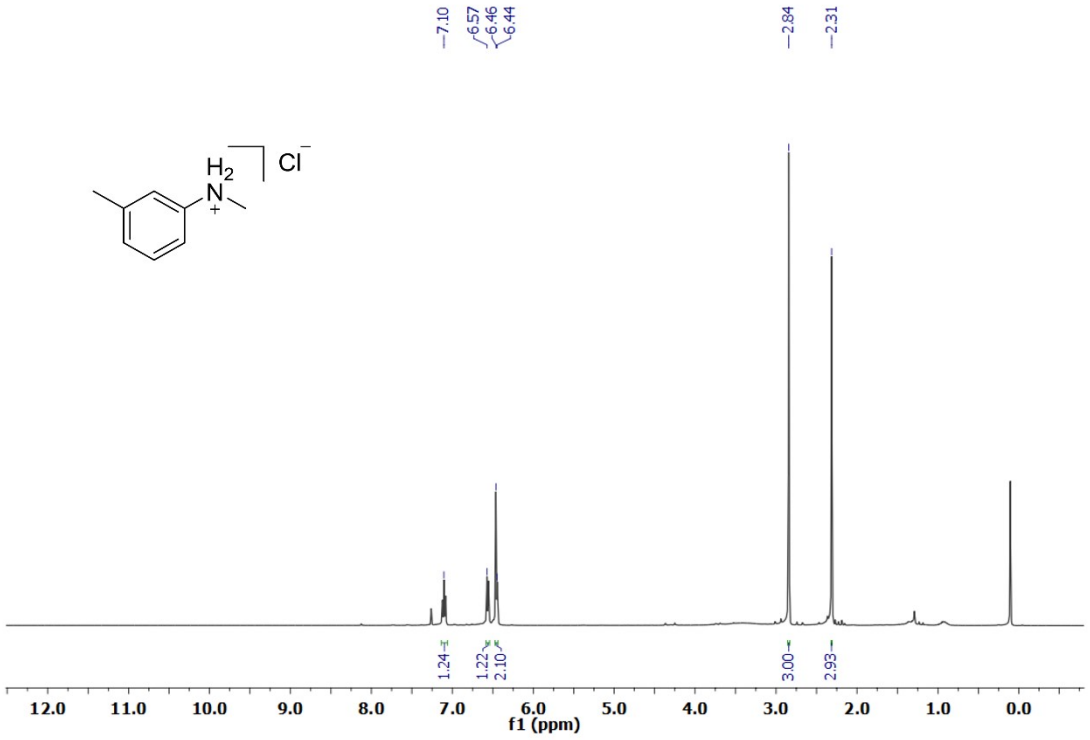

Figure S53. $^{13}C\{^{1}H\}$ NMR spectrum (101 MHz, $CDCl_3$) of *N*,3-dimethylaniline·HCl.

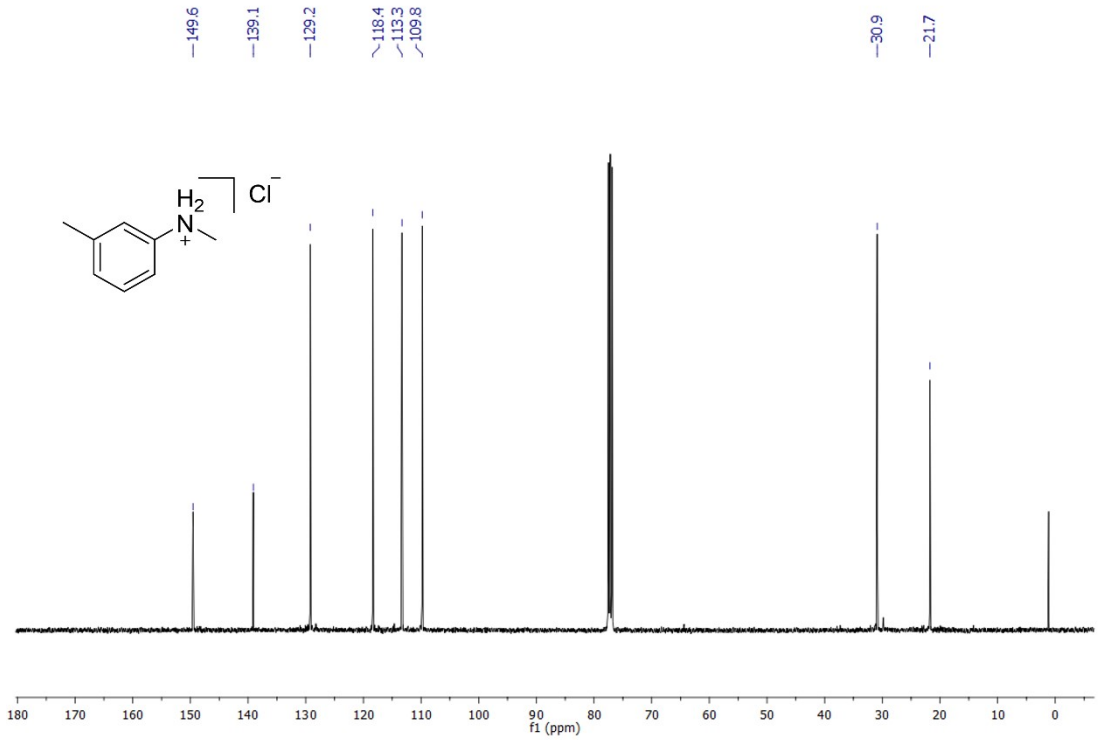

Figure S54. ^{1}H NMR spectrum (400 MHz, D_2O) of *N*-methyl-3-(trifluoromethyl)aniline·HCl.

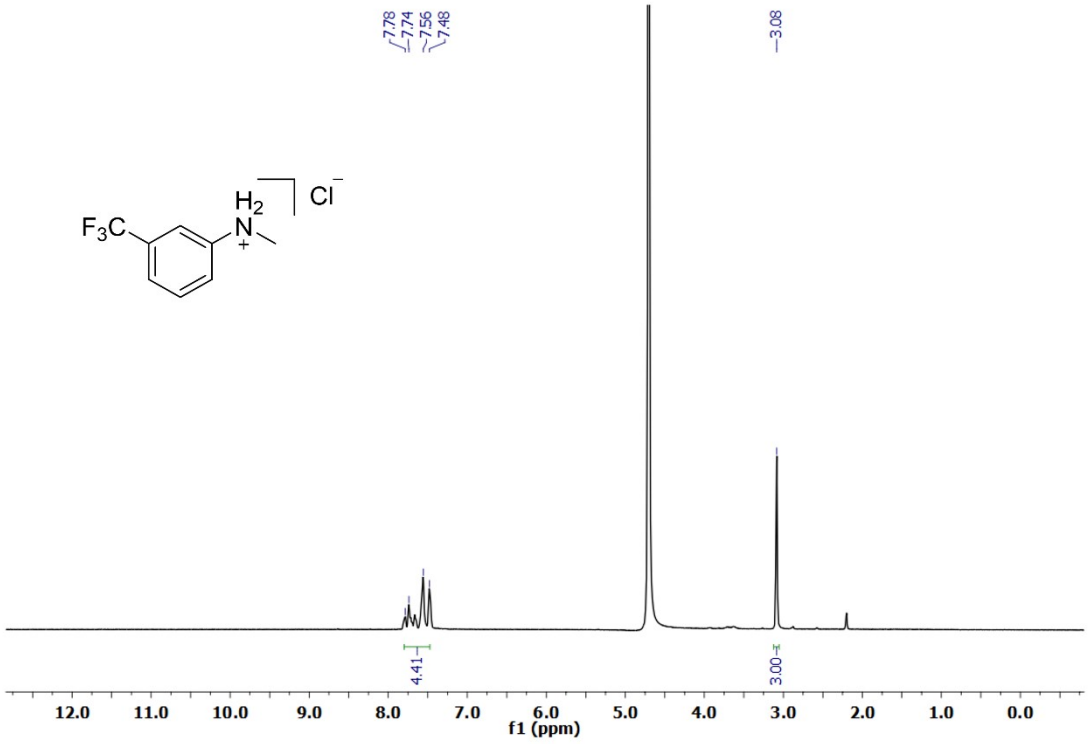

Figure S55. $^{13}C\{^{1}H\}$ NMR spectrum (101 MHz, D_2O) of *N*-methyl-3-(trifluoromethyl)aniline·HCl.

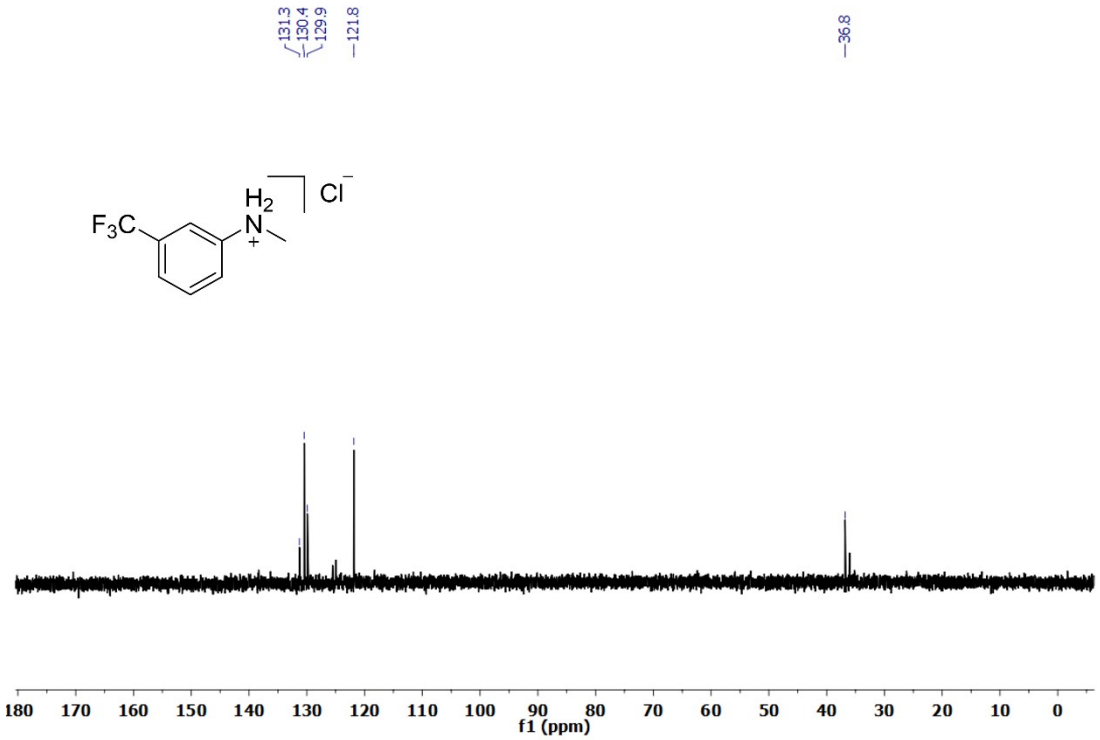

Figure S56. ^{19}F NMR spectrum (376 MHz, D_2O) of *N*-methyl-3-(trifluoromethyl)aniline·HCl.

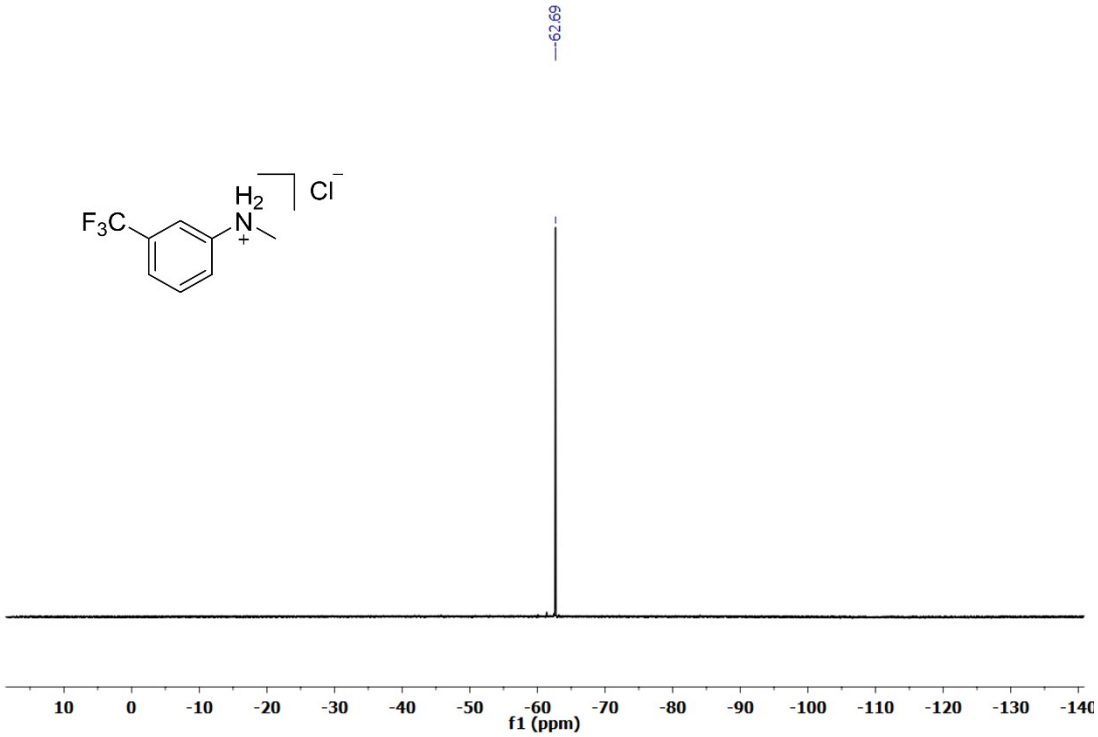

Figure S57. ^{1}H NMR spectrum (400 MHz, D_2O) of *N*,4-dimethylaniline·HCl.

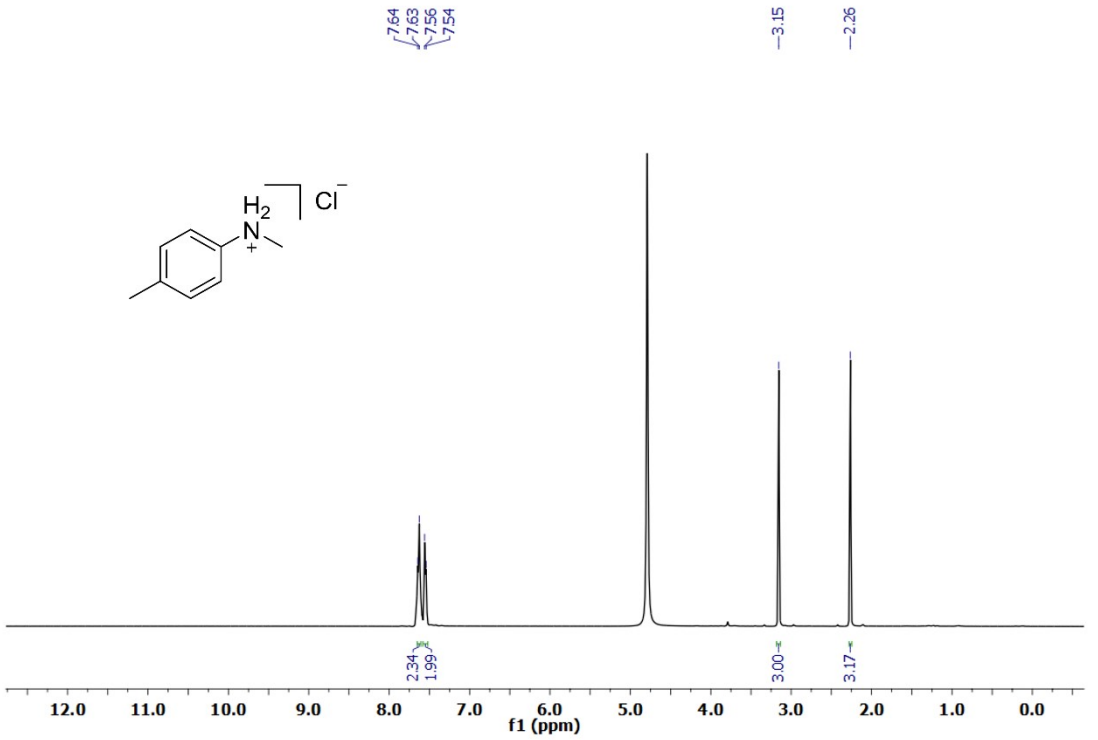

Figure S58. $^{13}C\{^{1}H\}$ NMR spectrum (101 MHz, D_2O) of *N*,4-dimethylaniline·HCl.

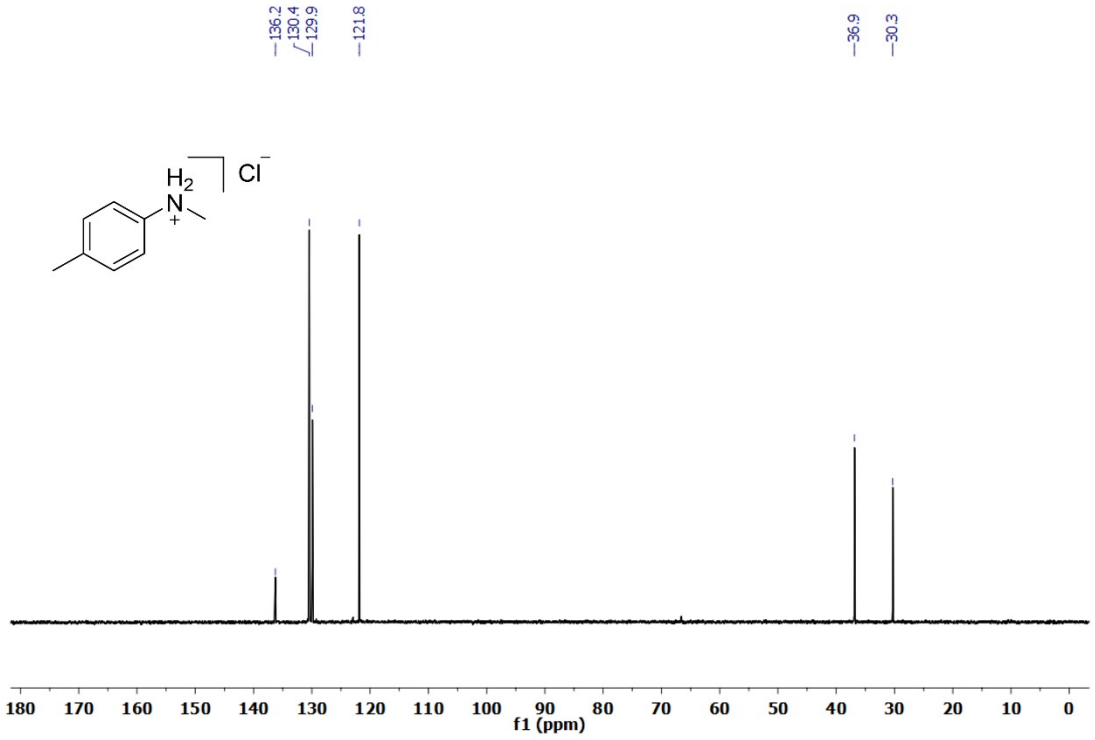

Figure S59. ^{1}H NMR spectrum (400 MHz, D_2O) of 4-Methoxy-*N*-methylaniline·HCl.

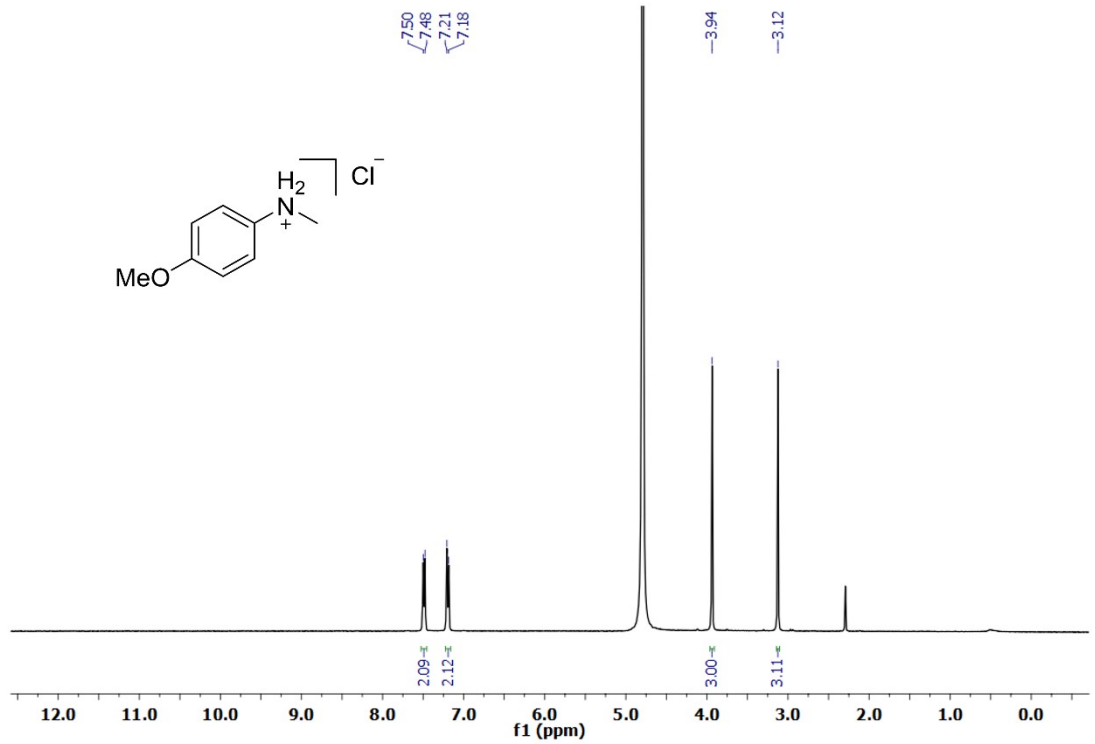

Figure S60. $^{13}C\{^{1}H\}$ NMR spectrum (101 MHz, D_2O) of 4-Methoxy-*N*-methylaniline·HCl.

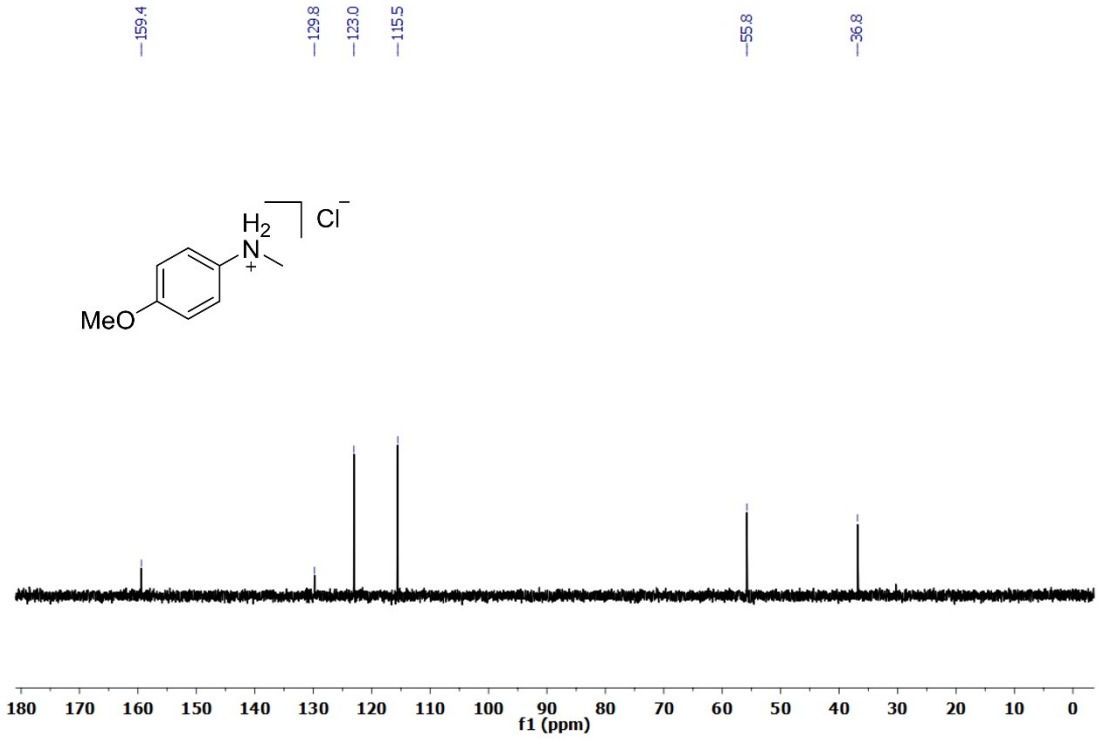

Figure S61. ^{1}H NMR spectrum (400 MHz, D_2O) of *N*,2-dimethylaniline·HCl.

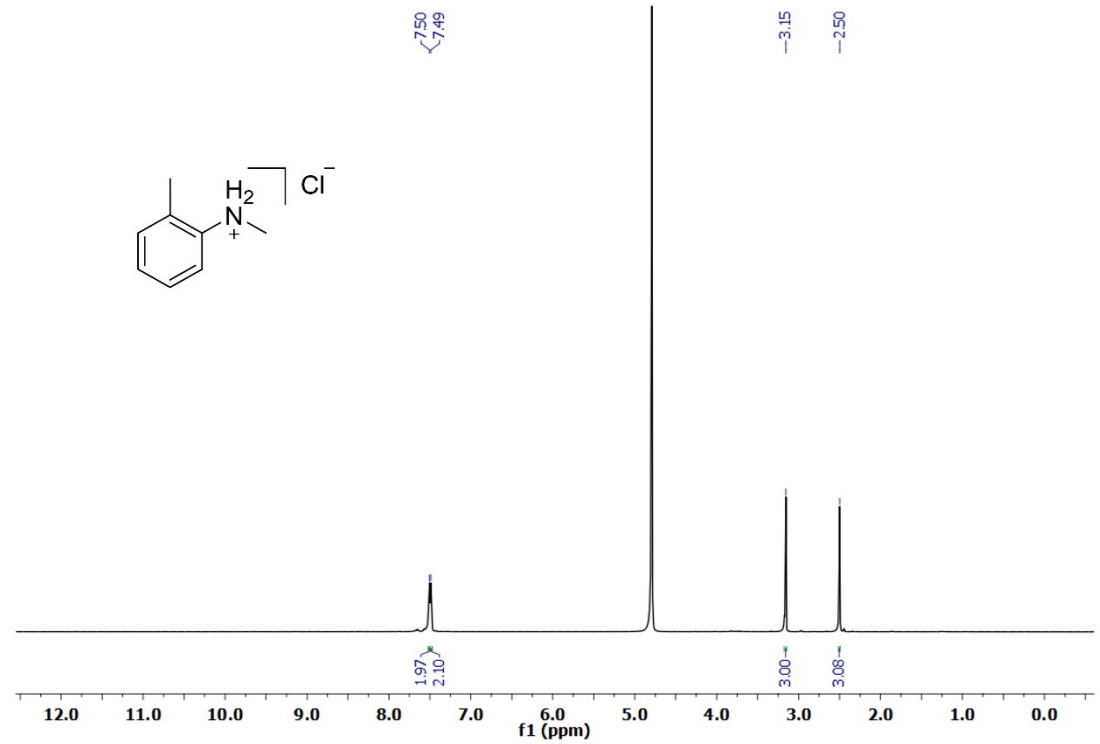

Figure S62. $^{13}C\{^{1}H\}$ NMR spectrum (101 MHz, D_2O) of *N*,2-dimethylaniline·HCl.

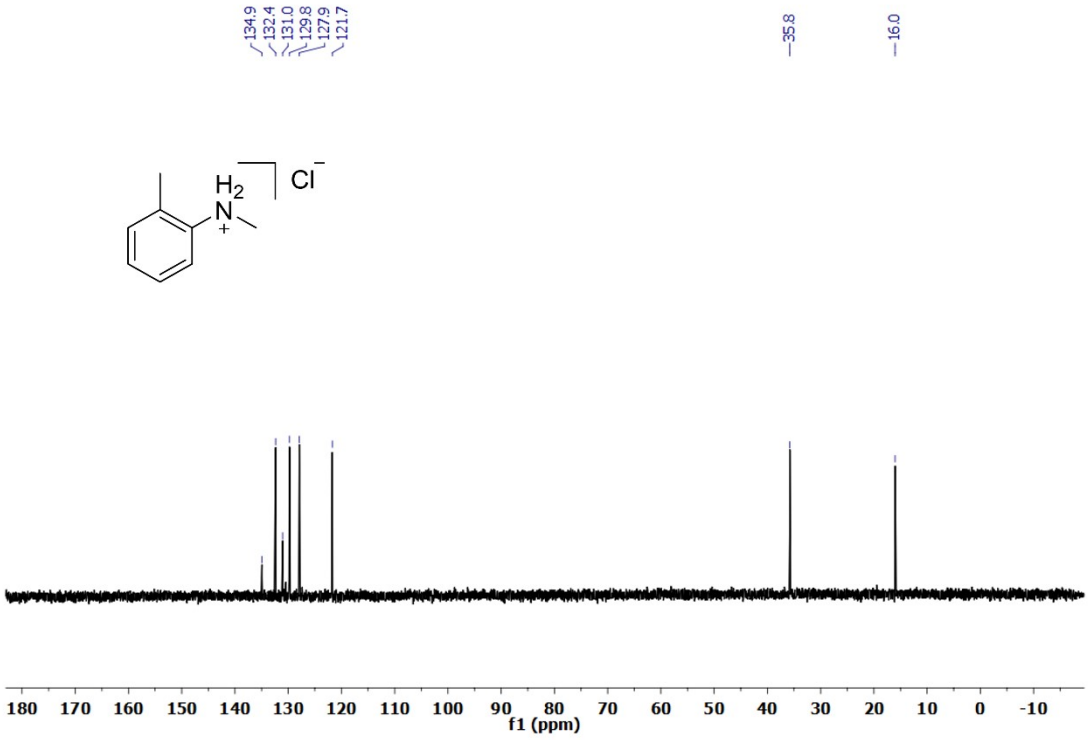

Figure S63. ^{1}H NMR spectrum (400 MHz, D_2O) of *N*-methyl-2-nitroaniline·HCl.

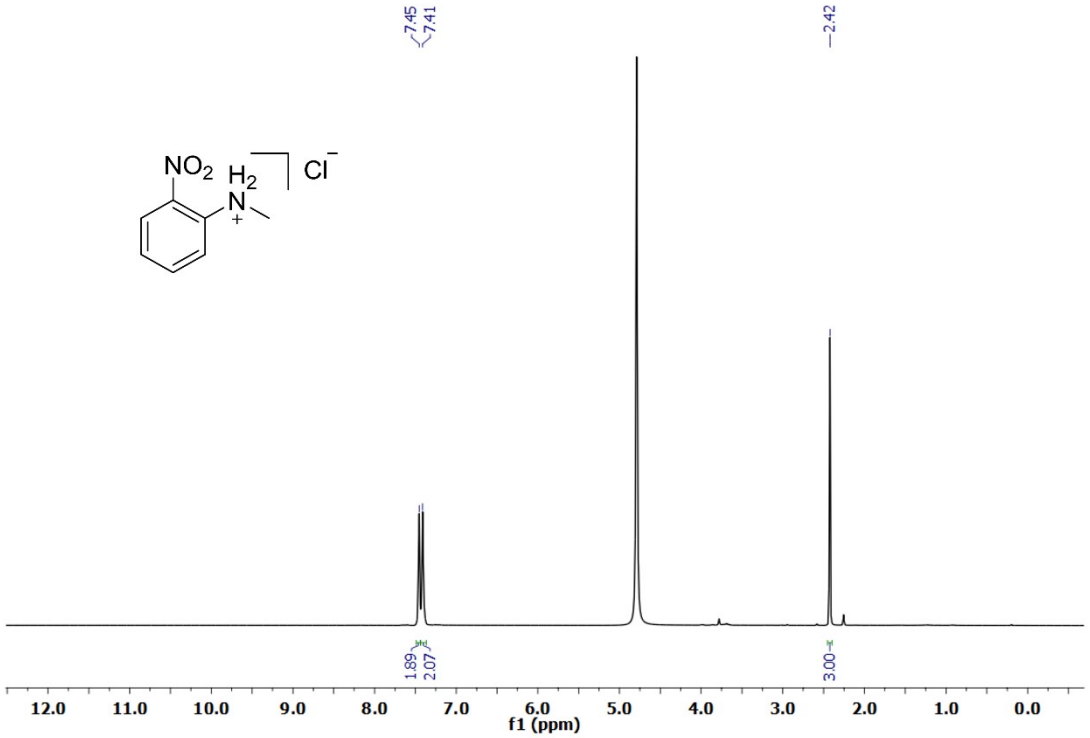

Figure S64. $^{13}C\{^{1}H\}$ NMR spectrum (101 MHz, D_2O) of *N*-methyl-2-nitroaniline·HCl.

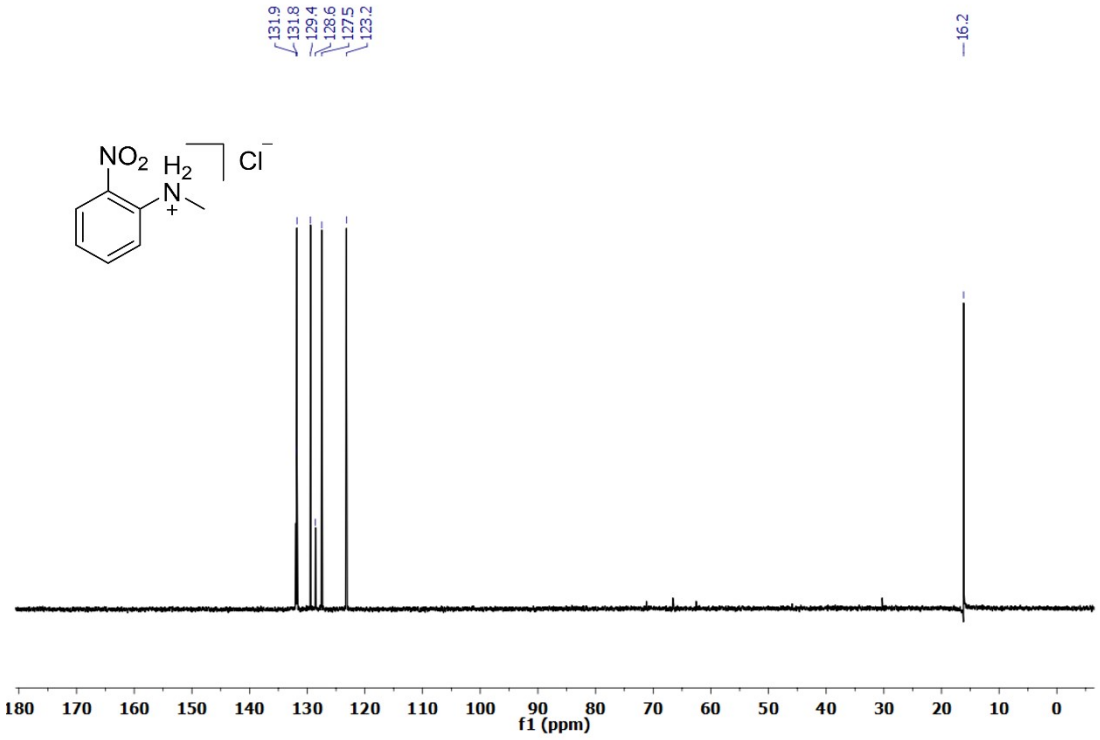

Figure S65. ^{1}H NMR spectrum (400 MHz, D_2O) of *N*-methylnaphthalen-1-amine·HCl.

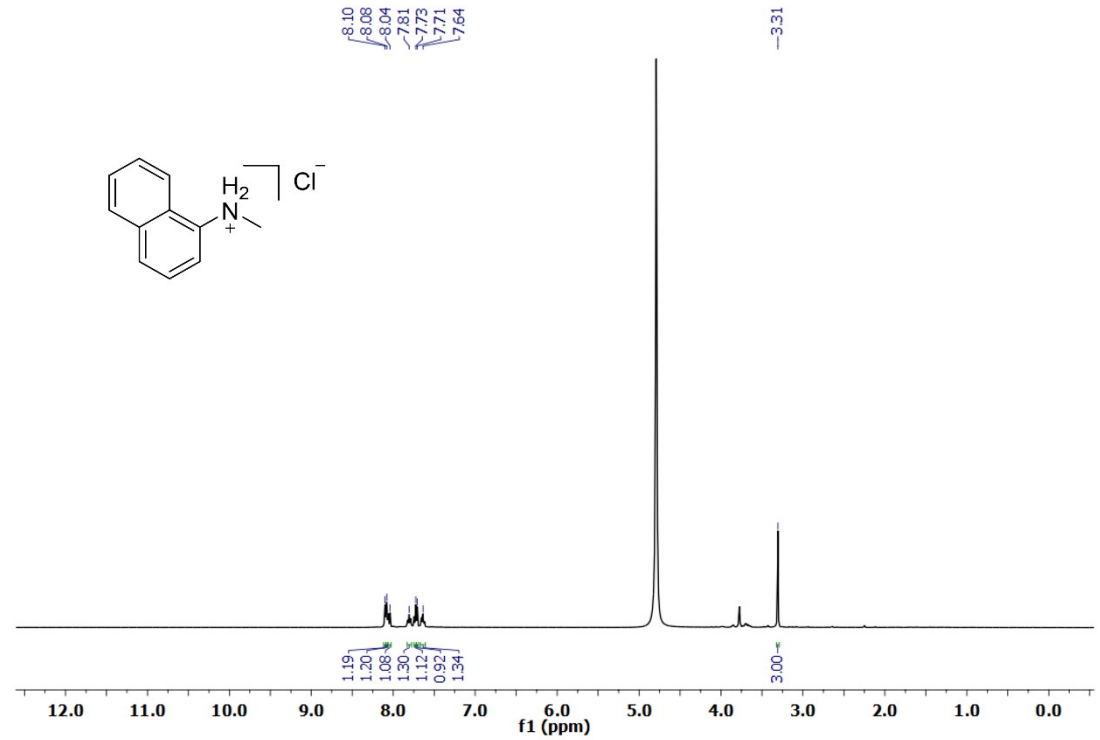

Figure S66. $^{13}C\{^{1}H\}$ NMR spectrum (101 MHz, D_2O) of *N*-methylnaphthalen-1-amine·HCl.

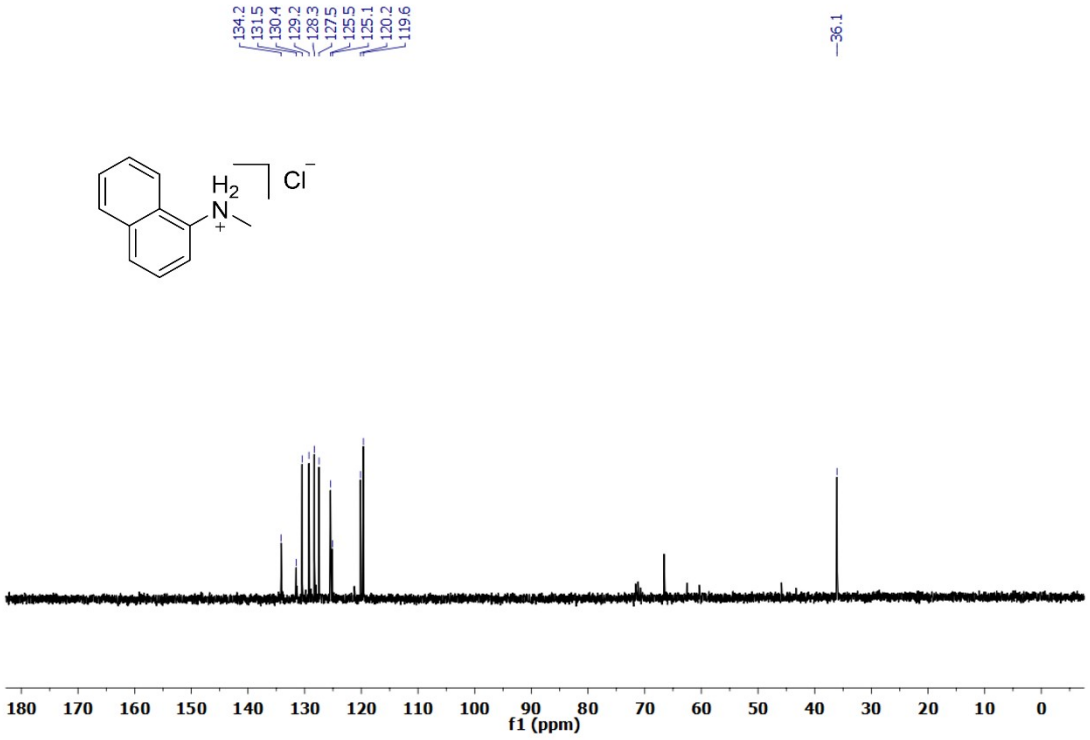

Catalytic protocols and control experiments

General GC-FID procedure.

The liquid phase reactions were analyzed using gas chromatography with a flame ionization detector (GC-FID) with an Agilent 7820 GC-FID system, equipped with a J&W HP-5 Intuvo GC fused silica column (30 m, 0.32 mm, 0.25 μm). The volume of injection was 1.0 μL. The GC system temperatures were as follows: temperature of the injector 250 °C; transfer line temperature 250 °C; oven temperature: 72 °C (2.0 min); 20 °C/min up to 150 °C (1.0 min); 10 °C/min up to 230 °C (3.0 min); finally, 30 °C/min. up to 250 °C (3.0 min). The samples for the injections were prepared taking a 20 μL aliquot from the reaction and adding 5 μL of mesitylene (internal standard), both dissolved in 980 μL of ethyl acetate.

Figure S67. Example of a GC-FID chromatogram for the reduction/*N*-methylation of nitrobenzene in methanol with 1 eq. of ^{t}BuOK catalyzed by 4 mol% [**3**]NO_3 (130°C ,18h).

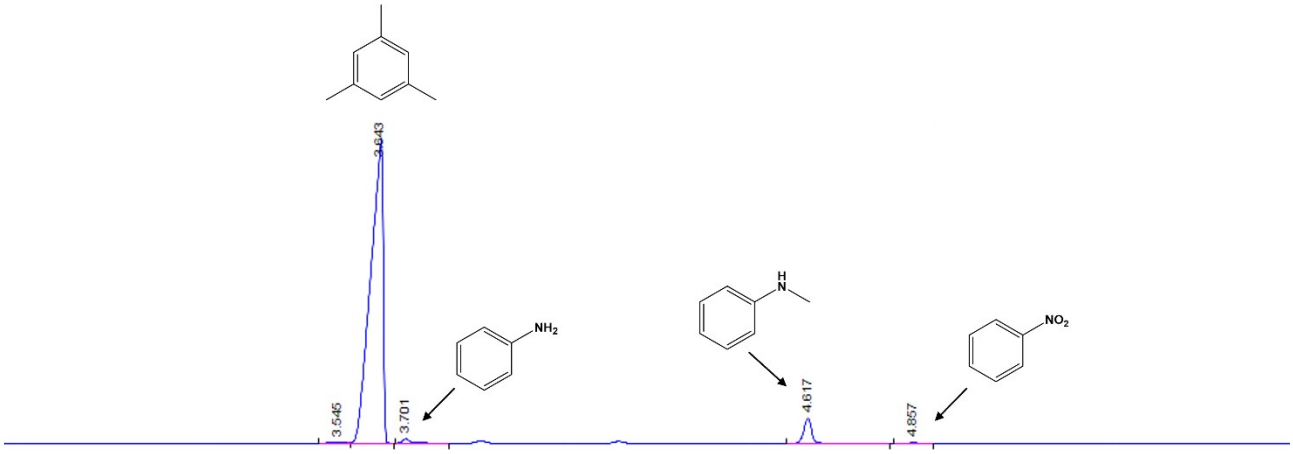

Kinetic studies.

Five reaction tubes were charged with nitrobenzene (0.5 mmol), [**3**]NO_3 (0.02 mmol), potassium tert-butoxide (0.5 mmol) and degassed methanol (1 mL). The reactions were performed under the standard conditions (130 °C, 0 to 18 h). After 1 h, 4 h, 8 h, 12 h and 18 h, one reaction tube was cooled to room temperature. The progress of the reaction was monitored by GC-FID analysis.

Table S5. Kinetic data for each reaction time

t (h)	**Nitrobenzene a1** (mol%)	**Aniline b1** (mol%)	***N*-Methylaniline c1** (mol%)
0	100	0	0
1	85	15	0
4	41	37	22
8	22	26	52
12	11	8	81
18	2	4	94

Reduction of azobenzene.

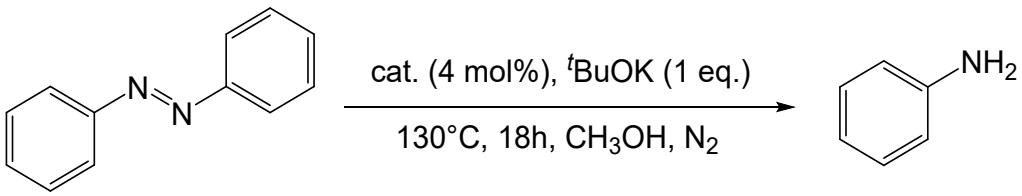

0.5 mmol of azobenzene, 0.5 mmol of potassium tert-butoxide and 0.02 mmol of [**3**]NO_3 were dissolved in 1 mL of methanol, previously degassed, in a Schlenk tube. The reaction was then left under stirring in an inert atmosphere (N_2) at 130 °C for 18 h. The progress of the reaction was monitored by GC-FID analysis.

Deuteration experiments.

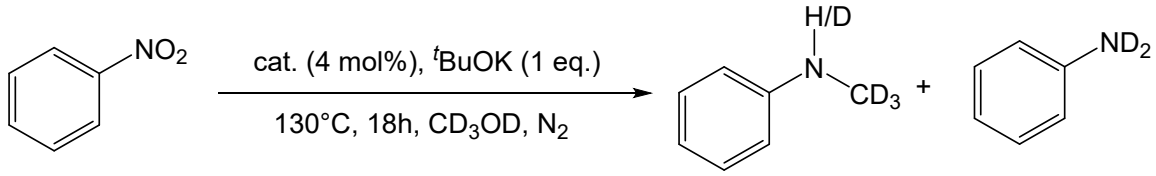

With CD_3OD. 0.5 mmol of nitrobenzene, 0.5 mmol of potassium tert-butoxide and 0.02 mmol of [**3**]NO_3 were dissolved in 1 mL of dry methanol-d_4, previously degassed, in a Schlenk tube. The reaction was then left under stirring in an inert atmosphere (N_2) at 130 °C for 18 h. The progress of the reaction was monitored by GC-FID analysis.

Figure S68. GC-FID chromatogram of the crude of the reduction/*N*-methylation of nitrobenzene with CD_3OD (1 eq. of ^{t}BuOK, 4 mol% [**3**]NO_3, 130°C ,18 h).

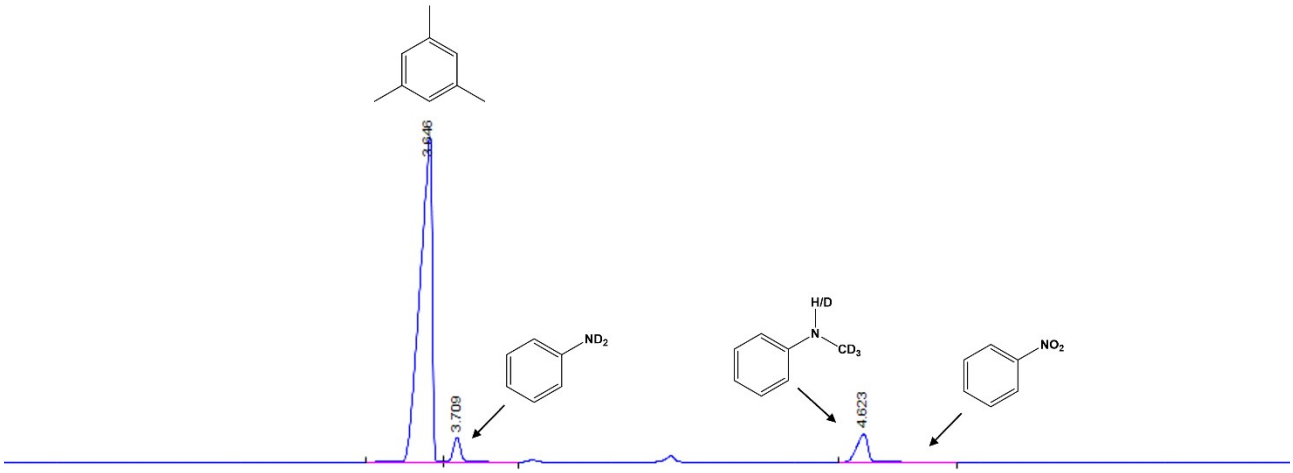

Figure S69. ^{1}H NMR spectrum (400 MHz, CD_3OD) of the crude of the reduction/*N*-methylation of nitrobenzene with CD_3OD (1 eq. of ^{t}BuOK, 4 mol% [**3**]NO_3, 130 °C ,18 h).

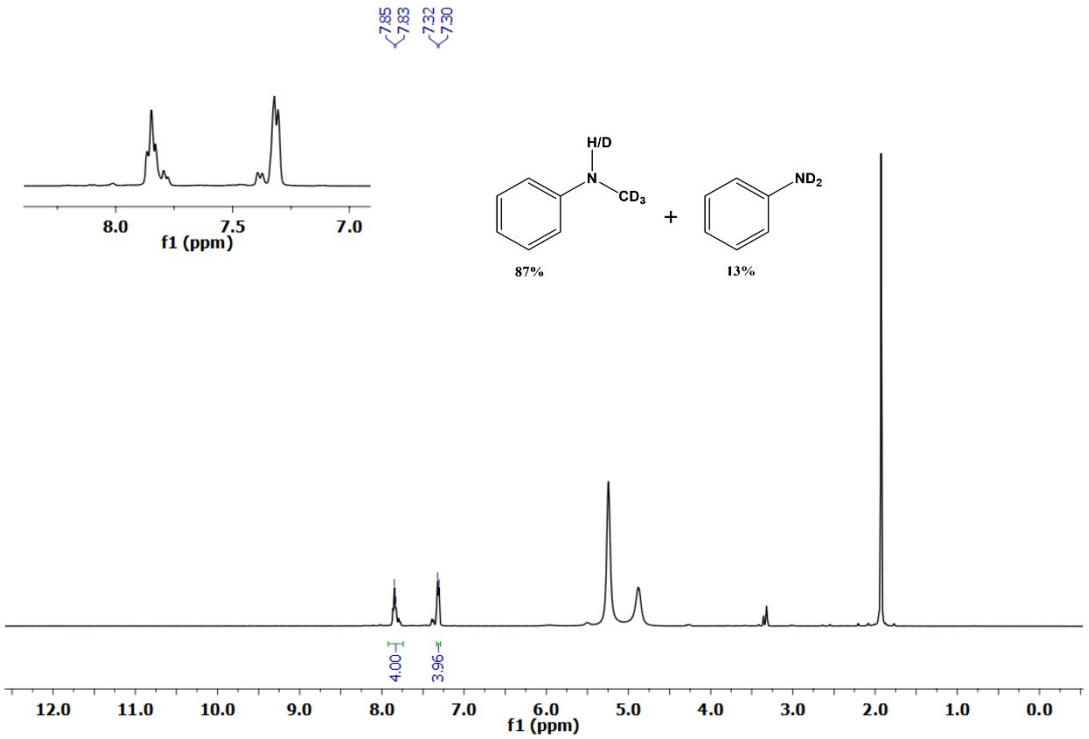

Figure S70. $^{13}C\{^{1}H\}$ NMR spectrum (101 MHz, CD_3OD) of the crude of the *N*-methylation of nitrobenzene with CD_3OD (1 eq. of ^{t}BuOK, 4 mol% [**3**]NO_3, 130 °C ,18 h). Magnification related to the signal of the N-***C***D_3 moiety (29.7 ppm, septet $^{1}J(^{13}C\text{-}^{2}H)$ = 20.6 Hz).

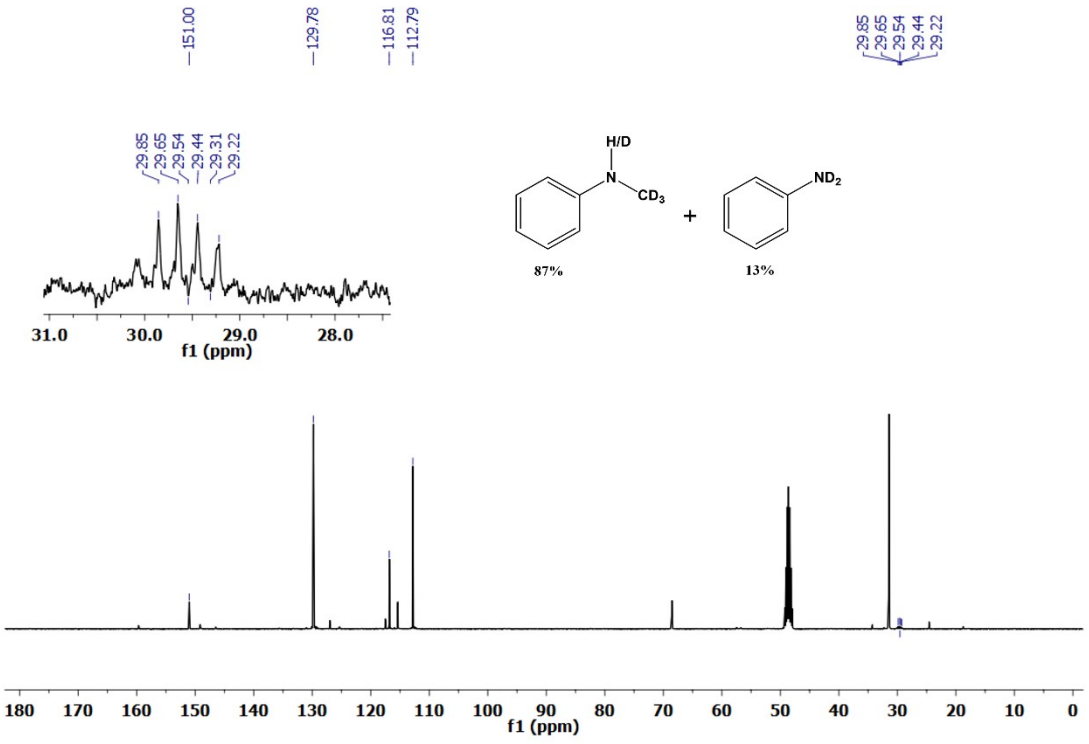

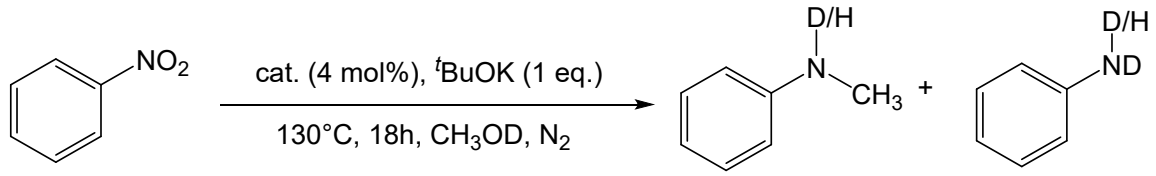

With CH_3OD. 0.5 mmol of nitrobenzene, 0.5 mmol of potassium tert-butoxide and 0.02 mmol of [**3**]NO_3 were dissolved in 1 mL of dry methanol-d_1, previously degassed, in a Schlenk tube. The reaction was then left under stirring in an inert atmosphere (N_2) at 130 °C for 18 h. The progress of the reaction was monitored by GC-FID analysis.

Figure S71. GC-FID chromatogram of the crude of the reduction/*N*-methylation of nitrobenzene with CH_3OD (1 eq. of ^{t}BuOK, 4 mol% [**3**]NO_3, 130°C ,18h).

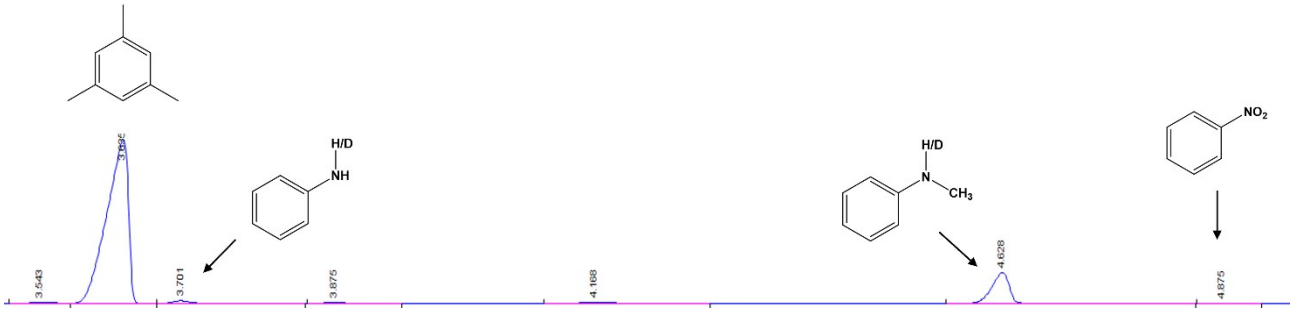

Figure S72. ^{1}H NMR spectrum (400 MHz, CH_3OD) of the crude of the reduction/*N*-methylation of nitrobenzene with CH_3OD (1 eq. of ^{t}BuOK, 4 mol% [**3**]NO_3, 130°C ,18 h).

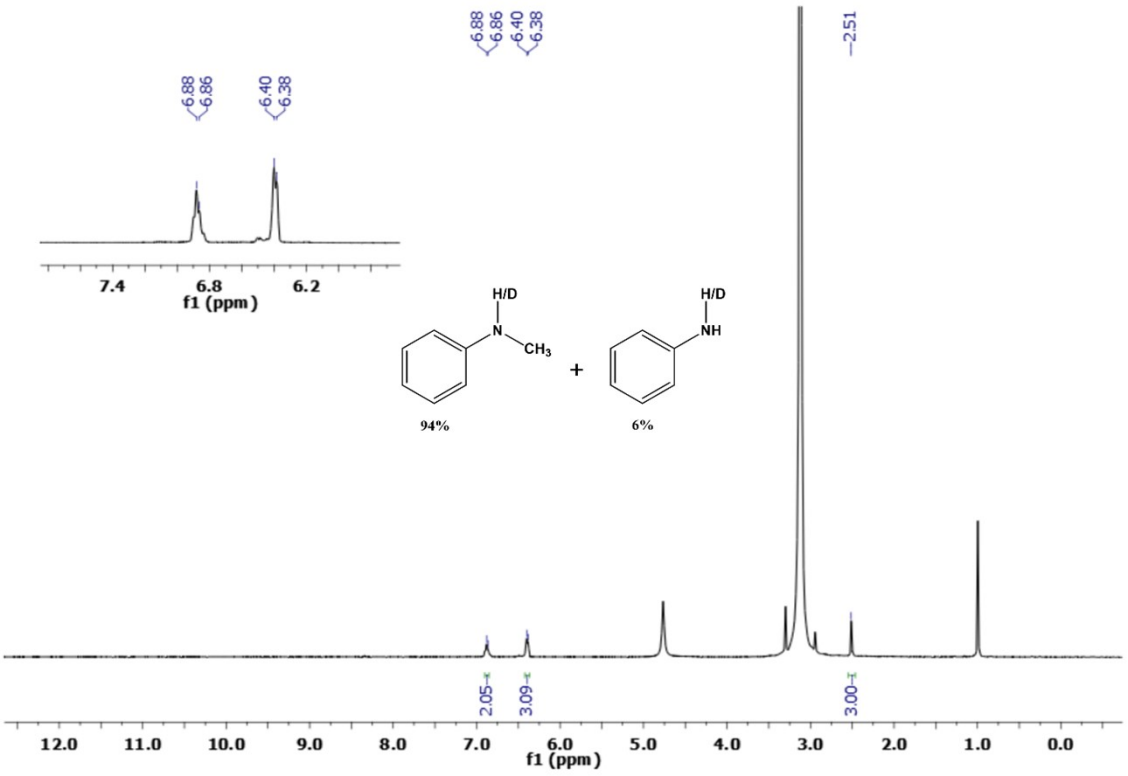

Figure S73. $^{13}C\{^{1}H\}$ NMR spectrum (101 MHz, CH_3OD) of the crude of the reduction/*N*-methylation of nitrobenzene with CH_3OD (1 eq. of ^{t}BuOK, 4 mol% [**3**]NO_3, 130°C ,18h). Magnification related to the signal of the N-***C***H_3 moiety (30.6 ppm, singlet).

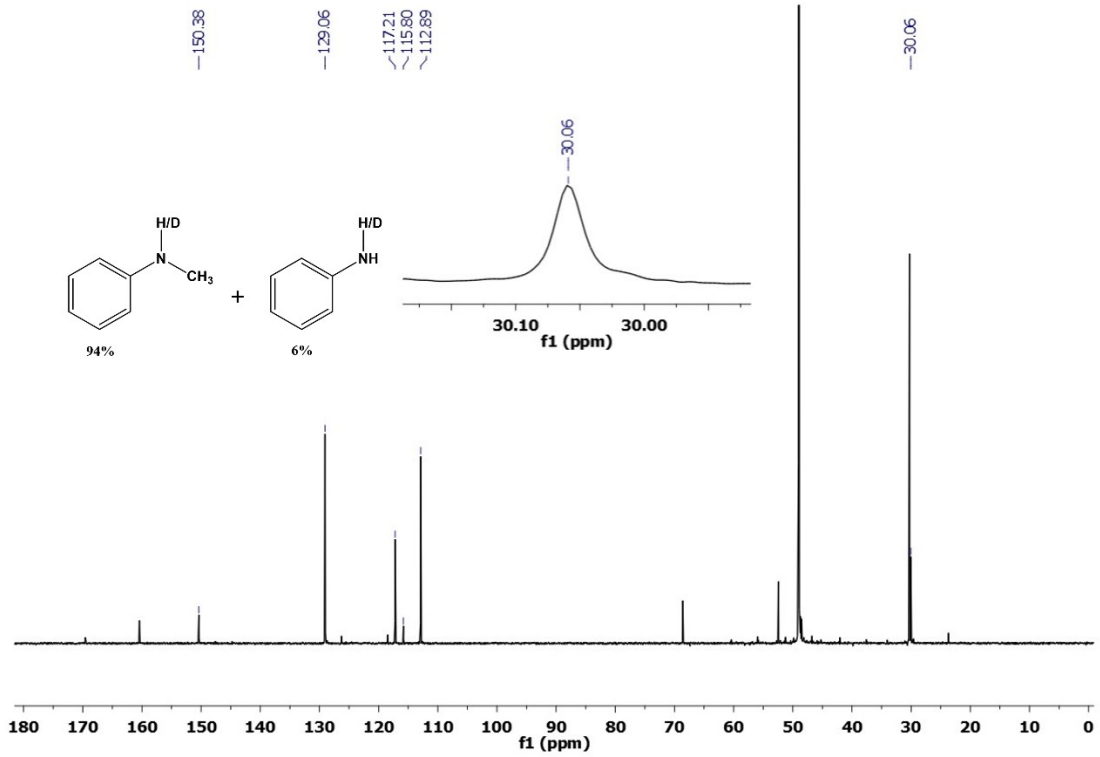

General procedure for the transfer hydrogenation of nitrobenzene.

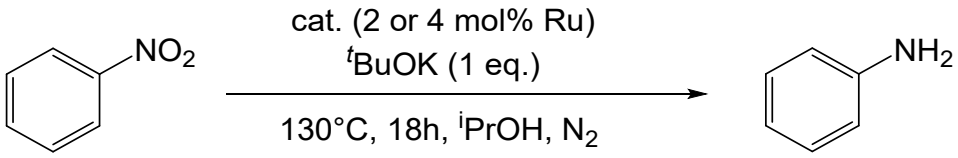

0.5 mmol of nitrobenzene, 0.5 mmol of potassium tert-butoxide and the selected amount of catalytic precursor (**D1**, **N2** or [**3**]NO_3) were dissolved in 1 mL of 2-propanol, previously degassed, in a Schlenk tube. The reaction was then left under stirring in an inert atmosphere (N_2) at 130 °C for 18 h. The progress of the reaction was monitored by GC-FID analysis.

General procedure for the *N*-methylation of aniline.

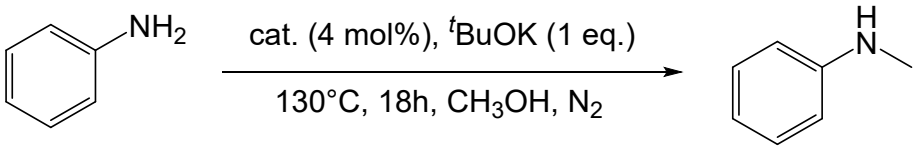

0.5 mmol of aniline, 0.5 mmol of potassium tert-butoxide and 0.02 mmol of [**3**]NO_3 were dissolved in 1 mL of methanol, previously degassed, in a Schlenk tube. The reaction was then left under stirring in an inert atmosphere (N_2) at 130 °C for 18 h. The progress of the reaction was monitored by GC-FID analysis.

MS and NMR investigations on $[3]^+$ under catalytically-relevant conditions.

Figure S74. ^{1}H NMR spectra (500 MHz, CD_3OD) of $[\mathbf{3}^{-2H}]^-$ (**a**, prepared with $[\mathbf{3}]NO_3$ + 2 eq ^{t}BuOK), after addition and ^{t}BuOK (20 eq.) and $PhNH_2$ (**b**) or $PhNO_2$ (**c**) at room temperature and after 20 h at reflux temperature (**d**).

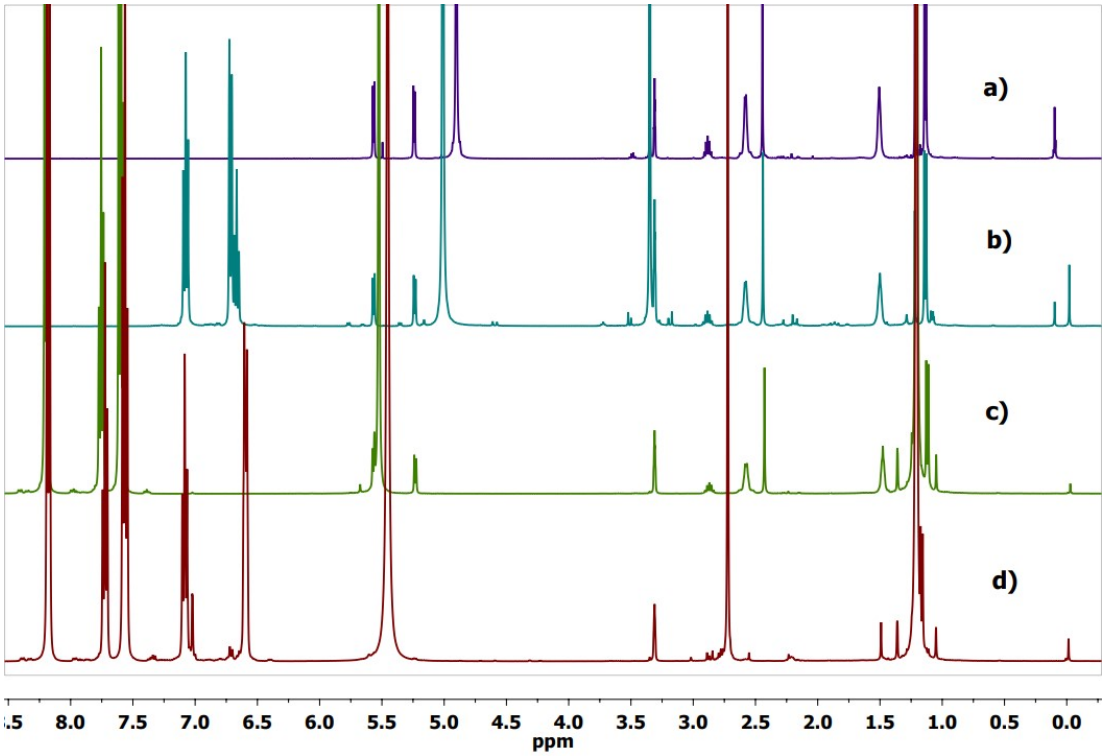

Figure S75. GC-MS chromatogram for the reduction/*N*-methylation of 3-methylnitrobenzene in methanol with 1 eq. of ^{t}BuOK catalyzed by 4 mol% $[\mathbf{3}]NO_3$ (130 °C ,18 h).

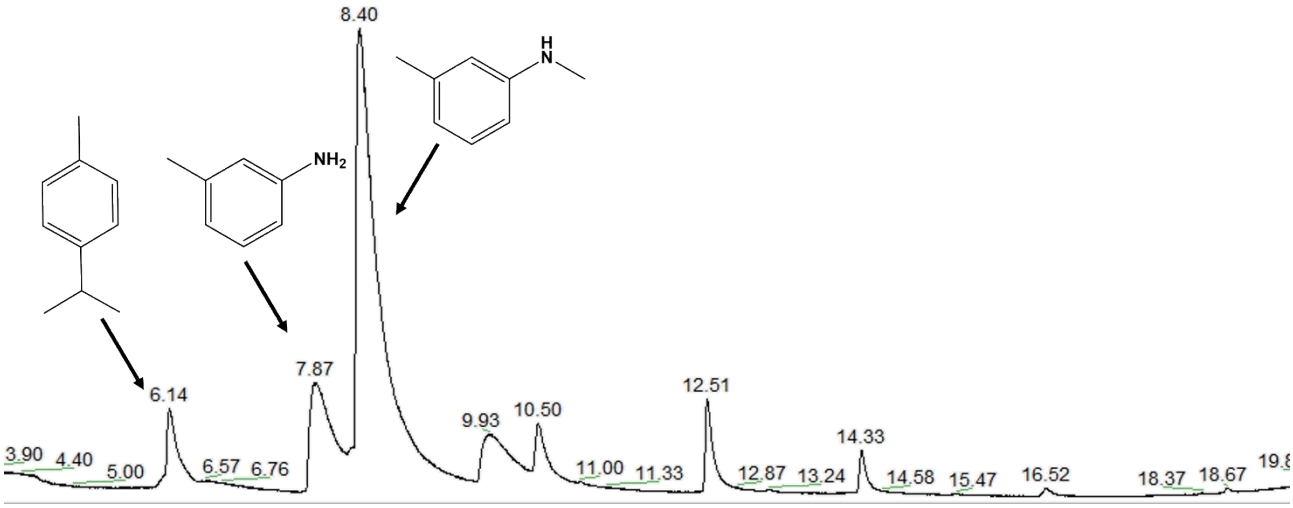

Figure S76. MS spectrum of *p*-cymene (t.r. 6.14).

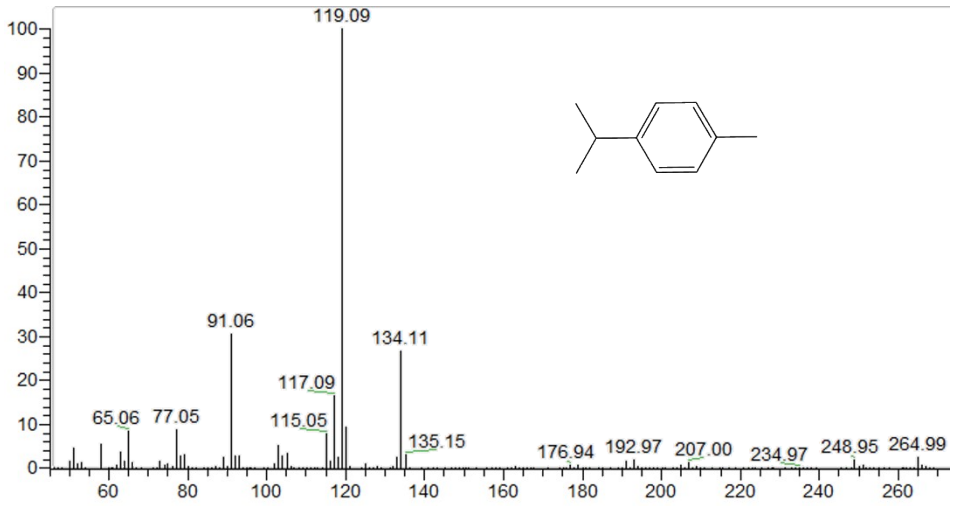

Figure S77. MS spectrum of 3-methylnitrobenzene (t.r. 7.87).

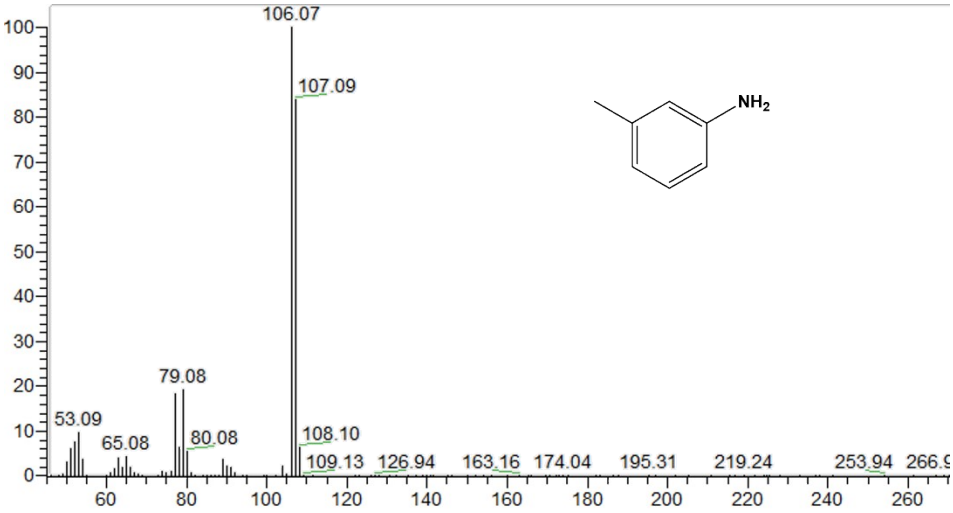

Figure S78. MS spectrum of *N*,3-dimethylaniline (t.r. 8.40).

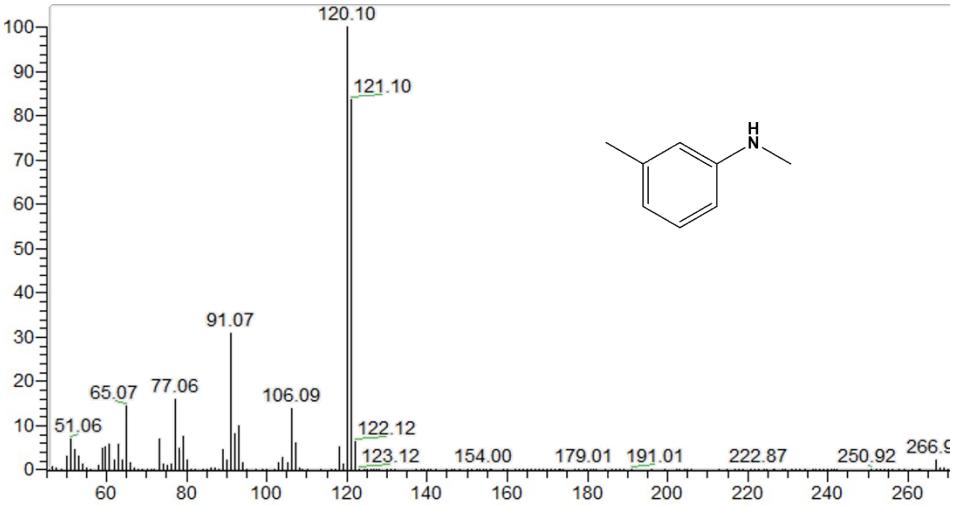

Notes and references

1 L. Biancalana, G. Pampaloni, S. Zacchini and F. Marchetti, *J. Organomet. Chem*. 2018, **869**, 201-211.

2 (a) M. A. Bennett, T.-N. Huang, T. W. Matheson and A. K. Smith, *Inorg. Synth*., 1982, **21**, 72–78. (b) S, L. Nongbri, B, Das and K. Mohan Rao, *J. Organomet. Chem*. 2009, **694**, 3881–3891. (c) L. E. Heim, S. Vallazza, D. van der Waals and M. H. G. Prechtl, *Green Chem*. 2016, **18**, 1469–1474.

3 Dissolution is presumably accompanied by dimer cleavage, with formation of $[RuCl_2(\kappa S\text{-DMSO})(\eta^6\text{-arene})]$. See ref. 1.

4 M. A. Bennett and J. P. Ennett, *Organometallics* 1984, **3**, 1365-1374.

5 M. J. Palmer, J. A. Kenny, T. Walsgrove, A. M. Kawamoto and M. Wills, J. Chem. Soc., *Perkin Trans*. 2001, **1**, 416–427.

6 S. Katsuta, H. Nomura, T. Egashira, T. Imoto, Y. Kudo and Y. Takeda, *Bull. Chem. Soc. Jpn*. 2011, **84**, 259–265.

7 B. Chatterjee and C. Gunanathan, *Chem. Commun*. 2014, **50**, 888-890.

8 (a) W. Huber, P. Bröhler, W. Wätjen, W. Frank, B. Spingler and P. C. Kunz, *J. Organomet. Chem*. 2012, **717**, 187-194. (b) M.-L. Hu, V. Safarifard, A. Morsali, T.-L. Shao and X.-C. Li, *Inorg. Chem. Commun*. 2013, **37**, 189–192.

9 (a) K.-J. Haack, S. Hashiguchi, A. Fujii, T. Ikariya and R. Noyori, *Angew. Chem Int. Ed*. 1997, **36**, 285-288. (b) L. Evanno, J. Ormala and P. M. Pihko, *Chem. Eur. J.* 2009, **15**, 12963–12967.

10 (a) M. A. Bennett, L. Yoong Goh, I. J. McMahon, T. R. B. Mitchell, G. B. Robertson and T. W. Turney, W. A. Wickramasinghe, *Organometallics* 1992, **11**, 3069-3085. (b) X. Lian Lu, W. Kee Leong, L. Yoong Goh, T. S. Andy Hor, J. J. Vittal, *Synth. React. Inorg. Met.-Org. Nano-Met. Chem*. 2005, **35**, 743–746.

11 Due to the lability of both coordinated nitrate and MeOH, the compound could exist as $[Ru(NO_3)(\kappa^2N\text{-}\{CH_2CH_2C{=}NOH\}_2)(\eta^6\text{-}p\text{-cymene})][NO_3]$ in the solid state and as a MeOH adduct in solution. Investigation of these aspects is out of the scope of the present work.